Identification of growth limiting factors in *Synechocystis* sp. PCC 6803

Volume 1 of 1

Alberto Abrantes Esteves Ferreira

A thesis submitted to the National University of Ireland, Galway

For the degree of Doctor of Philosophy

College of Science, School of Natural Science

Plant and AgriBiosciences Research Centre (PABC)

Under the supervision of Dr Ronan Sulpice

Head of School of Natural Sciences - Prof. Ciaran Morrison

February 2018

Contents

Declaration

I certify that this thesis is my own work and that I have not used this work in the course of another degree, either at the National University of Ireland Galway or elsewhere.

Signed:_____

Alberto Abrantes Esteves Ferreira

Abstract

In this study we showed that *Synechocystis* sp. PCC 6803 can achieve fast division rates using urea, a low-cost nitrogen source that does not require energy for uptake and hydrolysis, and releases CO_2 into to the cell during its assimilation. However, even using urea, we still observed a gradual decrease of growth rates in batch cultures. This was not explained by physiological or metabolic limitations. Further analyses also excluded the occurrence of quorum sensing or nutrients limitations and only self-shading (light limitation) had a moderate effect under moderate light intensity. The results indicate that growth rates are negatively affected by increases in cell density and *Synechocystis* likely present a cell-cell interaction mechanism that enable it to sense the increase of culture density and adjust its division rates to enter in stationary phase before facing light and nutrient limitations. This mechanism could not be bypassed with modifications of growth conditions, although the length of the lag phase was varying with light period in a temperature dependent way. The variations observed in the length of the lag phase are not explained by variations in the DNA replication rate or differences in the evolution of cell volume, and, thus, possibly might not be linked with photosynthesis and metabolism. Hence, it is possible that the internal signal triggered by cell-cell interaction is present when cells are transferred from high to low densities and the initiation of cell division may demand the depletion of this signal, which probably happen faster when *Syechocystis* is cultured in higher temperatures. Finally, molecular analysis showed that pili structures are not related with sensing cell density and, therefore, further efforts are necessary to identify the cell wall components and signalling pathway involved in the adjustment of growth rates by cell-cell interaction.

Acknowledgements

I would like to thank the Science Without Borders program and CAPES for the opportunity and financial support to study a PhD course abroad.

To Dr Ronan Sulpice, thanks for the patience, mainly during the first months of my PhD, when my English was not very good and I could not communicate very well. I also thank for the supervision, being always available for discussion that ended in new questions and headaches. They stimulated me to search the answers, try to explain them the best I could, and always have tablets of aspirin in my backpack.

To Dr Wagner Luiz Araújo, thanks for introducing me to Dr Ronan Sulpice and for the assistance since the application of my PhD project until today.

To my GRC committee members Prof Charles Spillane, Dr Peter McKeown and Dr Sara Farrona thanks for the discussions and ideas about my research.

To Dr Antoine Fort, thanks for the patience to answer the uncountable questions about where is and how can I do.

To Dr Masami Inaba, thanks for the ideas and assistance during my research.

To all colleagues from the different labs, thanks for the help and funny chats in the lunchroom.

Finally, special thanks to my parents Maria Alaide and Geraldo Alberto, my sisters Bárbara and Yasmim, my wife Kallyne, and some very close relatives and friends for all these years of attention, friendship and encouragement.

List of Abbreviations

° C	Degree Celsius
µg	Microgram
µL	Microliter
µM	Micromolar
µm	Micrometer
µmol	Micromol
2-OG	2-oxoglutarate
2-OGDC	2-oxoglutarate decarboxylase
2-OGDH	2-oxoglutarate dehydrogenase
ACC	Acetyl-CoA carboxylase
ADP	Adenosine diphosphate
AMP	Adenosine monophosphate
ArgD	n-acetylornithine aminotransferase
ATP	Adenosine triphosphate
BC	Biotin carboxylase
BCCP	Biotin carboxyl carrier protein
BG-11	Blue-Green medium
BG-11$_0$	Blue-Green medium without nitrogen source
C/N	Carbon/Nitrogen
c-di-GMP	Cyclic dimeric guanosine monophosphate
cDNA	Complementary deoxyribonucleic acid
CO_2	Carbon dioxide
CRP	Cyclic AMP receptor protein
cSt	Centistoke
CT	Carboxyltransferase
DNA	Deoxyribonucleic acid
ED	End of the day
EN	End of the night
ETC	Electron transport chain
FACS	Fluorescence-activated cell sorting
Fd	Ferredoxin

Fd^-	Reduced ferredoxin
FNT	Formate/nitrite transporter
GABA	Gamma-aminobutyric acid
GABA-AT	GABA aminotransferase
GC-MS	Gas chromatography coupled with mass spectrometry
GDC	Glutamate decarboxylase
GDH	Glutamate dehydrogenase
GFP	Green fluorescent protein
GOGAT	Glutamine oxoglutarate aminotransferase
GS	Glutamine synthetase
Gt	Generation time
GTP	Guanosine triphosphate
h	Hour
H_2	Atmospheric hydrogen
HL	High light intensity
HNO_2	Nitrous acid
$I_{0.5}$	Half-inhibitory concentration
ICL	Isocitrate lyase
kbp	Kilobase pairs
K_d	Dissociation constant
kDa	Kilodalton
k_m	Michaelis–Menten constant
Km^R	Kanamycin resistance
m	Mass
m^2	Meter square
Mg^{2+}	Magnesium
$MgCl_2$	Magnesium chloride
Min	Minutes
mL	Milliliter
ML	Moderate light intensity
mM	Millimolar
mm	Millimeter

Mn^{2+}	Manganese
MS	Malate synthase
N_2	Atmospheric nitrogen
NADH	Reduced nicotinamide adenine dinucleotide
NADPH	Reduced nicotinamide adenine dinucleotide phosphate
NAG	N-acetylglutamate
NAGK	N-acetylglutamate kinase
$NaHCO_3$	Sodium bicarbonate
NGS	Next-generation sequencing
Ni^{2+}	Nickel
nm	Nanometer
NtcA	Nitrogen control factor of cyanobacteria
O_2	Oxygen
OD	Optical density
PCC	Pasteur Culture Collection
PCR	Polymerase chain reaction
PII	Nitrogen regulatory protein PII
PipX	PII interacting protein X
PphA	Protein phosphatase A
PSI	Photosystem I
PSII	Photosystem II
RBD	Randomized block design
RNA	Ribonucleic acids
rpm	Rotations per minute
s	Seconds
SSA	Succinic semialdehyde
SSADH	Succinic semialdehyde dehydrogenase
TCA	Tricarboxylic acid
tsp	Transcription starting point
v	Volume
V_{max}	Maximum rate of reaction
WT	Wild type

List of Publications and Conferences Attended

Papers published

- Cavalcanti, JH, **Esteves-Ferreira AA**, Quinhones C, Pereira-Lima I, Nunes-Nesi A, Fernie A, Araújo WL (2014). Evolution and functional implications of the tricarboxylic acid cycle as revealed by phylogenetic analysis. Genome Biology and Evolution 6: 2830-2848.
- **Esteves-Ferreira AA**, Cavalcanti JHF, Vaz MGMV, Alvarenga LV, Nunes-Nesi A, Araújo WL (2017). Cyanobacterial nitrogenases: phylogenetic diversity, regulation and functional predictions. Genetics and Molecular Biology 40: 261-275.
- **Esteves-Ferreira AA**, Inaba M, Obata T, Fort A, Fleming GT, Araújo WL, Fernie AR, Sulpice R (2017). A novel mechanism, linked to cell density, largely controls cell division in *Synechocystis*. Plant Physiology 174: 2166-2182.
- Han X, Tohge T, Lalor P, Dockery P, Devaney N, **Esteves-Ferreira AA**, Fernie AR, Sulpice R (2017). Phytochrome A and B regulate primary metabolism in Arabidopsis leaves in response to light. Frontiers in Plant Science 8.

Manuscripts submitted

- **Esteves-Ferreira AA**, Inaba M, Fort A, Araújo WL, Sulpice R. Nitrogen metabolism in cyanobacteria: metabolic and molecular control, growth consequences and biotechnological applications. Submitted to: Critical Reviews in Microbiology.
- **Esteves-Ferreira AA**, Carvalho RA, Vaz MGMV, Alvarenga LV, Barros KA, Castro NV, DaMatta FM, Nunes-Nesi A, Sulpice R, and Araújo WL. Metabolic and physiological traits in cyanobacterial strains with distinct morphology and ecological origin. Submitted to: European Journal of Phycology.

Poster presentations

- **Esteves-Ferreira AA**, Sulpice R. Metabolic determinants of cyanobacteria growth through integrative data-driven modelling. 15th International Symposium on Phototrophic Prokaryotes, 2015, Tübingen - Germany.
- **Esteves-Ferreira AA**, Inaba M, Obata T, Fort A, Fleming GT, Araújo WL, Fernie AR, Sulpice R. Cell density is a major regulator of the rate of cell division in *Synechocystis* sp. PCC6803. 6th Congress of the International Society for Applied Phycology, 2017, Nantes - France.

Chapter 1: Nitrogen Metabolism in Cyanobacteria: Metabolic and Molecular Control, Growth Consequences and Biotechnological Applications

1.1 Introduction

Cyanobacteria are one of the earliest branching groups of organisms on Earth (Altermann and Kazmierczak, 2003). They are the only known prokaryotes to carry out oxygenic photosynthesis and played a key role in the formation of atmospheric oxygen 2.3 billion years ago (Bekker et al., 2004). Current agreement among the scientific community is that the plastids in green algae and land plants originated from the engulfment of free-living cyanobacteria by an ancient unicellular eukaryotic cell, which acquired photosynthetic capabilities via a cooperative relation, a process termed endosymbiosis or endocytobiosis (Martin et al., 2002; Atteia et al., 2004; Price et al., 2012; Ochoa de Alda et al., 2014). Thus, cyanobacteria are a key for the understanding of Earth's early biological and environmental history (Mulkidjanian et al., 2006; Tomitani et al., 2006; Knoll, 2008), and nowadays they are still among the most important primary producers on Earth (Ting et al., 2002).

These photosynthetic bacteria are one of the morphologically most diverse group of prokaryotes, exhibiting unicellular, colonial or filamentous forms (Komárek and Kastovský, 2003). This diversity in morphology, followed by changes in metabolism, has enabled cyanobacteria to inhabit almost every terrestrial and aquatic habitat on Earth (Schirrmeister et al., 2013). The adaptability of cyanobacterial species is likely due to the fact that they have withstood the challenges of evolutionary environmental change. Accordingly, the temporal and spatial variations in light, carbon dioxide (CO_2), nitrogen sources and oxygen (O_2) on Earth have been the driving force for the evolution and acquisition of many genes and physiological properties (Badger et al., 2006; Beck et al., 2012). Nitrate, nitrite, ammonium, urea, cyanate, and some amino acids, e.g. arginine, glutamine, and glutamate, can be assimilated by cyanobacteria, although ammonium is the preferred nitrogen source (Quintero et al., 2001; Valladares et al., 2002; Flores et al., 2005; Muro-Pastor et al., 2005; Kamennaya et al., 2008). Additionally, some cyanobacteria strains can also assimilate atmospheric nitrogen (N_2) by using different strategies to reconcile photosynthesis and N_2 fixation, thus avoiding nitrogenase inhibition by O_2 (Berman-Frank et al., 2003; Esteves-Ferreira et al., 2017a).

As photosynthetic organisms, cyanobacterial physiology is strongly affected by light availability. Too low light intensity and/or duration will not allow meeting the cellular demands, whilst an excess will require cells to dissipate part of the light energy as heat and fluorescence in order to avoid photo-degradation of their photosystems (Kirilovsky, 2007; Xu et al., 2012; Thurotte et al., 2015). In cyanobacteria, light

harvesting is performed by hydrophilic hemi-discoidal structures called phycobilisomes, located on the cytoplasmic surface of the thylakoid membrane (Mullineaux, 2008). The light energy is transferred from this antenna complexes to chlorophyll *a* present in the reaction centers of the photosystem I (PSI) and photosystem II (PSII) (Liu et al., 2013), thus leading to generation of most of the ATP and cellular reducing equivalents (i.e. NADPH and ferredoxin (Fd)) (Yang et al., 2002; Knoop et al., 2013), which will supply metabolic processes such as the Calvin-Benson cycle, nitrogen uptake and assimilation (Valladares et al., 2002; Flores et al., 2005).

Cyanobacteria are generally characterized by their high protein content (Becker, 2007; González López et al., 2010). In these organisms, nitrogen metabolism is regulated by a very conserved fine-tuning system which senses the cellular balance between carbon and nitrogen levels (Huergo and Dixon, 2015; Forchhammer and Lüddecke, 2016). In *Synechocystis* sp. PCC 6803 (hereafter termed *Synechocystis*), photosynthetic rates are positively correlated with amino acid and protein levels, but not with growth rates. In fact, high levels of these metabolites are associated with slow growth rates (Esteves-Ferreira et al., 2017b). Thus, a better understanding of the carbon and nitrogen network may allow us to comprehend how cyanobacteria allocate carbon from photosynthesis and how this can be converted in growth instead of storage. In this review, we describe the mechanisms involved in the control of nitrogen metabolism in unicellular and filamentous non-heterocytous (i.e. strains without nitrogen-fixing cells named heterocytes) cyanobacteria, at both metabolic and molecular levels. We then discuss how the nitrogen network may be related to the diurnal regulation of growth, and how manipulating it via genetic engineering might allow controlling the allocation of carbon and nitrogen resources between growth and the accumulation of reserves, thus increasing the biotechnological potential of these organisms.

1.2 Uptake and reduction of nitrogen by cyanobacteria

Ammonium is the most reduced inorganic form of nitrogen and maybe as a consequence the preferred source of nitrogen for cyanobacteria. As a result, when provided together with other nitrogen sources such as nitrate, nitrite, and urea, cyanobacteria will use ammonium primarily (Muro-Pastor et al., 2005). The presence of ammonium in the growth medium causes a general decrease in the abundance of nitrogen assimilatory enzymes and an inhibition of the activity of combined-nitrogen transport systems, a process known as global nitrogen control (Herrero et al., 2001; Forchhammer,

2004). In high concentration and at alkaline pH, a major fraction of the ammonium is in the form of ammonia, which can diffuse passively through membranes (Kleiner, 1981) (Figure 1.1A). However, in natural environments, ammonium is usually present at low concentration (Rees et al., 2006), and specific permeases (*amt1*, *amt2*, and *amt3*) are required for an efficient cellular uptake (Figure 1.1A), with Amt1 permease being the main permease responsible for ammonium uptake in *Synechocystis* (Montesinos et al., 1998).

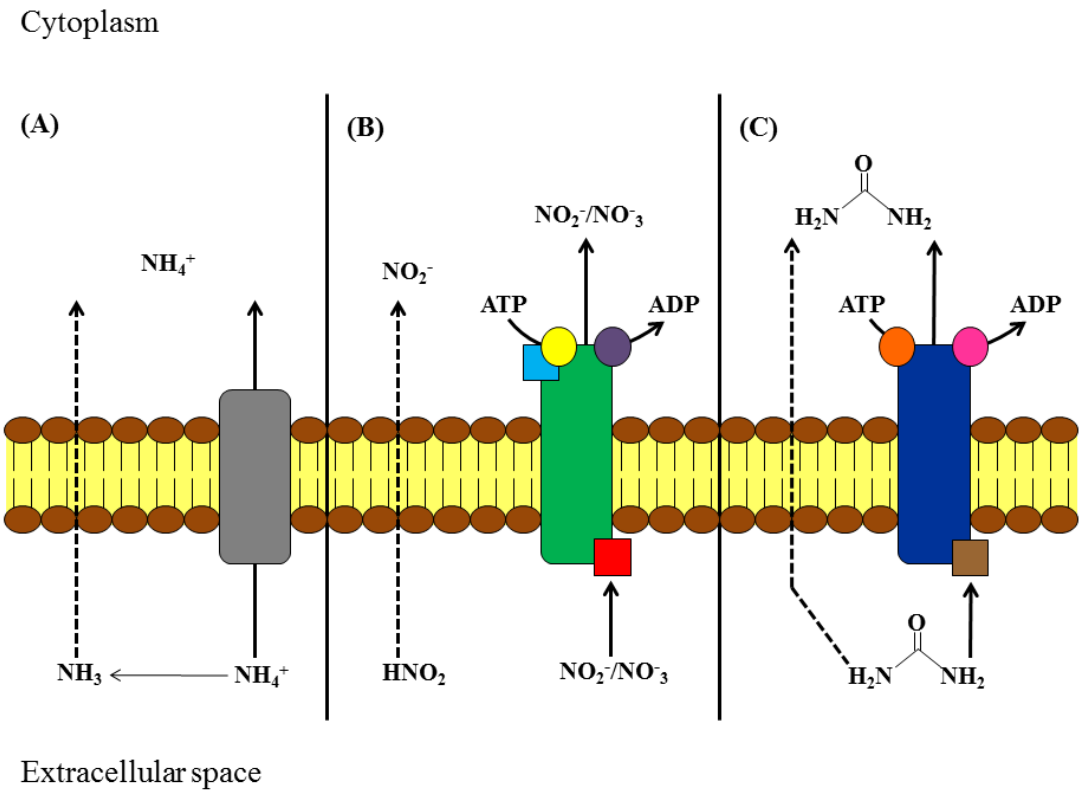

Figure 1-1: Nitrogen uptake in cyanobacteria.
A – ammonium passive diffusion (left) or by a specific permease (right); **B** – nitrite passive diffusion (left), and nitrite and nitrate active uptake by an ABC-type transporter, NrtA nitrate and nitrite periplasmic substrate-binding protein (red square), NrtB transmembrane protein (green rectangle), NrtC nitrate and nitrite cytoplasmic-binding site (blue square) and ATPase domain (yellow circle), and NrtD ATPase cytoplasmic protein (purple circle); **C** – urea passive diffusion (left) and urea active uptake by an urea ABC-type transporter, UrtA urea periplasmic-binding protein (brown square), UrtB and UrtC transmembrane proteins (blue rectangle), and UrtD and UrtE ATP-binding proteins (pink and orange circles).

Nitrate and nitrite are the most common sources of nitrogen for cyanobacteria (Guerrero et al., 1981; Su et al., 2005). At neutral pH, only nitrite can be converted to its protonated form (nitrous acid – HNO_2) and diffuse passively through the membrane (Figure 1.1B) (Sakamoto et al., 1999). However, due to the relatively low concentrations

of nitrate and nitrite in aquatic environments (micromolar range - μM) (Rees et al., 2006) and their negative residual charges, specific transporters are essential to concentrate these nitrogen sources inside the cell. The ABC-type NrtABCD transporter is observed only in freshwater cyanobacteria strains (Maeda et al., 2015), and actively transports both nitrate and nitrite (Figure 1.1B) (Luque et al., 1994b). The genes *nrtA*, *nrtB*, *nrtC*, and *nrtD* encode the proteins of the NrtABCD transporter. They are commonly present in the *nirA* operon (i.e. *nirA-nrtABCD-narB*) that also encode the enzymes Fd-nitrite reductase (NirA) and Fd-nitrate reductase (NarB), which lead to the formation of ammonium (see below). However, in *Synechocystis nirA* is separated from *nrtABCD-narB* (Omata et al., 1993; Aichi et al., 2001; Ohashi et al., 2011). NrtA is the periplasmic substrate-binding protein; NrtB is proposed to be the transmembrane protein and allows the passage of nitrate and nitrite through the membrane; NrtC has two distinct domains, the C-terminal domain that shares 30% of similarity with the amino acid sequence of NrtA and the N-terminal domain that is similar to NrtD, and is involved in the post-transcriptional regulation of the NrtABCD transporter; NrtD is a cytoplasmic ATPase with two subunits that act in the ATP binding and hydrolysis (Omata et al., 1989; Omata et al., 1993; Kobayashi et al., 2005; Koropatkin et al., 2006). The binding and subsequent hydrolysis of ATP on NrtD drive conformational changes of the membrane domain of NrtABCD, mediating the transport process (Davidson and Chen, 2004; Koropatkin et al., 2006). A second transporter, encoded by the gene *nrtP* (Sakamoto et al., 1999), also exhibit high affinity for nitrate and nitrite and was identified in the genome of cyanobacteria strains from freshwater, marine and saline environments (Bird and Wyman, 2003; Maeda et al., 2015). Moreover, certain cyanobacteria strains from marine and saline environments also present a nitrite transporter of the formate/nitrite transporter (FNT) family, and curiously the cyanate ABC-type transporter can also transport nitrite, although with a much lower affinity than for cyanate (Maeda and Omata, 2009; Maeda et al., 2015).

In order to be assimilated by cyanobacteria, nitrate needs to be reduced to ammonium via two sequential reactions catalysed by nitrate reductase and nitrite reductase (Figure 1.2). The reductions of nitrate to nitrite and nitrite to ammonium are Fd-dependent, consuming two and six electrons, respectively (Flores and Herrero, 2005). These reactions are energetically costly and can consume up to 30% of the reducing equivalents produced by the photosynthetic light reactions in cyanobacteria (Sakamoto et al., 1999).

Urea can be used as a nitrogen source by many microorganisms including bacteria, fungi, and algae (Ge et al., 1990; Singh, 1990) since it can easily diffuse across the lipid bilayers (Figure 1.1C). The concentration of urea in the ocean ranges from 0.1 to 1 µM, although it can rise in coastal and estuarine environments (Mitamura and Saijo, 1980; Antia et al., 1991). It has previously been shown that a number of cyanobacteria are able to import urea at concentrations as low as 0.1-0.6 µM (Mitamura et al., 2000). This is possible because these cyanobacteria, such as *Synechocystis*, do have a high-affinity urea ABC-type transporter (Figure 1.1C), encoded by *urt* genes (*urtA*, *urtB*, *urtC*, *urtD*, *and urtE*), which is capable of taking up urea at concentrations lower than 1 µM. These genes are normally organized in an operon, although in *Synechocystis* they are spread along the chromosome (Valladares et al., 2002). As for the nitrate ABC-type transporter, each gene encodes a protein responsible for a specific function within the transporter: UrtA is the periplasmic substrate binding protein, UrtB and UrtC the transmembrane proteins allowing urea to pass through the membrane, and UrtD and UrtE the proteins responsible for the ATP-binding and hydrolysis (Valladares et al., 2002).

Before assimilation, urea needs to be hydrolysed to ammonium and CO_2, and this reaction is catalysed in cyanobacteria by a Ni^{2+}-dependent urease (Figure 1.2) (Sakamoto and Bryant, 2001). The urease is usually described as a constitutive enzyme which is not regulated by nitrogen-containing compounds. Indeed, in cyanobacteria such as *Synechocystis*, the transcript abundance of the genes encoding urease and its activity do not vary when ammonium-grown cells are either maintained on ammonium or transferred on urea, nitrate or starved of any nitrogen source (Ludwig and Bryant, 2012). However, in some cyanobacteria strains, low urease activity has been reported when they were grown in presence of ammonium (Singh, 1992). The likely explanation for urease to be a constitutive enzyme is related to its role in the urea cycle. This cycle links catabolic and anabolic reactions in order to reallocate carbon and nitrogen among metabolic compounds (Allen et al., 2011). For example, during cyanophycin mobilization, urea is released from arginine by arginase and can then be re-assimilated as ammonium by urease (Figure 1.2), instead of diffusing passively out of the cell (Quintero et al., 2000).

Many non-heterocytous cyanobacterial strains can fix and reduce N_2 to ammonium when facing nitrogen deprivation, although well-known strains such as *Synechocystis* and *Arthrospira* (*Spirulina*) *maxima* cannot (Bergman et al., 1997; Esteves-Ferreira et al., 2017a). N_2 fixation is an energetically expensive metabolic reaction catalysed by nitrogenase, which is negatively affected by O_2 (Fay, 1992; Stal, 2008). To protect

nitrogenase from O_2, photosynthesis and N_2 fixation are temporally separated. High nitrogenase activity peaks 12 hours after the peak of photosynthesis, simultaneously with higher respiratory rates. This strategy allows nitrogenase an environment with very low O_2 tension and protects it from denaturation (Berman-Frank et al., 2003; Steunou et al., 2008). A different N_2 fixation strategy is exclusively observed in strains of the genera *Trichodesmium* (Bergman et al., 2013). In this genus, nitrogenase is located in approximately 20% of the cells of the filament, and curiously these cells exhibit high N_2 fixation rates at mid-day (Berman-Frank et al., 2001; Rodriguez and Ho, 2014). At the same time, photosynthesis is downregulated, whereas respiration, Mehler reaction, and the oxidative pentose phosphate pathway are upregulated, decreasing O_2 levels and providing reducing power and ATP for nitrogenase (Finzi-Hart et al., 2009; Sandh et al., 2011).

1.3 Nitrogen assimilation pathways in a cyanobacterial unbroken TCA cycle

Autotrophic growth requires constant synthesis or uptake of ammonium (Muro-Pastor et al., 2005). In cyanobacteria, ammonium is incorporated in carbon backbones via the glutamine synthetase/glutamine oxoglutarate aminotransferase (GS/GOGAT) cycle (Figure 1.2). The activity of this cycle requires ATP and reducing equivalents (Fd and NADH) (García-Domínguez et al., 1997; Okuhara et al., 1999). In the first step, GS catalyses the ATP dependent incorporation of ammonium into glutamate, forming glutamine (Eisenberg et al., 2000). In the next reaction, GOGAT catalyzes the transfer of one amide group from glutamine to 2-oxoglutarate (2-OG), releasing two molecules of glutamate (Okuhara et al., 1999; Flores and Herrero, 2005). Then, aminotransferases can transfer the amino group from glutamate to other carbon backbones to form additional amino acids (Mehta et al., 1993).

In most cyanobacteria, there is only one GS (GSI), encoded by the gene *glnA*. When cells are grown in presence of ammonium, GSI activity is negatively regulated via protein-protein interaction by two inactivating factors (i.e. IF7 and IF17). In contrast, in the presence of other nitrogen sources or under nitrogen deficiency, *glnA* expression is upregulated (García-Domínguez et al., 2000; Paz-Yepes et al., 2003; Saelices et al., 2011). Curiously, in some *Synechocystis* and *Synechococcus* strains, and also in *Gloeocapsa* sp. PCC 7428, there is a second type of GS encoded by *glnN*, known as GS type III (GSIII) (Reyes and Florencio, 1994). In *Synechocystis*, *glnN* transcription is more sensitive to ammonium and nitrate than *glnA*, and maximal transcript level and enzymatic

activity are only observed in cells under nitrogen starvation. However, GSIII activity can reach at most 24% of GSI activity (Reyes and Florencio, 1994; García-Domínguez et al., 1997; Reyes et al., 1997). In *Pseudanabaena* sp. strain PCC 6903 only the GSIII is present, being responsible for all ammonium assimilation. As observed in the other strains, nitrogen starvation lead to maximum GSIII expression and catalytic activity (Crespo et al., 1998). Therefore, the presence of an additional GS responsive to nitrogen availability, in some cyanobacteria strains, indicates a possible role of GSIII to enhance the efficiency of ammonium assimilation under nitrogen deficiency.

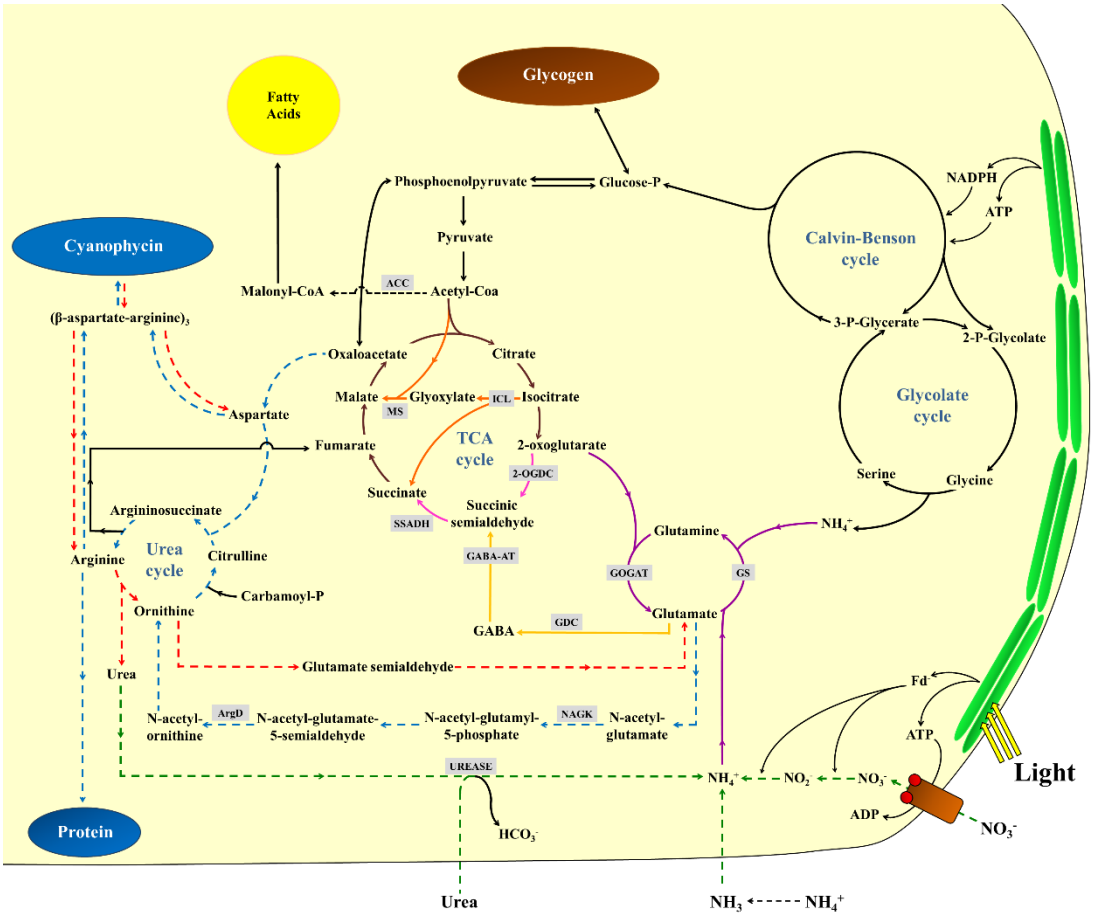

Figure 1-2: Nitrogen metabolism in cyanobacteria.
Green dashed lines: nitrogen uptake and ammonium synthesis; purple lines: ammonium assimilation by GS/GOGAT; brown lines: classical TCA cycle; pink lines: 2-OGDC/SSADH bypass; yellow lines: γ-aminobutyric acid (GABA) shunt; orange lines: glyoxylate cycle; blue dashed lines: arginine, protein and cyanophycin biosynthesis; red dashed lines: cyanophycin mobilization. Photoassimilates not used for nitrogen metabolism can be stored as glycogen and fatty acids. Abbreviations: Fd^- - reduced ferredoxin; TCA cycle - tricarboxylic acid cycle; GS - glutamine synthetase; GOGAT - glutamine oxoglutarate aminotransferase; GDC – glutamate decarboxylase; GABA - γ-aminobutyric acid; GABA-AT - γ-aminobutyric acid aminotransferase; 2-OGDC - 2-oxoglutarate decarboxylase; SSADH - succinic semialdehyde dehydrogenase; ICL - isocitrate lyase; MS - malate synthase ; NAGK - N-acetylglutamate kinase; ArgD - n-acetylornithine aminotransferase; ACC - Acetyl-CoA carboxylase.

GOGAT is usually described as a constitutive enzyme (Yang et al., 1999). However, its activity shows variations during *Synechococcus elongatus* PCC 7942 growth cycle (Lüddecke et al., 2017). Two different types of GOGAT are observed in photosynthetic organisms, a Fd-GOGAT encoded by *glsF* (commonly named *gltS*) and a NADH-GOGAT encoded by *gltB* (large subunit) and *gltD* (small subunit) (Muro-Pastor and Florencio, 2003). To date, all cyanobacteria which genome has been sequenced have a Fd-GOGAT (Muro-Pastor et al., 2005) and NADH-GOGAT has been reported only in *Synechocystis* and *Plectonema boryanum* (Navarro et al., 1995; Kaneko et al., 1996; Okuhara et al., 1999; Wang et al., 2004). In these strains, both enzymes are simultaneously active in laboratory growth conditions, although Fd-GOGAT has a more important role in ammonium assimilation and growth. Individually, *gltS*, *gltB*, and *gltD* are nonessential genes, but GOGAT null mutants cannot be obtained, suggesting that GS/GOGAT is the main path for nitrogen assimilation in cyanobacteria (Navarro et al., 1995; Okuhara et al., 1999).

Glutamate dehydrogenase (GDH) is present in the different morphological groups of the phylum Cyanophyta (Neilson and Doudoroff, 1973; Florencio et al., 1987; Chávez et al., 1995; Rangel et al., 2009), and catalyzes the synthesis of glutamate from 2-OG and ammonium in a NADPH dependent reaction. GDH can also perform the reverse reaction, although with lower efficiency (Florencio et al., 1987; Rangel et al., 2009). This enzyme is nonessential and presents a higher K_m for ammonium than GSI. Its absence does not affect nitrogen assimilation and exponential growth, although its level usually increases from linear to stationary phase, and null mutants show lower cell viability at these stages (Chávez et al., 1995; Chávez et al., 1999; Rangel et al., 2009). Thus GDH is unlikely involved with primary ammonium assimilation in cyanobacteria, and has been suggested to be involved in the consumption of excess of cellular ammonium, protecting the proton gradient within the thylakoid and periplasmic spaces (Chávez et al., 1999), or in amino acids assimilation during stationary phase (Rangel et al., 2009).

2-OG is the carbon skeleton necessary for nitrogen assimilation and an intermediate of the tricarboxylic acid (TCA) cycle (Figure 1.2). In bacteria, as in most other living organisms, the TCA cycle has two main functions, it oxidizes of acetyl-CoA for production of reducing power in the form of NADH and ATP, and provides essential precursor metabolites (e.g. oxaloacetate and 2-OG) required for the biosynthesis of other metabolites (Zhang and Bryant, 2011; Steinhauser et al., 2012).

Based on biochemical analyses performed on numerous cyanobacterial strains which showed the absence of 2-oxoglutarate dehydrogenase (2-OGDH) and succinyl-CoA synthetase activities, the enzymes which convert 2-OG to succinate (Smith et al., 1967; Pearce et al., 1969), cyanobacteria were classified as a phylum with an incomplete/unusual TCA cycle. The synthesis of 2-OG was considered to be the final step of the oxidative branch of the TCA cycle, and the main metabolic role of 2-OG was to provide carbon skeletons for the incorporation of ammonium through the GS/GOGAT cycle (Vázquez-Bermúdez et al., 2000).

Recently, alternative pathways which can complete the TCA cycle have been identified in different strains of cyanobacteria (Figure 1.2). In total, four variants of the TCA cycle are now described in cyanobacteria: (*i*) the classical open TCA cycle (Smith et al., 1967; Pearce et al., 1969); (*ii*) the 2-oxoglutarate decarboxylase (2-OGDC)/succinic semialdehyde dehydrogenase (SSADH) bypass (Zhang and Bryant, 2011); (*iii*) the γ-aminobutyric acid (GABA) shunt (Xiong et al., 2014; Zhang et al., 2016); and (*iv*) the glyoxylate cycle (Zhang and Bryant, 2015; Gründel et al., 2017). Notwithstanding, no more than two of these variants have been identified within the same strain.

Zhang and Bryant (2011) identified two enzymes in *Synechococcus* sp. PCC 7002 whose activities functionally substitute 2-OGDH and succinyl-CoA synthetase. The 2-OGDC converts 2-OG in succinic semialdehyde (SSA), and the SSADH converts the SSA into succinate (Figure 1.2). These enzymes produce NADPH, but not guanosine triphosphate (GTP). In *Synechococcus* sp. PCC 7002, the genes that encode these two enzymes are organized in an operon, and homologues of these genes have been identified in all sequenced genomes of cyanobacteria, at the exception of *Prochlorococcus* and marine *Synechococcus* spp. (Zhang and Bryant, 2011). Interestingly, these genes are not only present in cyanobacteria, but also in heterotrophic bacteria and chloroplast genomes of land plants (Tian et al., 2005; Cavalcanti et al., 2014). Furthermore, flux balance and metabolite analyses have shown that 2-OGDC/SSADH bypass is more active during dark than light periods (Hendry et al., 2016; Zhang et al., 2016).

The GABA shunt is likely present in a smaller fraction of cyanobacteria strains because the gene encoding glutamate decarboxylase (GDC) is absent in most of the sequenced cyanobacteria. Interestingly, some of the *Prochlorococcus* and marine *Synechococcus* strains lacking the 2-OGDC/SSADH bypass have the GABA shunt (Xiong et al., 2014), and both pathways are present in *Synechocystis.* The presence of the GABA shunt in *Synechocystis* is possible due to the bifunctionality of n-acetylornithine

aminotransferase (ArgD). This enzyme usually synthesises n-acetylornithine (Quintero et al., 2000), but in *Synechocystis* it also presents a GABA aminotransferase (GABA-AT) function (Xiong et al., 2014; Zhang et al., 2016), synthesising SSA from GABA (Figure 1.2). Isotope tracer analysis showed a higher production of succinate by GABA shunt, suggesting that this pathway is functionally more important than the 2-OGDC/SSADH bypass in *Synechocystis* (Xiong et al., 2014). In good agreement, a genome-wide reconstruction of the metabolic network revealed that photoautotrophic growth is reduced when metabolites are oxidized by 2-OGDH or 2-OGDC/SSADH, but not by the GABA shunt (Nogales et al., 2012). On the other hand, flux balance analysis indicates that 2-OGDC/SSADH bypass and the GABA shunt present similar stoichiometry, leading to similar biomass yields, although their yields are lower compared to those achieved by 2-OGDH in plants (Knoop et al., 2013).

The glyoxylate cycle is an alternative pathway for acetate assimilation that skips the two decarboxylation steps of the TCA cycle. The final product of this bypass is the production of succinate, which can be converted to oxaloacetate and used as a precursor for the synthesis of amino acids and carbohydrates (Figure 1.2) (Kornberg, 2000; Berg et al., 2002). Even though isocitrate lyase (ICL) and malate synthase (MS) activities were reported previously in *Anacystis nidulans* (*Synechococcus*) (Pearce and Carr, 1967; Eley, 1988) and *Synechocystis* (Yang et al., 2002), the identification of the genes that encode both enzymes was first reported in *Cyanothece*, and no homologous genes were observed in other cyanobacterial genomes (Bandyopadhyay et al., 2011). Moreover, ICL activity was not detected in partially purified extracts from *Synechocystis* (Knoop et al., 2013). In good agreement, recent studies showed that ICL and MS are present only in nitrogen-fixing cyanobacteria (Zhang and Bryant, 2015; Gründel et al., 2017). In *Cyanothece* sp. PCC 7424, the glyoxylate cycle is active during the dark period, however, it is not able to promote heterotrophic growth using acetate as the main carbon source. For this reason, it has been associated with the storage of reserves overnight (e.g. cyanophycin and polyhydroxybutyrate) that can be used during the light period to promote growth (Zhang and Bryant, 2015; Gründel et al., 2017).

As previously described in plants, cyanobacteria seem to perform preferentially a non-cyclic TCA cycle during the light period. Then the TCA cycle works as an anaplerotic pathway to provide the intermediates 2-OG and oxaloacetate that will be used as carbon skeleton for nitrogen assimilation and amino acids synthesis, and to metabolize the fumarate produced in pathways such as the urea cycle (Figure 1.2) (Quintero et al.,

2000; Sweetlove et al., 2010; Steuer et al., 2012). The higher activity of the first steps of the TCA cycle over the last ones is in good agreement with data obtained in *Synechocystis* and *Synechococcus* sp. PCC 7002, where fumarate and malate were absent or at very low levels when the strains were cultured under photoautotrophic conditions (Xiong et al., 2014; Zhang et al., 2016). Additionally, succinate dehydrogenase and fumarate hydratase were characterized as nonessential enzymes in *Synechococcus elongatus* PCC 7942, with the steps between 2-OG and oxaloacetate also described as nonessential (Rubin et al., 2015). Therefore, a non-cyclic TCA cycle during the light period might be a consequence of the higher efficiency of the photosynthetic reactions over the respiratory ones to produce ATP and reducing equivalents.

As a result of the discovery of metabolic variants that can complete TCA cycle in cyanobacteria, the 2-OG function as a sole source of carbon skeleton for nitrogen metabolism is now challenged. The presence of a complete TCA cycle opens new questions, especially about the respiratory process. Moreover, the identification of succinate production in 2-OGDC/SSADH and GABA shunt null mutants of *Synechocystis* and *Synechococcus* sp. PCC 7002 suggests that there are still unknown pathways linked to the TCA cycle (Xiong et al., 2014; Zhang et al., 2016). The identification of those pathways will be a very important step towards a better comprehension of how cyanobacteria regulate their carbon-nitrogen (C/N) balance and adjust their growth in response to changes in environmental conditions. 2-OG concentrations are linked to the C/N levels, working as an indicator of the C/N balance and cellular redox status (Alfonso et al., 2001; Forchhammer, 2004). In other words, 2-OG is not only a central metabolite but also a signalling molecule (Huergo and Dixon, 2015).

1.4 Global nitrogen control: the interactions between 2-oxoglutarate, PII, PipX and NtcA link metabolite levels and gene expression

The nitrogen regulatory protein PII (PII) can interact with 2-OG, the binding being dependent upon the 2-OG concentrations. The binding of 2-OG on PII leads to conformational changes of PII, affecting its interaction with other proteins and then their activity or binding properties (Forchhammer and Lüddecke, 2016). Among these proteins, the PII interacting protein X (PipX), is released from PII to interact with the nitrogen control factor of cyanobacteria (NtcA), affecting the transcription efficiency of nitrogen related genes (Llácer et al., 2010). Thus, a complex network link 2-OG with PII,

PipX, and NtcA, and allows these proteins to regulate the activity and expression of transporters and enzymes related to nitrogen and carbon metabolism (Figure 1.3).

1.4.1 Protein PII is a sensor of 2-oxoglutarate and regulates nitrogen metabolism, including nitrogen storage as cyanophycin

PII connects gene expression and metabolism by sensing 2-OG levels, its phosphorylated state being a good indicator of the C/N balance (Figure 1.3). This protein is a universal 2-OG sensor found in all bacteria, nitrogen-fixing archaea, and in chloroplasts of algae and plants (Sant'Anna et al., 2009; Chellamuthu et al., 2013). In *Synechocystis* and *Synechococcus elongatus* PCC 7942 there are two *glnB* (encoding PII) promoters: one is constitutive, and the other is NtcA inducible. In *Synechocystis* these promoters overlap and exhibit two different sites for transcription initiation, with the NtcA-dependent site upstream of the constitutive, and activated only under nitrogen-limited conditions (García-Domínguez and Florencio, 1997). On the other hand, in *Synechococcus elongatus* PCC 7942, both promoters are separated, with the NtcA-inducible promoter located downstream of the constitutive one and activated when cells are grown on nitrate or face nitrogen deficiency (Lee et al., 1999). PII is a homotrimer comprising 12-13 kDa subunits with a practically hemispheric body from which three T-loops exit. Additionally, small structures called B and C loops are present on opposite sides of each subunit (Xu et al., 2003). The T-loops are important for PII protein-protein interaction, and host at their base a binding site for 2-OG. An ATP/ADP binding site is located in each intersubunit cleft formed by B and C loops from different subunits and shows 2 to 3 times more affinity to ATP than ADP (Fokina et al., 2010a; Fokina et al., 2011).

PII senses the cellular nitrogen, carbon availability and redox power by interacting with ATP, magnesium (Mg^{2+}) and 2-OG, which leads to conformational changes in the T-loops and regulate its interaction with different proteins. ATP-Mg must first bind on PII to create the 2-OG binding site and then allow 2-OG interaction with PII (Fokina et al., 2010a). Opposite, ADP binding on PII blocks 2-OG binding on that subunit and decreases the affinity of the other subunits for 2-OG (Fokina et al., 2011). The three 2-OG binding sites present on PII protein exhibit anti-cooperativity. The binding of the first 2-OG leads to structural changes in the second binding site, increasing its dissociation constant (K_d) and consequently decreasing the affinity for 2-OG. The same process occurs between the second and third 2-OG binding sites and among ATP/ADP binding sites

(Fokina et al., 2010a; Ma et al., 2014). Therefore, PII occurs in four different states, a dephosphorylated one and three phosphorylated states with a different number of phosphorylated subunits: PII-(ATP/2-OG)$_1$, PII-(ATP/2-OG)$_2$, and PII-(ATP/2-OG)$_3$ (Zeth et al., 2014). As a result, a progressive increase in the cellular levels of ATP and 2-OG is required for PII complete phosphorylation, making PII a good sensor of carbon and energy cellular levels (Forchhammer and Hedler, 1997; Fokina et al., 2010b).

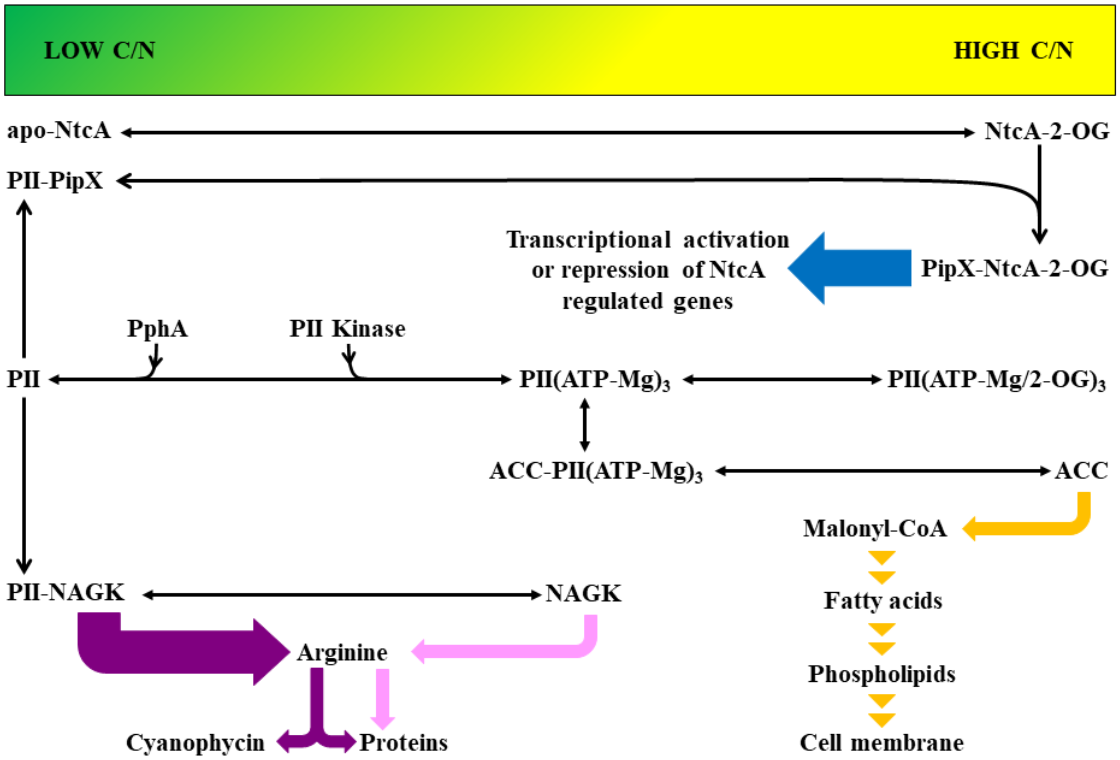

Figure 1-3: Global nitrogen control in cyanobacteria.
Interaction network between 2-oxoglutarate, PII, PipX, and NtcA, and their regulatory roles in ACC, NAGK activity, and gene expression. Unphosphorylated PII interacts with NAGK, increasing its activity, and then supplying enough arginine for both protein and cyanophycin biosynthesis. On the other hand, phosphorylated PII interacts with ACC and blocks malonyl-CoA synthesis. Abbreviations: C/N – carbon/nitrogen balance; NtcA - nitrogen control factor of cyanobacteria; PII - nitrogen regulatory protein PII; PipX - PII interacting protein X; 2-OG – 2-oxoglutarate; PphA - protein phosphatase A; Mg- magnesium; NAGK - N-acetylglutamate kinase; ACC - Acetyl-CoA carboxylase.

PII protein kinase specifically uses ATP to phosphorylate PII at serine 49 (Fokina et al., 2010a), however, the gene which encodes it remains unknown. Its kinase activity is regulated negatively by ammonium and positively by 2-OG (Forchhammer and de Marsac, 1995), which is characteristic of NtcA activated genes. In agreement, a NtcA null mutant (*ntcA*$^-$) strain is not able to phosphorylate PII completely, even under nitrogen-limited conditions (Lee et al., 1999). Moreover, the application of a given dose of nitrate can lead to different PII phosphorylation states depending on carbon and light availability.

Cells grown on high CO_2 or light levels or glucose supplementation exhibited elevated PII phosphorylation state, whereas ambient CO_2 and low light lead to an unphosphorylated PII (Forchhammer and Tandeau de Marsac, 1995; Hisbergues et al., 1999; Lee et al., 1999; Irmler and Forchhammer, 2001; Kloft and Forchhammer, 2005). These effects of light or glucose on PII phosphorylation state raise the question whether they are solely driven by changes in 2-OG levels, or if there is also an additional signalling process, possibly via the generation of ATP, linked to the redox state of the thylakoid electron transport chain (ETC) that could also affect PII phosphorylation.

The dephosphorylation of PII is catalysed by the protein phosphatase A (PphA), which is a member of the PP2C family (Irmler and Forchhammer, 2001). PphA has a Mn^{2+} or Mg^{2+} dependent activity, with Mn^{2+} leading to higher dephosphorylation efficiency. ATP and 2-OG indirectly affect PphA activity by interacting with PII and blocking PphA-PII association. However, to prevent PphA activity, all three ATP and 2-OG binding sites of PII need to be occupied (Ruppert et al., 2002). PphA amounts respond to nitrogen sources, low levels being observed in *Synechocystis* cells grown on ammonium or under nitrogen starvation, and high levels when grown on nitrate and nitrite. Thus, PphA is not under the global nitrogen control (Kloft and Forchhammer, 2005; Kloft et al., 2005), in line with the observation that *ntcA*$^-$ strains have a PII phosphatase activity (Lee et al., 1999). Additionally, an interesting relation between PII kinase and phosphatase has been described. Because nitrate and nitrite induce PII kinase synthesis and then promote PII phosphorylation, higher levels of PphA will be required to rapidly dephosphorylate PII. Opposite, when cells are grown on ammonium, they have a low kinase activity, then high levels of PphA are not necessary.

PII is involved in the post-transcriptional regulation of different proteins and proteins complexes. Hence, its regulatory activity has been described on the ABC-type nitrate transporter NrtABCD and nitrate reductase (Kobayashi et al., 2005; Takatani et al., 2006), ABC-type cyanate transporter (Chang et al., 2013), high-affinity bicarbonate transporters (Hisbergues et al., 1999), acetyl-CoA carboxylase (ACC) (Hauf et al., 2016), N-acetylglutamate kinase (NAGK) (Heinrich et al., 2004; Llácer et al., 2007), and PipX (Espinosa et al., 2006). Because PII is a relatively abundant protein, its cellular concentration is higher than those proteins (Guerreiro et al., 2014), allowing PII to regulate the activity of different proteins simultaneously.

PII coordinates, independently of its phosphorylation state, the activities of the NrtABCD transporter, nitrate reductase, ABC-type cyanate transporter and high-affinity

bicarbonate transporters. The activities of NrtABCD transporter, nitrate reductase and ABC-type cyanate transporter are repressed by ammonium only in the presence of PII. In the case of NrtABCD, the C-terminal domain of NrtC interacts with PII to regulate this ammonium-dependent repression. However, how the C-terminal domain of NrtC associates with PII remains unclear (Kobayashi et al., 1997; Lee et al., 1998; Kobayashi et al., 2005; Chang et al., 2013).

PII regulates negatively the activity of ACC, but only in a fully phosphorylated state and in presence of low levels of 2-OG (Hauf et al., 2016). ACC is a protein complex composed of four proteins, the biotin carboxyl carrier protein (BCCP), the biotin carboxylase (BC), and the α and β subunits of the carboxyltransferase (CT) (Sasaki and Nagano, 2004). This heteromeric enzyme catalysis the carboxylation of acetyl-CoA to malonyl-CoA (Figure 1.2), the first step of fatty acids biosynthesis (Knoop et al., 2013). The consumption of acetyl-CoA by ACC leads to a decrease in 2-OG levels, favouring the interaction of fully phosphorylated PII with the BCCP subunit (Figure 1.3). This interaction inhibits ACC activity and thus the synthesis of malonyl-COA, leading to a progressive increase in the levels of acetyl-CoA, and consequently 2-OG. The increment in the physiological levels 2-OG allows its binding to PII. When all three binding sites are occupied PII dissociate from ACC (Figure 1.3), and the excess of acetyl-CoA is used again for fatty acids synthesis (Hauf et al., 2016). This fine-tuning control of ACC activity by PII is a highly conserved mechanism, with similar regulations observed in green algae and land plants (Feria Bourrellier et al., 2010; Zalutskaya et al., 2015).

NAGK is the rate-limiting enzyme in the arginine biosynthetic pathway (Figure 1.2). The phosphorylation of PII at serine 49 prevents PII-NAGK association and inhibits NAGK activity. In its non-activated state, NAGK has a low activity, providing basal a level of arginine for protein synthesis (Figure 1.3). Under conditions where nitrogen is in excess or cannot be used (e.g. low C/N ratio), dephosphorylated PII binds to NAGK, enhancing the activity of the enzyme (Heinrich et al., 2004; Llácer et al., 2007; Fokina et al., 2010b). In this complex, two PII trimers interact with one hexameric NAGK, thus each subunit of PII binds to one subunit of NAGK (Lüddecke and Forchhammer, 2013). Within the PII-NAGK complex, the B-loops of PII interact with the C-domains of NAGK containing the arginine sites, and the T-loops interact with the N-domains of NAGK containing the N-acetylglutamate (NAG) sites (Llácer et al., 2007). The binding of PII increases NAGK maximal velocity (V_{max}) by 2-4 folds and also decreases its K_m for NAG by 10 folds. In addition, PII-NAGK is less sensitive to arginine concentration than

NAGK, with an increase in the half-inhibitory concentration of arginine ($I_{0.5}$) by 15 folds (Llácer et al., 2007). Thus, PII binding to NAGK leads to a higher synthesis rate of arginine, with the excess of what is required for protein synthesis being stored as cyanophycin (Figures 1.2 and 1.3) (Stephan et al., 2000; Maheswaran et al., 2006; Llácer et al., 2008). Finally, this consumption of the assimilated nitrogen for storage leads to an increase of the C/N balance and allows the dissociation of the PII-NAGK complex, which is achieved when all 2-OG binding sites of PII are occupied (Figure 1.3) (Fokina et al., 2010b).

PipX is a protein with 89 amino acids encoded by the gene *pipX*. Homologues of this protein were identified in all cyanobacteria genomes sequenced so far, but not in any organisms from other phyla (Espinosa et al., 2006). In low C/N conditions, when PII is unphosphorylated, PipX interacts with PII, forming a complex composed of three PipX proteins and one PII (Figure 1.3). Under high C/N, this protein is bound with NtcA (Llácer et al., 2010). Thus, PipX is always associated with either PII or NtcA according to the C/N balance (Figure 1.3) and has never been reported in a non-associated state. Interestingly, the first PII null mutants (*pII*$^-$) were discovered to carry a spontaneous null mutation of PipX (*pipX*$^-$) (Forchhammer and de Marsac, 1995; Espinosa et al., 2009), leading the authors to hypothesise that PipX is toxic for cells in the absence of PII. Further studies confirmed the hypothesis, showing that (*i*) homozygous *pII*$^-$ could only be obtained using a *pipX*$^-$ background strain (Espinosa et al., 2009; Espinosa et al., 2010); (*ii*) cyanobacterial strains with two copies of *pipX* also had a second copy of *pII* (Laichoubi et al., 2011), (*iii*) constitutive expression of *pipX* leading to a high PipX/PII ratio was lethal for cells (Laichoubi et al., 2012); and recently, (*iv*) the selection of homozygous *pII*$^-$ in a *Synechococcus elongatus* PCC 7942 strain carrying a wild type PipX was only achieved when cells were grown in conditions leading to a high C/N, thus when most PipX is associated with NtcA (Chang et al., 2013). Therefore, PII essentiality in cyanobacteria is associated with the requirement to avoid the free PipX toxicity under low C/N conditions. Under high C/N conditions, PII interacts with ATP and 2-OG, and PipX dissociates from PII and binds to NtcA, leading to the formation of the PipX-NtcA complex, and then changes in gene expression (Figure 1.3 and below) (Llácer et al., 2010).

1.4.2 NtcA driven regulation of transcription is dependent on 2-oxoglutarate and PipX via modulation of its DNA binding properties

NtcA is a homodimeric DNA-binding protein that belongs to a cyclic AMP receptor protein (CRP) family of transcriptional activators (Vega-Palas et al., 1992). This protein is highly conserved in all of the sequenced cyanobacteria, with more than 61% similarity in amino acid sequence (Frías et al., 1993; Herrero et al., 2001). Each subunit of the homodimer has two distinct domains, a N-terminal 2-OG binding domain and a C-terminal DNA-binding domain, connected by a C-helix (Zhao et al., 2010).

The efficiency of NtcA binding to a promoter is enhanced by 2-OG and PipX (Figure 1.3). In the presence of $MgCl_2$, 2-OG increases synergistically the binding of NtcA on NtcA-dependent promoters. This binding is not dependent on ATP or another nucleoside triphosphate (Tanigawa et al., 2002; Vázquez-Bermúdez et al., 2002). Mechanistically, the two 2-OG binding sites of the NtcA homodimer present cooperativity between them, the interaction of the first 2-OG molecule with one of the N-terminal domains increasing the affinity of the second binding site to 2-OG (Forcada-Nadal et al., 2014). The binding of 2-OG promotes conformational changes that are transmitted onward the two C-helices until both C-terminal DNA-binding domains, allowing an optimal distance and orientation for DNA binding. Thus, NtcA presents two forms, an inactive one (apo-NtcA) and an active one (NtcA-2-OG). Both forms possess the capacity to bind DNA, although the interaction of NtcA with 2-OG promote conformational changes that increase the affinity between NtcA and its DNA binding site (Figure 1.3) (Zhao et al., 2010).

The conformational changes promoted by 2-OG binding on NtcA allow its binding to PipX (Llácer et al., 2010). One PipX binds with each NtcA subunit and stabilises the NtcA active form by increasing NtcA affinity to 2-OG from 3.5 up to 9 times (Forcada-Nadal et al., 2014). Hence, PipX promotes maximal NtcA-dependent regulation of transcription by probably helping to recruit RNA polymerase. NtcA alone can bind DNA and regulate gene transcription, but far less efficiently than in the presence of PipX (Espinosa et al., 2007; Espinosa et al., 2014). Therefore, maximal changes in expression of the genes regulated by NtcA are achieved when there is an increase in 2-OG concentrations which drives NtcA to an active state, allowing the formation of the 2-OG-NtcA-PipX complex (Figure 1.3).

NtcA binds to type II promoters that contain a -10 box in the form TAN_3T and an enhancer sequence (NtcA binding site) containing the palindromic motif $GTAN_8TAC$,

which compensates the lack of the -35 box (Luque et al., 1994a; Asayama and Imamura, 2008). Both triplets of the NtcA binding site are complementary to each other and the C-terminal DNA-binding domain of each subunit of the dimer interacts with one triplet (Herrero et al., 2001). Usually, eight nucleotides between the triplets are the ideal space, although binding sites with 7 and 9 nucleotides space were also reported. Variations in the NtcA binding box can affect the interaction of NtcA and 2-OG, and decrease the affinity between NtcA and DNA binding sites (Jiang et al., 2000; Forcada-Nadal et al., 2014).

Depending on the location of the NtcA binding site on a promoter, NtcA can activate or repress the transcription of genes and operons. Hence, when NtcA binding sites are located upstream the transcription starting point (tsp), NtcA can activate transcription by increasing the transcription efficiency of the RNA polymerase (Niu et al., 1996; Osanai et al., 2014). Opposite, NtcA represses gene expression when its binding site overlaps the -10 box (RNA polymerase-binding site) or the tsp, blocking the access of the RNA polymerase to the promoter (Asayama and Imamura, 2008; Kuniyoshi et al., 2011).

Two different *ntcA* genes, varying in their promoter sequence, are present in *Synechocystis*, one being expressed constitutively and responsible for NtcA basal expression, and the other regulated by the cellular redox status and nitrogen availability (Alfonso et al., 2001). In *Synechocystis*, *ntcA* is an essential gene (Osanai et al., 2014), and in the presence of nitrogen sources other than ammonium, or under nitrogen starvation, NtcA activates the transcription of a set of genes involved in (Table 1.1): (*i*) mobilization of nitrogen stored as phycobilisome (*nblA*) (Luque et al., 2001); (*ii*) transcriptional activation of the *nirA* operon (*ntcB*) (Suzuki et al., 1995); (*iii*) uptake of nitrogen sources such as nitrate/nitrite (*nrtABCD* and *nrtP*) (Luque et al., 1994a; Sakamoto et al., 1999), ammonium (*amt1*) (Paz-Yepes et al., 2007), urea (*urtABCDE*) (Valladares et al., 2002), and cyanate/nitrite (*cynABD*) (Harano et al., 1997); (*iv*) reduction of nitrate and nitrite to ammonium, so nitrate and nitrite reductase (*narB and nirA*) (Luque et al., 1994a), and nitrite reductase related protein (*nirB*) (Suzuki et al., 1995); (*v*) cyanate hydrolysis to ammonium by cyanate lyase (*cynS*) (Harano et al., 1997); (*vi*) assimilation of ammonium, so isocitrate dehydrogenase (*icd*) (Muro-Pastor et al., 1996), nitrogen stress-induced RNA 4 (*nsiR4*) (Klähn et al., 2015), GSI (*glnA*) and GSIII (*glnN*) (Luque et al., 1994a; Reyes et al., 1997; Vázquez-Bermúdez et al., 2002); (*vii*) sugar catabolism, with sigma factor E (*sigE*) and response regulator Rre37 (*rre37*) (Muro-

Pastor et al., 2001; Azuma et al., 2011); and (*viii*) sensing and controlling cellular nitrogen homeostasis, with PII (*glnB*) (García-Domínguez and Florencio, 1997), PII kinase (Forchhammer and de Marsac, 1995), and NtcA itself (*ntcA*) (Luque et al., 1994a; Alfonso et al., 2001). On the other hand, in the presence of other nitrogen sources than ammonium, or under nitrogen starvation, NtcA represses transcription of the GS inactivating factors IF7 (*gifA*) and IF17 (*gifB*) (Table 1.1) (García-Domínguez et al., 2000; Saelices et al., 2011).

Interestingly, NtcA binding sites have also been identified in genes related to microcystin synthesis, a hepatotoxin synthesised by some bloom-forming cyanobacteria strains (Rastogi et al., 2014). However, apparently conflicting results have been reported with NtcA acting as both activator (Ginn et al., 2010; Pimentel and Giani, 2014) and repressor (Kuniyoshi et al., 2011) of the transcription of the microcystin gene cluster (Table 1.1). Thus, in the context of the ecological and public health importance of microcystin (Rastogi et al., 2014), further studies are required.

The regulatory role of NtcA is not restricted to nitrogen metabolism. NtcA seems to have regulatory functions on photosynthetic light reactions and carbon uptake, concentration and assimilation (Sauer et al., 1999; Su et al., 2005; Espinosa et al., 2014). Therefore, NtcA is likely not only involved in the coordination of genes associated with nitrogen metabolism but also plays a role in the regulation of carbon metabolism (Table 1.1) (Osanai et al., 2006; Osanai et al., 2007; Azuma et al., 2011). However, how NtcA regulates photosynthesis in response to nitrogen availability remains unclear.

1.5 Possible crosstalk between the nitrogen control network and the diurnal regulation of growth

Cyanobacteria are the unique prokaryotic phylum which presents a circadian regulation of growth (Foster et al., 2007). In these organisms, the cell cycle is light-dependent since photosynthesis is the main provider of cellular energy to promote growth (Yang et al., 2002; Knoop et al., 2013). Hence, an increase in light availability/intensity should stimulate cell division. However, a circadian gating control and a cell-cell interaction mechanism can prevent a light-driven growth stimulation, slowing down or even stopping cell division (Mori and Johnson, 2001; Yang et al., 2010; van Alphen and Hellingwerf, 2015; Esteves-Ferreira et al., 2017b). In contrast, DNA replication seems not to be regulated by the circadian clock, because replication rates are constant under continuous light (Mori et al., 1996; Pando and van Oudenaarden, 2010). Moreover, the

Table 1-1: Major components in the regulatory network of carbon and nitrogen balance in cyanobacteria

Name	Gene(s)	Function	Regulation	Reference
Phycobilisome degradation protein	*nblA*	Mobilization of nitrogen stored as phycobilisome	Transcriptionally activated by NtcA	Luque et al., 2001
Nitrite-responsive transcriptional activator	*ntcB*	Transcriptional activation of the *nirA* operon	Transcriptionally activated by NtcA	Suzuki et al., 1995
Nitrate ABC-type transporter	*nrtABCD*	Nitrate/nitrite uptake	Transcriptionally activated by NtcA Post-transcriptionally regulated by PII	Luque et al., 1994a Kobayashi et al., 2005
Nitrate/nitrite permease	*nrtP*	Nitrate/nitrite uptake	Transcriptionally activated by NtcA	Sakamoto et al., 1999
Ammonium permease	*amt1*	Ammonium uptake	Transcriptionally activated by NtcA	Paz-Yepes et al., 2007
Urea ABC-type transporter	*urtABCDE*	Urea uptake	Transcriptionally activated by NtcA	Valladares et al., 2002
Cyanate ABC-type transporter	*cynABD*	Cyanate/nitrite uptake	Transcriptionally activated by NtcA Post-transcriptionally downregulated by PII	Harano et al., 1997 Chang et al., 2013
Ferredoxin-nitrate reductase	*narB*	Nitrate reduction to nitrite	Transcriptionally activated by NtcA Post-transcriptionally regulated by PII	Luque et al., 1994a Kobayashi et al., 2005
Ferredoxin-nitrite reductase	*nirA*	Nitrite reduction to ammonium	Transcriptionally activated by NtcA	Luque et al., 1994a
Nitrite reductase related protein	*nirB*	Control of nitrite reductase activity	Transcriptionally activated by NtcA	Suzuki et al., 1995
Cyanate lyase	*cynS*	Cyanate degradation	Transcriptionally activated by NtcA	Harano et al., 1997
Isocitrate dehydrogenase	*icd*	Synthesis of 2-oxoglutarate	Transcriptionally activated by NtcA	Muro-Pastor et al., 1996
Nitrogen stress-induced RNA 4 (NsiR4)	*nsiR4*	Post-transcriptional downregulation of IF7	Transcriptionally activated by NtcA	Klähn et al., 2015
Glutamine synthetase I (GSI)	*glnA*	Glutamine synthesis/ ammonium assimilation	Transcriptionally activated by NtcA Post-transcriptionally downregulated by IF7 and IF17	Luque et al., 1994a Saelices et al., 2011
Glutamine synthetase III (GSIII)	*glnN*	Glutamine synthesis/ ammonium assimilation	Transcriptionally activated by NtcA	Reyes et al., 1997

Table 1.1: Major components in the regulatory network of carbon and nitrogen metabolism in cyanobacteria

Name	Gene(s)	Function	Regulation	Reference
Sigma factor E	*sigE*	Transcriptional activation of nitrogen assimilation at stationary phase, and sugar catabolism pathways.	Transcriptionally activated by NtcA	Muro-Pastor et al., 2001
Response regulator Rre37	*rre37*	Transcriptional activation of sugar catabolism pathways.	Transcriptionally activated by NtcA	Azuma et al., 2011
Nitrogen regulatory protein PII (PII)	*glnB*	Post-transcriptional regulation of nitrogen related proteins	Transcriptionally activated by NtcA Post-transcriptionally regulated by 2-OG, PII kinase and PphA	García-Domínguez and Florencio, 1997 Forchhammer and de Marsac, 1995 Irmer and Forchhammer et al., 2001 Fokina et al., 2010a
PII Kinase	Unknown	PII phosphorylation	Transcriptionally activated by NtcA	Forchhammer and de Marsac, 1995
Nitrogen control factor of cyanobacteria	*ntcA*	Transcriptional activation or repression of nitrogen related genes	Transcriptionally activated by NtcA Post-transcriptionally regulated by 2-OG and PipX	Luque et al., 1994a Zhao et al., 2010 Llácer et al., 2010
GSI inactivating factor IF7	*gifA*	Post-transcriptional downregulation of GSI	Transcriptionally repressed by NtcA Post-transcriptionally downregulated by NsiR4	García-Domínguez et al., 2000 Klähn et al., 2015
GSI inactivating factor IF17	*gifB*	Post-transcriptional downregulation of GSI	Transcriptionally repressed by NtcA	García-Domínguez et al., 2000
Microcystin synthetase gene cluster	*mycA-J*	Microcystin synthesis	Transcriptionally activated by NtcA Transcriptionally repressed by NtcA	Ginn et al., 2010 Kuniyoshi et al., 2011

decrease in the rate of DNA replication during dark periods has been associated with the oxidative state of the ETC (Ohbayashi et al., 2013; Ohbayashi et al., 2017). In cyanobacteria strains such as *Synechococcus* and *Synechocystis* cell division and DNA replication occur during the light period, albeit cell division showing more sensitivity to diurnal variations in light/dark cycles than DNA replication, probably due to the high amount of energy required by the division process. Thus, when cells are transferred from light to dark, they normally stop cell division, even when they are close to the end of the process (Marino and Asato, 1986; Mori and Johnson, 2001; Asato, 2003). On the other hand, DNA replication will only stop in cells that are in the early stages of genome replication, the cells close to complete the replication cycle finishing it even if they are in the dark (Ohbayashi et al., 2017).

Other cellular components such as transcripts, proteins and metabolites related to photosynthesis, TCA cycle, carbon metabolism and amino acid biosynthesis also show diurnal variations in their cellular levels (Steuer et al., 2012; Beck et al., 2014; Guerreiro et al., 2014). Among them, NtcA and PII, the main proteins of the nitrogen regulatory network, exhibit diurnal fluctuations of their transcript levels. This was observed when cells were grown under various growth conditions (e.g. different nitrogen sources, light, and CO_2 levels) (Esteves-Ferreira et al., 2017b).

Photosynthesis is light dependent, and during this period it supplies redox power and photoassimilates, allowing the maintenance of all metabolic processes and the promotion of growth. The increase in energy and carbon availability associated with photosynthesis, together with the activity of a non-cyclic TCA cycle, leads to increments in 2-OG levels (Figure 1.2). The higher cellular content of 2-OG drives adjustments on the nitrogen control network, due to changes in PII interaction with ATP and 2-OG, and NtcA activation by 2-OG and PipX (Figure 1.3) (Llácer et al., 2010; Zeth et al., 2014; Zhang et al., 2016). Hence, those proteins can transcriptionally and post-transcriptionally regulate processes related to nitrogen uptake and assimilation to fulfil the cellular demand for nitrogen, and then fine-tune the balance between carbon and nitrogen levels that are both diurnally changing (Su et al., 2005; Forchhammer and Lüddecke, 2016). This highly regulated process will ensure the timely supply amino acids, especially during the first hours of the light periods when high rates of protein synthesis are observed (Beck et al., 2014). Consequently, photoassimilates are used as carbon skeletons for the synthesis of amino acids or phospholipids, the balance between both biosynthetic pathways being under the control provided by the interaction between PII and ACC (Figures 1.2 and 1.3;

see above) (Hauf et al., 2016). Amino acids will then be used by the cell machinery to synthesize proteins related to all cellular processes, including structural proteins and protein complexes that will be inserted to phospholipid bilayers to form both thylakoids and cell membranes (Peschek et al., 2004; van de Meene et al., 2006; Wang et al., 2009). Thus, the regulation provided by the nitrogen control network might not only allow to properly balance C/N resources, but also be of major importance for regulating temporally within the diurnal cycle the maintenance and biogenesis of the cell membrane systems, and consequently cell division. Indeed, it is important for cells to coordinate temporally the synthesis of large sets of proteins with the biosynthesis of phospholipids in order to be able to assemble and insert protein complexes in new membranes.

Both fatty acids and amino acids that are not used for growth will be stored as lipid bodies and cyanophycin, respectively. Their levels are indirectly affected by PII regulation on ACC and NAGK (Figures 1.2 and 1.3) (Maheswaran et al., 2006; Hauf et al., 2016). Moreover, the excess of photoassimilates can be polymerized to form glycogen, which is the carbon/energy source for dark periods (Díaz-Troya et al., 2014), or released to the extracellular environment in order to control the cellular homeostasis and avoid inhibition of photosynthesis by negative sugar feedback (Esteves-Ferreira et al., 2017b). Hence, it is likely that the nitrogen control network has a very important role in synchronizing temporally the flux of carbon from photosynthesis to synthesis of the metabolites directly related with cell division, and is not solely involved in the regulation of the metabolism in response to environmental factors. Therefore, the importance of this network is probably higher than currently assumed. NtcA promoters were identified in genes involved in photosynthesis and PipX seems also required for the activation of those genes (Su et al., 2005; Espinosa et al., 2014). Thus, this network is likely not only involved in controlling the flux of carbon originating from photosynthesis, but also directly related to its regulation.

During the dark period, growth is limited due to a decrease of the energy available and the circadian gating control of cell division. During this period, glycogen is the main source of carbon and energy (Figure 1.2), and its full oxidation through a cyclic TCA cycle provides energy to support processes such as active transport through membranes, transcription, translation, and DNA repair (Steuer et al., 2012; Beck et al., 2014; Guerreiro et al., 2014). The decrease in carbon level entails in a lower cellular demand for nitrogen and probably affects negatively NtcA activation state and PII interaction with ATP and 2-OG. Hence, during the night, the regulations of genes and proteins by NtcA and PII is

expected to be different compared to the light period. We would expect a decrease of the NtcA repression on the transcription of the inactivating factors IF7 and IF17, and a consequent binding of these factors on GSI (Saelices et al., 2011), thus a reduction of nitrogen assimilation. Additionally, NtcA may have an indirect effect on glycogen degradation, because it upregulates the expression of SigE and Rre37, proteins directly involved in sugar catabolism (Muro-Pastor et al., 2001; Osanai et al., 2006; Osanai et al., 2007; Azuma et al., 2011). In good agreement, a *Synechocystis* strain overexpressing *ntc*A, when grown on nitrogen replete conditions, showed higher growth rates compared to the wild type strains, followed by lower levels of glycogen and higher content of sugar phosphates (Osanai et al., 2014). Therefore, changes in NtcA levels clearly affect the carbon metabolism and glycogen levels. Thus, NtcA may regulate positively glycogen degradation during the night, and a diurnal analysis of glycogen levels and NtcA regulated genes will help to answer this hypothesis.

1.6 Biotechnological potential of the nitrogen control network

The positive effect of *ntc*A overexpression on growth shows the potential of the nitrogen control network for improving cyanobacterial biomass and production of biomolecules. Under nitrogen depletion, this mutant strain showed a 3-fold increase in the expression levels of a bidirectional hydrogenase (Osanai et al., 2014). This enzyme catalyses both hydrogen (H_2) synthesis and degradation (Tamagnini et al., 2002). H_2 is considered one of the future clean fuels since it is a renewable energy source and its combustion releases high amounts of energy and water vapour instead of greenhouse gases. The use of microorganisms such as cyanobacteria shows economic viability, due to the low production costs compared to electrochemical production (Dutta et al., 2005). Bearing this in mind, considerable research efforts have been expended into increasing cyanobacterial H_2 production to make it an economically viable alternative to the replacement of fossil fuels (Bradley et al., 2013; McCormick et al., 2013).

Changes in PII protein-protein interactions can also lead to increases in the production of cyanobacterial biomolecules. A *Synechocystis* strain carrying a PII variant that constitutively binds and activates NAGK exhibited higher NAGK activity and cyanophycin content during the entire growth cycle. The higher production of cyanophycin did not affect growth when nitrate was used as the nitrogen source. Notably, when transferred to phosphate and potassium limiting conditions, this strain overaccumulated cyanophycin in a range between 47 up to 57% of its dry weight (Watzer

et al., 2015). Cyanophycin is a natural source of polyaspartic acid and a seducing alternative to replace polyacrylic acids, as it is water-soluble and biodegradable. These proprieties allow the use of polyaspartic acid from cyanophycin by the medical and cosmetic sectors for the production of biodegradable plastics, bioflocculants, additives, dispersants and polymeric hydrogels (Schwamborn, 1998; Frommeyer et al., 2014). A second target could be manipulating PII/ACC interaction to affect the carbon flow from acetyl-CoA and increase cellular lipid content. The deletion of PII in *Synechocystis* led to lower acetyl-CoA levels and a small increase in the fatty acids content when cells were grown on ammonium or nitrogen-starved. However, this small increase was only observed at the beginning of the exponential growth (Hauf et al., 2016). In contrast, strains of *Chlamydomonas reinhardtii* with reduced PII levels exhibited a higher number and larger lipids bodies when submitted to nitrogen starvation and only one of these strains showed a small decrease of its growth rate when cultured under nitrogen replete conditions (Zalutskaya et al., 2015). Since PII regulatory role on ACC is very similar between cyanobacteria and chloroplasts from green algae, the metabolic changes observed in *Chlamydomonas* could possibly be translated to cyanobacterial strains and lead to an increase in their lipid production. Compared to green algae, unicellular cyanobacteria have faster growth rates and a higher photosynthetic capacity, converting up to 10% of the solar energy into biomass (Parmar et al., 2011; Yu et al., 2015). Thus, cyanobacteria might be a more economically effective alternative for lipid production to food and biofuel applications. Therefore, further molecular investigations should be carried out for a better understanding of the metabolic aspects associated with the biotechnological applications of cyanobacteria. We anticipate that there is a large untapped potential for metabolic improvements which will lead to an economically sustainable use of cyanobacteria.

1.7 Conclusion

Nowadays, the regulatory role of the cyanobacterial nitrogen control network on carbon and nitrogen metabolism is well understood, with the identification of a large number of genes and proteins under its control (Table 1.1). However, we are probably still missing a number of genes encoding for proteins and metabolic pathways that are controlled by this highly intricated network (Su et al., 2005; Labella et al., 2016; Forcada-Nadal et al., 2017). Among these genes, those related to photosynthetic light reactions, carbon uptake, and assimilation deserve a special attention, since these processes are

providing carbon and energy for cell growth and maintenance. Thus, understanding these regulations and their link with the ultimate control of growth and metabolic composition may allow achieving economic viability of cyanobacteria-based biomass and bioproducts, reducing the production costs for large-scale industrial production.

Chapter 2: General Material and Methods

2.1 Strain selected

We selected the strain *Synechocystis* sp. PCC 6803 (hereafter termed *Synechocystis*) for our study since it is a major cyanobacterial model with very large amount of literature available about its physiology and molecular characteristics. The strain was obtained directly from the French Pasteur Culture Collection (PCC strain) and shows positive phototaxis when grown on BG-11 agar plates (Kanesaki et al., 2012).

2.2 Experimental protocols to evaluate the effect of different nitrogen sources, light and CO_2 levels on growth

Synechocystis was cultivated under two light intensities (50 and 200 µmol photons m^{-2} s^{-1}), two CO_2 concentrations (ambient and 2.5 mM bicarbonate) and three nitrogen sources (nitrate, ammonium and urea), for a total of 10 different growth conditions. All cultures were grown under 18h/6h day/night photoperiod, at a constant temperature of 26° C ± 1° C, and constantly shaken at 120 rpm. To allow complete acclimation to each treatment, *Synechocystis* was cultivated 3 times from log to stationary phase in all growth conditions before analyses were performed.

Cultures were initiated with 3 mL of inoculum in a conical flask (500 mL) containing 147 mL of BG-11 medium (2% v/v) (Rippka et al., 1979), for a starting cell density ranging from 4 to 6 x 10^6 cells mL^{-1}. BG-11_0 (without nitrogen) was supplemented with sodium nitrate (17.7 mM) or ammonium (5 mM) or urea (2.5 mM). Due to the release of CO_2 when urea is hydrolyzed, the same concentration of CO_2 (2.5mM) was added in ammonium and nitrate cultures in the form of sodium bicarbonate ($NaHCO_3$ – hereafter CO_2). To maintain the pH at 7.5 ± 0.5, HEPES (20 mM) was added to the medium.

2.3 Estimation of generation time and cell size

Growth cycle was evaluated by counting cells in a Neubauer chamber (Optik Labor, Germany) at intervals of 24 h until the third consequent day showing no significant increases in cell density (stationary phase). The generation time (Gt) for each treatment was calculated using a regression of the data within the logarithmic growth period. Cell size was determined using the software AxioVision Rel. 4.8.2 (Carl Zeiss, Germany) to measure the diameter of cells from photomicrographs taken using an Olympus microscope (model BX51) with coupled camera (model XC10).

2.4 Experimental protocols to test nutrient limitation, quorum sensing and self-shading

To evaluate the possibility that nutrient depletion and/or quorum sensing affects cell density at stationary phase, *Synechocystis* was cultured for 15 days in the different growth conditions described above, in order to reach stationary phase. Then, all the volume was centrifuged. The pellet was resuspended in a fresh BG-11 medium (new BG-11), and the volume adjusted to 150 mL. The supernatant (old BG-11) was filtered on a nitrocellulose membrane (47 mm x 0.22 µm; Sarstedt) and inoculated with 3 mL of the respective resuspended pellet (Figure 2.1). Cell density was determined and cultures were grown in the same conditions as previously. After four days of cultivation, the cellular density was determined to assess growth rates.

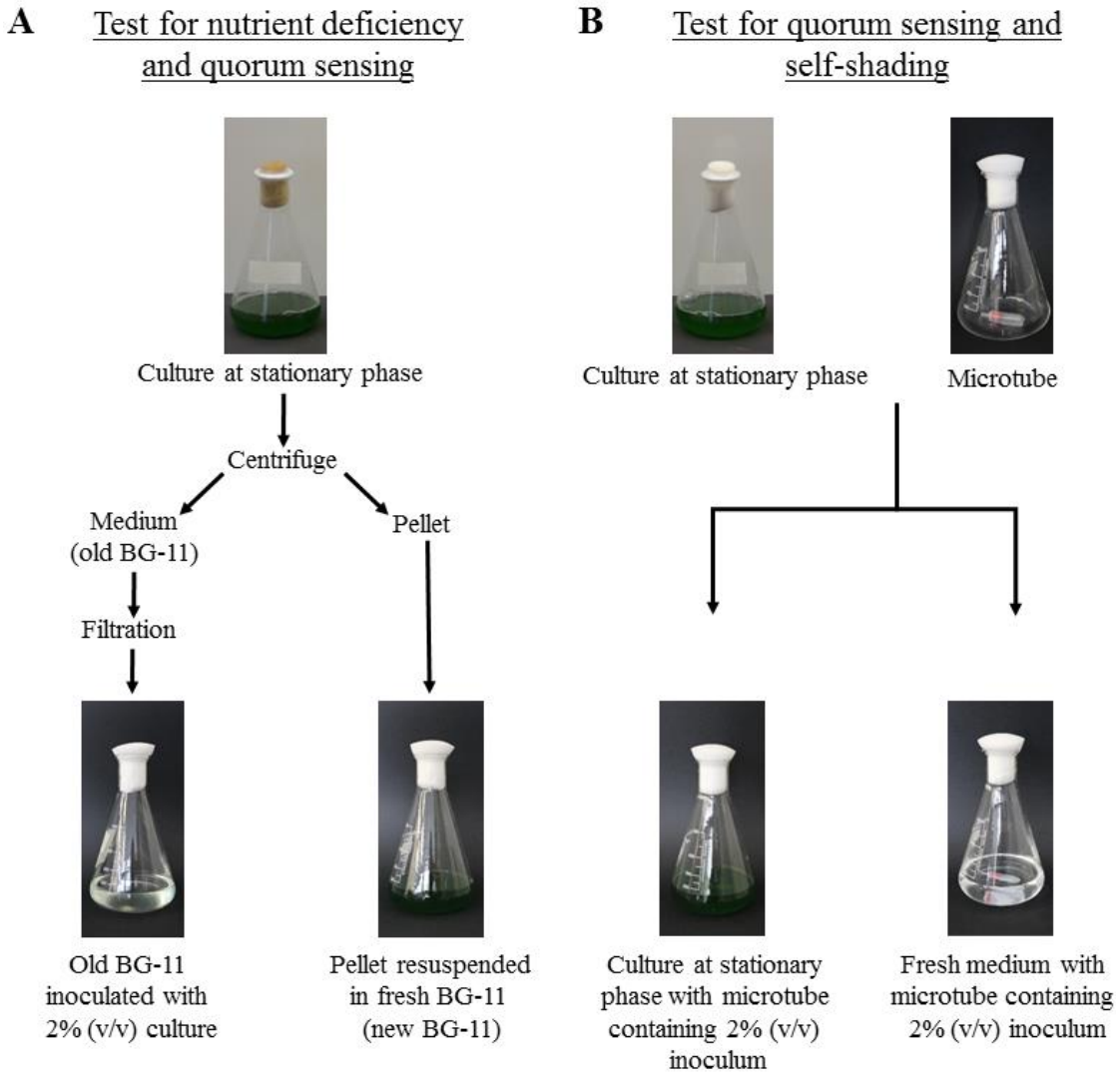

Figure 2-1: Experimental setup for the identification of the processes involved in the onset of stationary phase.

One growth condition, urea as the nitrogen source and the light intensity of 200 µmol photons m^{-2} s^{-1}, for which maximum growth rates were achieved, was selected to evaluate how many growth cycles of *Synechocystis* BG-11 medium could support. *Synechocystis* was cultured for eight days in fresh BG-11 medium until the onset of stationary phase. Subsequently, the entire culture was centrifuged and the supernatant (old BG-11) was filtered and used to grow an inoculum obtained from the resuspended pellet for an additional eight days. At the end of this period, cultures were centrifuged and the supernatant was filtered and reused again (reused old BG-11) to culture for eight days an inoculum obtained from the previous pellet. Finally, cultures were divided into two equal volumes and supplemented in a proportion of 1:1 with fresh BG-11 or water, and kept growing for eight more days.

To test for quorum sensing and light quality/intensity, cultures of *Synechocystis* were cultivated on urea at 50 or 200 µmol photons m^2 s^{-1} for 15 days in order to obtain a culture at saturation phase. For both light intensities, three translucent microtubes (2 mL) were filled with 1.5 mL of BG-11 culture medium (supplemented with urea) containing 2% (v/v) of the respective *Synechocystis* culture. These tubes were glued to the bottom of conical flasks (500 mL) after being sealed with filters (Sigma Iso-Disc™ Filters PFTE-4-4; 4 mm x 0.45 µm). The filters allowed for medium exchange, but without transfer/passage of cells. Then the conical flasks were filled with 150 mL of the respective *Synechocystis* culture at stationary phase or with fresh BG-11 culture medium (Figure 2.1). The flasks were kept shaking in the same light intensity the cultures grew before. After four days of culture, the cellular density in the tubes was determined.

2.5 Experimental protocol to evaluate the effect of cell density on growth

To investigate whether a cell-cell interaction can negatively affect the growth rate of *Synechocystis*, and how the effect is related quantitatively to the cell density of the culture, three different experiments were performed. All the experiments were performed with cultures on urea under 200 µmol photons m^{-2} s^{-1}, where maximum growth rates were achieved.

In the first experiment growth cycle of *Synechocystis* was evaluated in cultures starting with four different initial cell densities: 2 x 10^6, 4 x 10^6, 6 x 10^6 and 2 x 10^7 cells mL^{-1}. The growth cycle and Gt of each treatment were calculated as described before.

In the second experiment, cell density was artificially increased by 10 times during log phase. For that, cultures of 150 mL were grown until a density of 1 x 10^7 cells mL^{-1}

was reached. They were then separated into three groups: (1) cultures were used as controls (i.e. they were maintained growing), (2) cultures were centrifuged and concentrated 10 times to a final density of 1 x 10^8 cells mL^{-1} and (3) cultures were submitted to the same pipetting and centrifuging steps than in group 2, but resuspended without being concentrated (centrifuged controls). The growth of the three groups was then monitored daily as described above.

In the third experiment, *Synechocystis* was grown under fed-batch conditions to evaluate how its growth responds to different dilution rates and cell densities. Firstly, cultures were grown as batch, to assess if their growth properties in a photoreactor were similar to the ones observed previously in conical flasks. Once cultures reached stationary phase with a similar growth cycle as previously, cultures were diluted at a density of 4 x 10^6 cells mL^{-1}. The medium feed pump was started after 24 h, and the medium was fed at a rate of 5.6 mL h^{-1}. This was carried out only during the 18 h of the light period, which meant a daily volume of 100 mL of medium and a daily dilution rate of 0.5 time, as the initial volume of culture in the photoreactor was 200 mL. Every day at the beginning of the light period, the volume of the cultures was readjusted to the initial volume of 200 mL. A second daily dilution rate of 2 times was also tested by adding medium at a rate of 33.4 mL h^{-1} during the light period. Both dilution experiments were also performed with cultures at stationary phase (2 x 10^8 cells mL^{-1}).

2.6 Experimental setups to assess the effect of different culture conditions on growth rate and cell density at stationary phase

Synechocystis was cultivated under 200 µmol photons m^{-2} s^{-1}, in two temperatures (26° C and 32° C), five light regimes (4.5/1.5 light/dark, 6/2 light/dark, 9/3 light/dark, 18/6 light/dark and continuous light), and homogenized under two shaking speeds (60 and 120 rpm) or air bubbling. To allow complete acclimation to each treatment, *Synechocystis* was cultivated 3 times from log to stationary phase in all growth conditions before analyses were performed. For all these conditions, cultures were initiated with 3 mL of inoculum (2% v/v) in a conical flask (500 mL) containing 147 mL of BG-11 medium supplemented with urea, for a starting cell density ranging from 2 to 4 x 10^6 cells mL^{-1}, and kept at the conditions described above. Then, growth performance was evaluated as described previously in section 2.3.

2.7 Experimental protocol to determine the effect of viscosity on growth rate and cell density at stationary phase

Dextran was used as the crowding agent to increase the viscosity of BG-11 supplemented with urea. The viscosity of the medium containing 1%, 2.5%, 5% and 10% of dextran was measured using a Cannon-Fenske viscometer tube (size 25 – Sigma Aldrich Z275263). *Synechocystis* was inoculated in the different medium and cultured 3 times under 50 and 200 µmol photons m^{-2} s^{-1} from log to stationary phase to allow complete acclimation. Then, 3 mL of the acclimated cultures (2% v/v) were inoculated in a conical flask (500 mL) containing 147 mL of BG-11 medium supplemented with urea and different concentrations of dextran (0%, 1%, 2.5%, and 5%), for a starting cell density ranging from 2 to 4 x 10^6 cells mL^{-1}. Growth performance was evaluated as described previously in section 2.3.

2.8 Determination of DNA content and cell volume

The cellular volume and DNA content were analyzed by flow cytometry using an Accuri C6 flow cytometer (BD-bioscience, USA). For DNA content analysis, cells were harvested, stained with SYBR green (Sigma Aldrich S9430) in a proportion of 1:100 and the fluorescence of the SYBR green/DNA complex was determined at 520 nm. Cell area was measured from the same samples based on the forward scatter. From this value, the radius and subsequently the volume was calculated using the formulas:

$$r = \sqrt{\frac{A}{\pi}} \qquad V = \frac{3}{4}\pi r^3$$

Where: A is cellular area, r cellular radius and V cellular volume.

2.9 Biomass, photosynthesis and metabolic profile

All the physiological, metabolic and molecular analyses were performed with samples harvested at day four (log phase) and three days after the onset of the stationary phase, both at the end of the day and night.

2.9.1 Dry Biomass

Biomass was determined by filtering 50 mL of cultures on nitrocellulose membranes, which had been previously weighed. The material was dried at 70 ºC for 48 h, and then maintained for 24 h in a desiccation chamber with blue silica gel. The weight

of the membrane plus biomass was then determined, and the dry biomass weight was obtained by subtraction of the membrane weight.

2.9.2 Oxygen evolution analysis

Photosynthesis was analyzed using non-invasive optical oxygen sensors (PreSens - Germany). Oxygen sensor spots were glued inside the conical flasks (500 mL) so that they were in contact with the culture. The instrument was calibrated using a solution of sodium hydrosulphite to set 0% saturation, and after with distilled water. The analysis was started at the end of the dark period and after obtaining a stable readout of oxygen levels, the light was switched on. Oxygen evolution was then measured for at least 10 min.

2.9.3 Determination of metabolite contents

Samples were collected with a syringe filled with a quenching solution (60% v/v methanol in water) precooled to <-20°C. The solutions were then quickly transferred to centrifuge tubes stored in an ice bath. Each quenched sample was centrifuged for 20 min at 4000 rpm (Young et al., 2011). Pellets were subjected to hot ethanol extraction (Cross et al., 2006). The soluble fraction was used for the determination of chlorophyll *a* (Ritchie, 2006), and total amino acid contents (Schippers et al., 2008). In the insoluble fraction protein and glycogen contents were determined according to Lowry et al. (1951) and Hendriks et al. (2003), respectively. Total soluble sugars were determined as described previously (Dubois et al., 1956). The determination of a large set of primary metabolites was performed by gas chromatography coupled with mass spectrometry (GC-MS) (Krall et al., 2009), using palatinose as an internal standard. For cyanophycin and phycocyanin determination, samples were sonicated (40% amplitude for 4 min) and subsequently centrifuged for 40 min at 4000 rpm. Phycocyanin was determined from the supernatant (Tandeau de Marsac, 1977), and cyanophycin was extracted from the remaining pellet as previous described (Burnat et al., 2014), and determined by Sakaguchi reaction (Messineo, 1966).

2.10 Transformation

2.10.1 Construction of plasmids containing disrupted *sigF* and *pilA1A2* genes

DNA was extracted from *Synechocystis* as described by Kim et al. (2012). The sequence of *sigF* (slr1564), *pilA1* (sll1694) and *pilA2* (sll1695) genes were obtained from the Cyanobase website (http://genome.microbedb.jp/cyanobase/). For *sigF* disruption, a

1.9-kbp PCR product containing the 3' part of slr1563, slr1564 (the *sigF* gene), slr1565 and 5' part of slr1566 was amplified from the genomic DNA isolated from *Synechocystis* using the Q5 High-fidelity DNA polymerase kit (NEB), the forward primer RS017 (5'-GGATCTGTGGTCTGGCAATGGC-3') and the reverse primer RS018 (5'-CAAATCA GGCA GGAGATTGCGG-3'), following the manufacturer's instructions. This sequence was cloned into pMiniT vector using a PCR Cloning Kit (NEB), resulting in pMini-*sigF*. Then, a 1.2-kbp PCR product containing Tn903-derived kanamycin resistance (Km^R) gene was amplified from pUC4K using MyTaq™ Red Mix (Bioline), the forward primer RS021 (5'-gatcggtaccgatatcGGGAAAGCCACGTTGTGTCTC-3') and the reverse primer RS022 (5'-cgatctgcagCTGAGGTCTGCCTCGTGAAG-3'), according to the manufacturer's instructions. This sequence was digested by *Eco*RV and *Pst*I and inserted into *Pst*I-*Stu*I site of pMini-*sigF*. The resultant plasmid was designated p*sigF*::Km^R (Figure 2.2A).

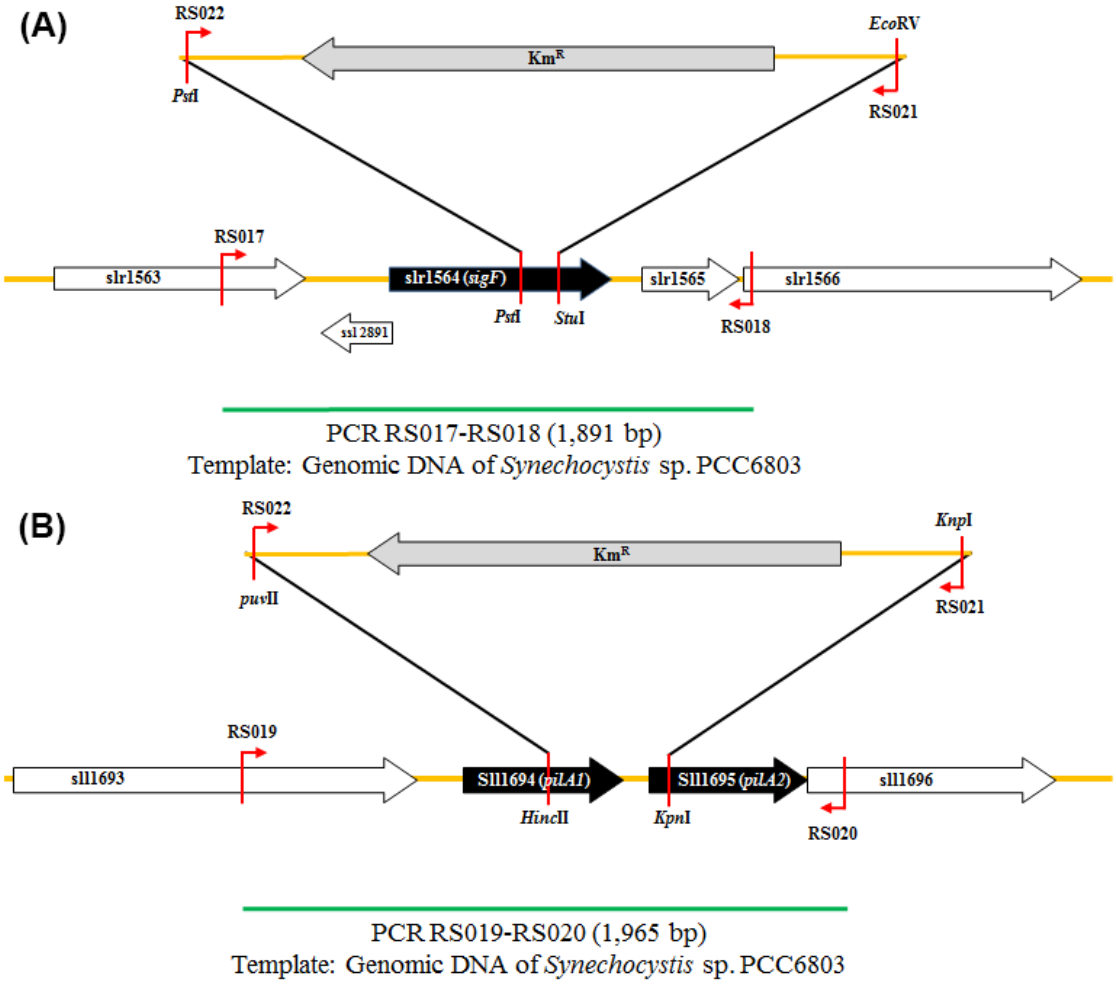

Figure 2-2: p*sigF*::Km^R (A) and p*pilA1A2*::Km^R (B) constructs.

For *pilA1A2* disruption, a 2.0-kbp fragment of genomic DNA containing the 3' part of sll1693, the tandemly arranged *pilA1* and *pilA2* genes (sll1694 and sll1695) and 5' part of sll1696 was obtained using the forward primer RS019 (5'-TGGAGCTAATCAGCAT GGTGGAC-3') and the reverse primer RS020 (5'-TCAGTCAAAGACTGCCCTGGAG-3') and cloned into pMiniT, resulting in pMini-*pilA1A2*. The 1.2-kbp PCR product containing Km^R gene was digested by *Kpn*I and *Pvu*II and inserted into *Hinc*II-*Kpn*I site of pMini-*pilA1A2*, resulting in p*pilA1A2*::Km^R (Figure 2.2B).

2.10.2 Transformation of *Synechocystis*

Synechocystis was transformed by homologous recombination. Cells were grown on BG-11 supplemented with sodium nitrate (17.7 mM) under a light intensity of 50 µmol photons m^{-2} s^{-1}, 18h/6h day/night photoperiod, at a constant temperature of 26° C ± 1° C, and constantly shaken at 120 rpm until the culture reached mid-logarithmic phase (OD ≅ 0.8; cell density of 4.6 $x10^7$ cells mL^{-1}). The entire volume (150 mL) was centrifuged for 20 min at 4000 rpm and the pellet was resuspended in 1.5 mL. Then, 0.5 µg of p*sigF*::Km^R or p*pilA1A2*::Km^R was added in 100 µL of concentrated culture and incubated overnight at 28° C under low light (20 – 30 µmol photons m^{-2} s^{-1}). The following day, cells were plated on BG-11 agar supplemented with sodium nitrate and incubated at 28° C under low light. After two days, one side of the agar plates was supplemented with kanamycin (5 µg/mL), and the kanamycin resistant colonies were transferred to new plates containing kanamycin (10 µg/mL). For complete segregation of *sigF* null mutant (Δ*sigF*) and *pilA1A2* null mutant (Δ*pilA1A2*), cells from the kanamycin resistant colonies were transferred to agar plates with increasing concentration of kanamycin. To confirm that all copies of the chromosome contained interrupted sequences of *sigF* and *pilA1A2* with the kanamycin cassette, DNA was isolated from individual colonies for PCR analyses.

2.10.3 Mobility assay and growth characterization

The phototaxis/mobility assay was performed by streaking cells from the kanamycin resistant colonies of Δ*sigF* and Δ*pilA1A2* on BG-11 agar plates and growing them under unidirectional light. For growth rate analysis, cells from three Δ*sigF* and Δ*pilA1A2* colonies were transferred to liquid BG-11 supplemented with sodium nitrate (17.7 mM) and cultured three times under a light intensity of 50 µmol photons m^{-2} s^{-1}, 18h/6h day/night photoperiod, at a constant temperature of 26° C ± 1° C, and constantly shaken at 120 rpm, allowing their complete acclimation. Then, 3 mL of the acclimated

cultures (2% v/v) were inoculated in a conical flask (500 mL) containing 147 mL of BG-11 medium supplemented with urea, for a starting cell density ranging from 2 to 4 x 10^6 cells mL^{-1}, and kept at the conditions described above. Finally, their growth performance and cell size were evaluated as described previously in section 2.3.

2.11 Gene expression analysis

RNA was extracted according to Kim et al. (2006), applying the freeze-thaw step described by Kim et al. (2012) before disrupting the cells in a Tissuelyser (Qiagen). RNA concentration was quantified spectrophotometrically at 260 nm, and its integrity was checked by electrophoresis on a denaturing agarose gel (1.6% m/v) (Goda and Minton, 1995). Due to the presence of DNA, samples were treated with RNase-free DNase I (Sigma) according to the manufacturer's instructions. For cDNA synthesis, 1000 ng of total RNA was reverse transcribed with SensiFAST cDNA Synthesis Kit (Bioline) in a final volume of 20 µL, following the manufacturer's instructions. Subsequently, cDNA was diluted 3 times and stored at -20° C. The RT-qPCRs were performed on 96-well PCR plates covered with a sealing tape (Thermo), using SensiMix™ SYBR® No-ROX Kit (Bioline), following the manufacturer's instructions. To calculate the relative expression levels of *ntcA* (nitrogen control factor of cyanobacteria), *pII* (nitrogen regulatory protein PII), *ftsZ* (cell division protein FtsZ), *pilA1* (pilin polypeptide PilA1), *pilA2* (pilin polypeptide PilA2) and *sigF* (Cyanobacterial SigF-related sigma factor), *rnpB* (RNA subunit of ribonuclease P) was selected as the reference gene, as previously described (Pinto et al., 2012).

2.12 Experimental design and statistical analysis

The experiments were performed and analyzed according to a randomized block design (RBD) with three replications. The data obtained at the end of the day and night were subjected to Student's *t* test at 5% probability. Analysis of variance (ANOVA, $P < 0.05$) was performed to compare the data obtained for the different growth conditions, and the means were compared by Tukey's test at 5% probability, using the lowest value as a reference. All these analyses were performed with the software package SPSS 22 Windows & Macintosh (Armonk/New York). Finally, the results obtained were independently analyzed via Spearman's correlation, using Excel 2013 (Microsoft).

Chapter 3: A Novel Mechanism, Linked to Cell Density, Largely Controls Cell Division in *Synechocystis*

3.1 Introduction

Cyanobacteria were the first organisms on Earth that performed oxygenic photosynthesis, and nowadays they are widespread on a variety of terrestrial and aquatic habitats, showing extensive metabolic, physiological and morphological diversity (Tomitani et al., 2006; Beck et al., 2012; Schirrmeister et al., 2013). This diversity among cyanobacteria has been related to their capability to adapt to series of changes which occurred on earth, affecting the availability of the atmospheric oxygen (O_2), light, carbon dioxide (CO_2) and reduced nitrogen (Catling et al., 2001; Herrero et al., 2001; Kasting and Siefert, 2002; Kuhl et al., 2005; Muramatsu and Hihara, 2011; Hagemann et al., 2016).

Synechocystis sp. PCC 6803 (hereafter termed *Synechocystis*) is one of the cyanobacterial species commonly used for metabolic and genetic studies. It is easy to culture under phototrophic, mixotrophic and heterotrophic conditions, its entire genome is sequenced, and exhibits natural competence for incorporation of exogenous DNA (Kanesaki et al., 2012; Yu et al., 2013). Like all photosynthetic organisms, the physiology and cell cycle of *Synechocystis* is affected both by light availability and intensity (Yang et al., 2010; Schuurmans et al., 2015). Light harvesting is performed by phycobilisomes composed of a core of allophycocyanins and branches of phycocyanin (Mullineaux, 2008; Arteni et al., 2009). The light energy is transferred from the phycobilisomes to chlorophyll *a* present in the reaction centers of photosystems I (PSI) and II (PSII) (Liu et al., 2013). These transfers lead to the generation of reducing power which supplies metabolic processes such as the Calvin-Benson cycle and nitrogen uptake and reduction (Valladares et al., 2002; Flores et al., 2005). The efficiency of CO_2 fixation and assimilation is (at least partially) under the control of a carbon concentration mechanism (CCM), which increases the CO_2 concentration around the Rubisco catalytic site (Price et al., 1998), allowing it to operate close to its maximal velocity (V_{max}) (Badger et al., 2006). *Synechocystis* can uptake and metabolize different nitrogen sources (nitrate, nitrite, ammonium, urea and some amino acids) (Quintero et al., 2000; Valladares et al., 2002; Flores et al., 2005; Muro-Pastor et al., 2005). Intriguingly, the control of the expression and activity of transporters and enzymes related to nitrogen metabolism is regulated by a complex network involving 2-oxoglutarate, NtcA (nitrogen control factor of cyanobacteria), PII (nitrogen regulatory protein PII) and PipX (PII interacting protein X) (Alfonso et al., 2001; Herrero et al., 2001; Llácer et al., 2010; Zhao et al., 2010; Espinosa et al., 2014; Lüddecke and Forchhammer, 2015).

In photo-bioreactors, *Synechocystis* can typically achieve growth rates ranging from 1.7 to 2.5 divisions day^{-1}, i.e. doubling times of between 14.1 and 9.6 h (Kim et al., 2011). Faster doubling times of 6 and 5.6 h were reported by Hihara et al. (2001) and Zavřel et al. (2015), respectively, however, in the case of the latter study, these division rates could not be maintained for more 120 h. Many studies have attempted to identify growth limiting factors in *Synechocystis* (e.g. nutrients and light) (Kim et al., 2011; Lea-Smith et al., 2014; Burnap, 2015; Touloupakis et al., 2015; van Alphen and Hellingwerf, 2015). Understanding of the factors controlling the limitation of *Synechocystis* growth would facilitate the use of this strain as a cell factory (Yu et al., 2013) for the production of biomass (Joseph et al., 2014), pigments (Sekar and Chandramohan, 2008), secondary metabolite natural products (Frommeyer et al., 2014), biofuel (Dexter and Fu, 2009; Baebprasert et al., 2011; Liu et al., 2011) and other high value compounds.

The commercialisation of cyanobacteria-based biomass and biomolecules still requires optimization for sustainable economic viability (Schenk et al., 2008; Brennan and Owende, 2010; Wijffels et al., 2013). One recently adopted approach in this view is the use of low-cost sources of CO_2, nutrients and water (Markou and Georgakakis, 2011; Slade and Bauen, 2013; Iijima et al., 2015). In this chapter, we grew *Synechocystis* in various growth conditions, using three different nitrogen sources, in combination with two light intensities and two CO_2 concentrations. Urea is seemingly a potent source of nitrogen supporting the growth of *Synechocystis*, as it promoted high cell division rates and is less costly than nitrate and ammonium. That said, after four days of culture, growth was inhibited for all conditions tested, and this inhibition was not related to a metabolic limitation. Indeed, we observed an uncoupling of photosynthesis and growth, leading to the accumulation of unused reserves in the cells, and even their release to the culture medium. We further investigated the reasons behind this non-metabolic growth limitation and conclude that nutrient limitation and quorum sensing are not responsible for the decrease in growth rates during the log phase and for the onset of the stationary phase. Our data also suggest that self-shading is not responsible for the growth limitation. We hypothesise that *Synechocystis* may be able to sense the gradual increase of cell density occurring in batch cultures via cell-cell interaction, leading to a gradual decrease of division rate until the onset of stationary phase.

3.2 Results

3.2.1 Rates of cell division peak at start of log phase and then gradually decrease

The growth cycle and Gt of *Synechocystis* varied in response to the nitrogen source, light intensity and CO_2 concentration (Figure 3.1; Table 3.1).

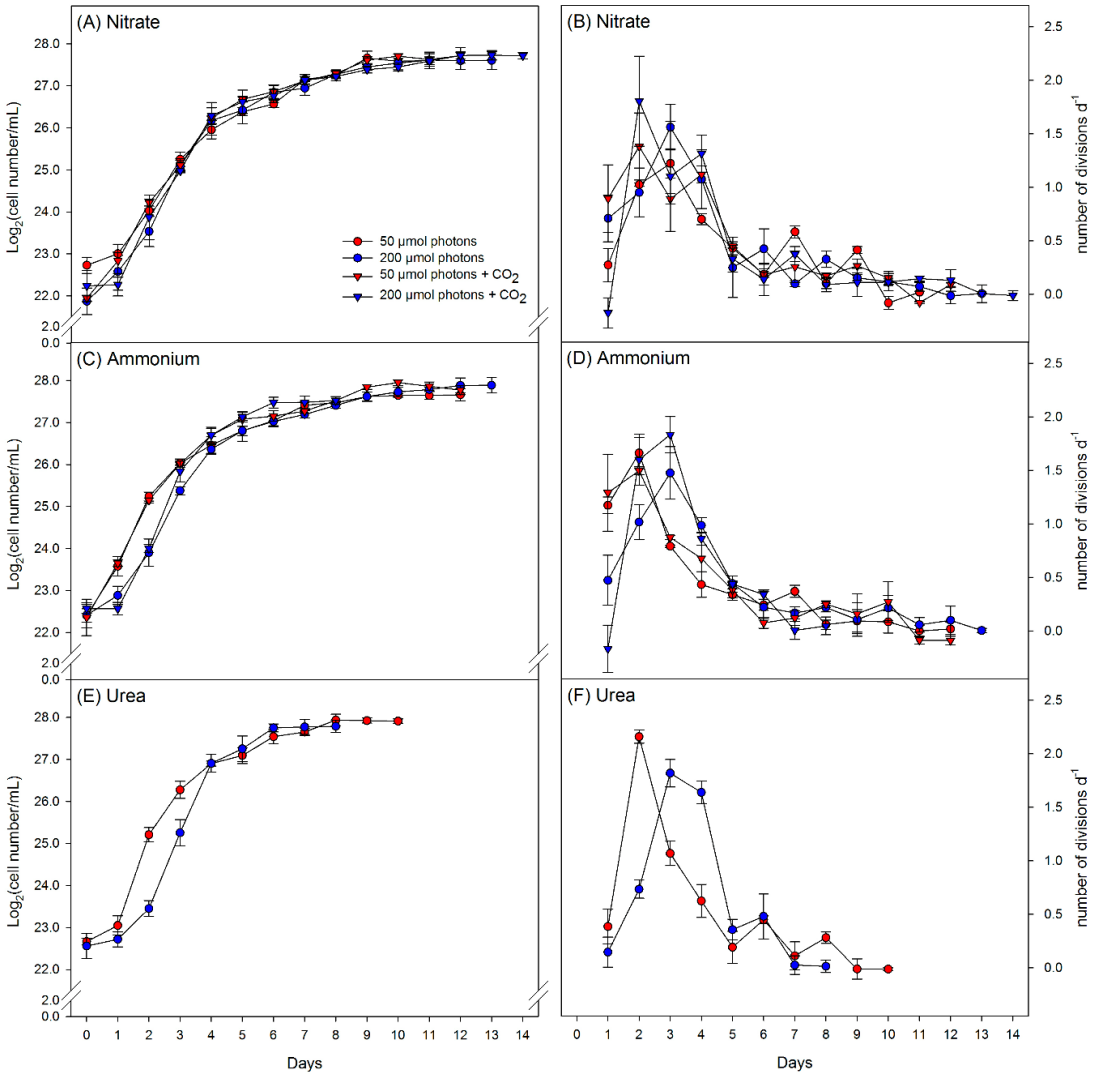

Figure 3-1: *Synechocystis* growth cycles.
Growth curves represented on a Log(cell) basis (**A**, **C** and **E**) and daily number of division (**B**, **D** and **F**) of *Synechocystis* grown on ten different culture conditions. Cultures on nitrate (**A-B**), ammonium (**C-D**) and urea (**E-F**) were submitted to two different light intensities, 50 µmol photons m^{-2} s^{-1} (red) and 200 µmol photons m^{-2} s^{-1} (blue). Cultures grown on ammonium and nitrate were supplemented with 2.5 mM bicarbonate (triangles), or not supplemented (circles).

A lag phase was not observed when cells were grown in the presence of ammonium under moderate light intensity (ML; 50 µmol photons m^{-2} s^{-1}), nitrate under ML with CO_2 supplementation, and nitrate under high light intensity (HL; 200 µmol photons m^{-2} s^{-1}; Figure 3.1A-D). The highest number of divisions per day were typically achieved at days two or three and gradually decreased afterwards (Figure 3.1B, D and F).

Table 3-1: Generation time of *Synechocystis* grown under ten culture conditions.

Culture	Generation time	
	ML	**HL**
Nitrate	21.41 ± 1.26 **fg**	20.15 ± 1.63 **efg**
Ammonium	16.95 ± 0.57 **abcd**	19.30 ± 0.95 **def**
Urea	14.88 ± 0.61 **abc**	13.89 ± 0.20 **a**
Nitrate + CO_2	22.40 ± 0.17 **g**	17.91 ± 0.37 **cde**
Ammonium + CO_2	17.44 ± 2.26 **bcde**	14.70 ± 0.44 **ab**

Generation time (hours) was calculated using a regression of the data within the logarithmic growth period at 50 µmol photons m^{-2} s^{-1} (**ML**) and 200 µmol photons m^{-2} s^{-1} (**HL**), with or without addition of CO_2. Values represent means ± standard deviation (n = 3). Means followed by the same letter do not differ by 5% probability (Tukey's test).

The cultures reached a stable stationary phase after 8 to 14 days (Figure 3.1). Curiously, the stationary phase occurred at similar cell densities (2.1 to 2.6 x 10^8; Figure 3.1; Table 3.2), despite a large variation in the duration of the growth cycles in nine of the ten growth conditions studied.

Table 3-2: Cell number in log and stationary phases

Culture	Log	
	ML	**HL**
Nitrate	6.51 x10^7 ± 5.90 x10^6 **a**	7.79 x10^7 ± 2.41 x10^7 **ab**
Ammonium	9.30 x10^7 ± 1.29 x10^7 **abc**	8.64 x10^7 ± 7.11 x10^6 **ab**
Urea	1.25 x10^8 ± 5.29 x10^6 **c**	1.27 x10^8 ± 1.84 x10^7 **c**
Nitrate + CO_2	7.87 x10^7 ± 2.81 x10^6 **ab**	8.24 x10^7 ± 1.08 x10^7 **ab**
Ammonium + CO_2	1.09 x10^8 ± 1.15 x10^7 **bc**	1.09 x10^8 ± 1.48 x10^7 **bc**
Culture	**Stationary**	
	ML	**HL**
Nitrate	2.14 x10^8 ± 2.27 x10^7 **ab**	2.10 x10^8 ± 3.25 x10^7 **ab**
Ammonium	2.13 x10^8 ± 2.11 x10^7 **ab**	2.51 x10^8 ± 2.62 x10^7 **ab**
Urea	2.57 x10^8 ± 2.39 x10^7 **b**	2.34 x10^8 ± 1.79 x10^7 **ab**
Nitrate + CO_2	2.21 x10^8 ± 1.13 x10^7 **ab**	2.23 x10^8 ± 2.86 x10^7 **ab**
Ammonium + CO_2	2.59 x10^8 ± 1.28 x10^7 **b**	1.93 x10^8 ± 1.28 x10^7 **a**

Cell number (cell number mL^{-1}) determined on the fourth day of culture (log phase) and three days after the onset of the stationary phase at 50 µmol photons m^{-2} s^{-1} (**ML**) and 200 µmol photons m^{-2} s^{-1} (**HL**), with or without addition of CO_2. Values represent means ± standard deviation (n = 3). Statistics are as described for Table 3.1.

In order to confirm whether cells were in the stationary phase, we analysed the expression of *ftsZ* gene, which encodes the cell division protein FtsZ (Figure 3.2). The

relative *ftsZ* expression levels of the cells at stationary phase, at the end of the day (ED), were 4 to 10 times lower than the levels observed for cells in log phase (Figure 3.2A). In addition, as observed previously (Mori and Johnson, 2001), the *ftsZ* expression levels were very low at the end of the night (EN), with little differences between the growth stages (Figure 3.2B), thus confirming that cells do not divide at night.

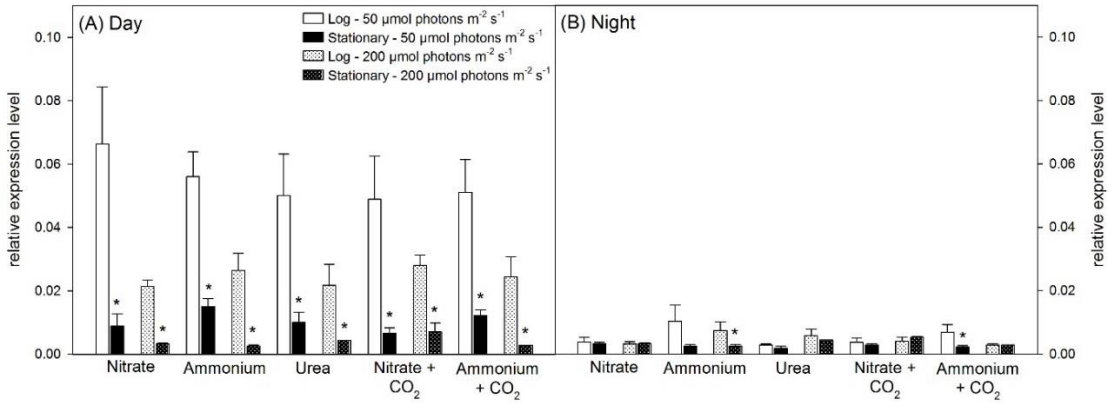

Figure 3-2: Relative expression levels of *ftsZ*.
Levels at the end of the day (A) and at the end of the night (B) on the fourth day of culture (log phase – white bars) and three days after the onset of the stationary phase (black bars). Values represent the mean ± standard deviation (n = 3). The asterisk represents a significant difference between samples from the same growth conditions harvested in log and stationary phases ($P < 0.05$, paired Student's *t* test).

The gradual decrease in the number of division per day observed from the third or fourth day of culture and the fact that cultures reached stationary phase with comparable cell densities regardless of differences in nitrogen source, light intensity and CO_2 concentration raised questions about a similar metabolic limitation occurring for all these growth conditions. We hypothesised it could be due to: (1) nutrient starvation; (2) a reduction in light intensity or quality due to high cell density (self-shading); (3) or a regulatory limitation of growth due to quorum sensing. In order to test these hypotheses, we analysed the photosynthetic rates, cellular metabolic contents, and evaluated the possibilities of nutrient depletion, quorum sensing and self-shading.

3.2.2 Metabolic and physiological traits during the log phase

The varied growth conditions did not affect the *Synechocystis* cell size (Table 3.3). Then, as our aim was to document the metabolic contents of the cells and relate this information to growth rates, the data were normalised on a per cell basis and not on a biomass basis. This method avoids biases due to specific growth conditions leading to cells containing more metabolites and then being heavier. Indeed, expressing our data on a biomass basis would have wrongly led to the conclusion of higher growth rates for some

growth conditions whilst in fact it could just be caused by cells accumulating more metabolites.

Table 3-3: Cell size in log and stationary phases

Culture	Log		Stationary	
	ML	**HL**	**ML**	**HL**
Nitrate	4.85 ± 0.45 **ab**	5.03 ± 0.40 **ab**	5.15 ± 0.31 **ab**	4.88 ± 0.51 **a**
Ammonium	4.98 ± 0.50 **ab**	5.03 ± 0.51 **ab**	5.32 ± 0.35 **ab**	5.03 ± 0.48 **ab**
Urea	4.75 ± 0.54 **a**	5.03 ± 0.40 **ab**	5.36 ± 0.40 **ab**	4.95 ± 0.38 **a**
Nitrate + CO_2	4.93 ± 0.41 **ab**	5.08 ± 0.49 **ab**	5.32 ± 0.42 **ab**	5.00 ± 0.47 **ab**
Ammonium + CO_2	5.12 ± 0.37 **ab**	5.07 ± 0.40 **ab**	5.05 ± 0.45 **ab**	4.98 ± 0.37 **ab**

Cell size (µm) determined on the fourth day of culture (log phase) and three days after the onset of the stationary phase at 50 µmol photons m^{-2} s^{-1} (**ML**) and 200 µmol photons m^{-2} s^{-1} (**HL**), with or without addition of CO_2. Values represent the mean ± standard deviation (n = 3). Statistics are as described for Table 3.1.

The rate of photosynthesis, as estimated by the determination of O_2 release, varied between the treatments (Table 3.4). Under HL, cells grown in the presence of nitrate supplemented with CO_2, ammonium and urea exhibited the highest photosynthetic rates (Table 3.4). In addition, photosynthetic rates of cells cultured with ammonium and urea showed a light effect, with an increase of almost 60% when grown under HL (Table 3.4). By contrast, nitrate cultures displayed similar photosynthetic rates and were not affected by increases in light intensity or CO_2 supplementation (Table 3.4).

Table 3-4: Photosynthetic rate in log phase.

Culture	Photosynthetic rate	
	ML	**HL**
Nitrate	$6.06 \times 10^{-10} \pm 2.50 \times 10^{-11}$ **def**	$5.44 \times 10^{-10} \pm 8.00 \times 10^{-11}$ **cde**
Ammonium	$4.61 \times 10^{-10} \pm 6.18 \times 10^{-11}$ **abcd**	$7.23 \times 10^{-10} \pm 4.69 \times 10^{-11}$ **f**
Urea	$3.89 \times 10^{-10} \pm 2.92 \times 10^{-11}$ **ab**	$6.20 \times 10^{-10} \pm 7.56 \times 10^{-11}$ **ef**
Nitrate + CO_2	$5.29 \times 10^{-10} \pm 2.92 \times 10^{-11}$ **bcde**	$5.72 \times 10^{-10} \pm 7.41 \times 10^{-11}$ **def**
Ammonium + CO_2	$4.01 \times 10^{-10} \pm 2.47 \times 10^{-11}$ **abc**	$3.18 \times 10^{-10} \pm 3.64 \times 10^{-11}$ **a**

Photosynthetic rate (µmol oxygen L^{-1} s^{-1} $Cell^{-1}$) determined on the fourth day of culture (log phase) at 50 µmol photons m^{-2} s^{-1} (**ML**) and 200 µmol photons m^{-2} s^{-1} (**HL**), with or without addition of CO_2. Values represent means ± standard deviation (n = 3). Statistics are as described for Table 3.1.

After four days of culture, the cellular dry weight (hereafter termed biomass) was higher under ML than HL for all the treatments, except for ammonium without CO_2 supplementation for which the biomass did not differ (Table 3.5).

Table 3-5: Cellular dry weight in log phase.

Culture	Cellular dry weight	
	ML	**HL**
Nitrate	$1.90 \times 10^{-9} \pm 9.21 \times 10^{-11}$ **e**	$1.05 \times 10^{-9} \pm 7.81 \times 10^{-11}$ **bc**
Ammonium	$9.41 \times 10^{-10} \pm 2.88 \times 10^{-11}$ **b**	$9.68 \times 10^{-10} \pm 4.38 \times 10^{-11}$ **bc**
Urea	$1.18 \times 10^{-9} \pm 1.69 \times 10^{-10}$ **cd**	$8.50 \times 10^{-10} \pm 4.82 \times 10^{-11}$ **ab**
Nitrate + CO_2	$1.87 \times 10^{-9} \pm 8.07 \times 10^{-11}$ **e**	$1.06 \times 10^{-9} \pm 8.75 \times 10^{-11}$ **bc**
Ammonium + CO_2	$1.36 \times 10^{-9} \pm 2.84 \times 10^{-11}$ **d**	$6.89 \times 10^{-10} \pm 3.70 \times 10^{-11}$ **a**

Cellular dry weight (mg dry weight $cell^{-1}$) determined on the fourth day of culture (log phase) at 50 µmol photons m^{-2} s^{-1} (**ML**) and 200 µmol photons m^{-2} s^{-1} (**HL**), with or without addition of CO_2. Values represent the mean ± standard deviation (n = 3). Statistics are as described for Table 3.1.

Chlorophyll *a* (hereafter termed chlorophyll) content was affected by nitrogen source and mostly by light intensity. In general, its content was higher under ML, in particular for cultures supplemented with nitrate (Figure 3.3A). The highest concentrations of phycocyanin were registered for cultures grown in the presence of nitrate and urea under ML, and the lowest for cultures grown in the presence of ammonium and nitrate under HL (Figure 3.3B). Levels of total soluble sugars were almost constant among the different growth conditions (Figure 3.3C). As previously documented (Mikkat et al., 1997), sucrose levels were below the level of detection with the exception of cells grown on nitrate in the presence or absence of CO_2 under ML (Tables 3.6 and 3.7). Total soluble sugars were also detected in the growth medium; however, their concentrations were similar for almost all treatments (Figure 3.3D). Glycogen amounts at ED were relatively constant for all growth conditions and only cells grown under HL and supplemented with CO_2 accumulated significantly more glycogen, independently of the nitrogen source (ammonium or nitrate; Figure 3.3E). A significant amount of the glycogen accumulated at ED was used during the night for all growth conditions (from 17.1 % to 66.6%), except for cells grown in the presence of nitrate with ML (Figure 3.3E). Levels of total soluble amino acids were very stable in cells grown under ML and did not exhibit diurnal variation. In contrast, their levels showed large variations between the treatments under HL (Figure 3.3F). The cellular protein content did not vary diurnally and was relatively similar between ammonium and urea growth conditions. Cells grown on nitrate displayed significantly higher protein content (Figure 3.3G). Cyanophycin levels did not vary diurnally and showed small variations between all growth conditions (Figure 3.3H).

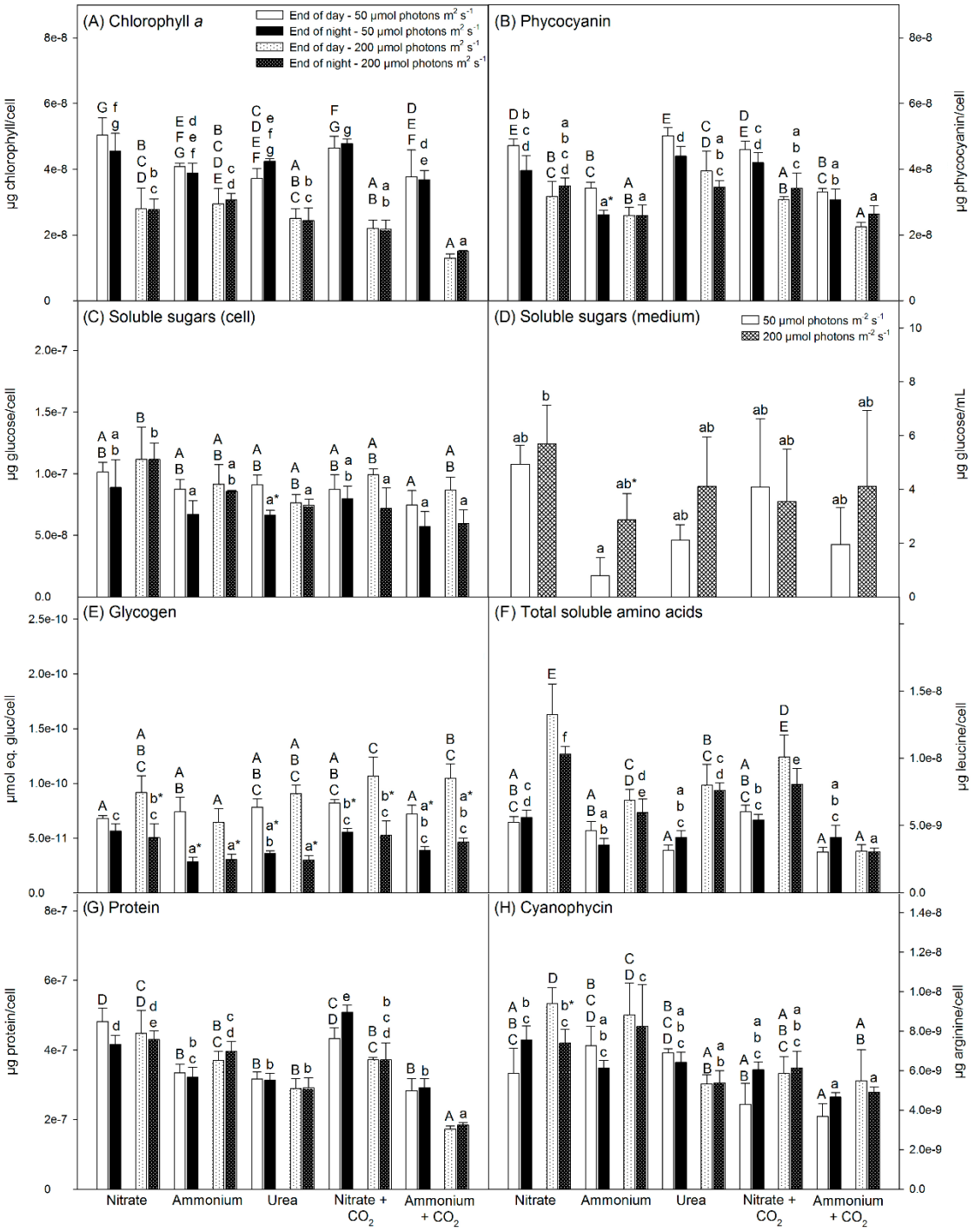

Figure 3-3: Pigments and metabolites determined on the fourth day of culture (log phase). Chlorophyll *a* (A), phycocyanin (B), total soluble sugars (cell) (C), total soluble sugars (medium) (D), glycogen (E), total soluble amino acids (F), proteins (G) and cyanophycin (H). Values represent the mean ± standard deviation (n = 3). Means followed by the same letter do not differ by 5% probability (Tukey's test). Capital letter show differences among samples harvested in the end of the day, and small letters in the end of the night. The asterisk represents a significant difference between samples from the same growth conditions harvested at the end of day and end of night ($P < 0.05$, paired Student's *t* test). For (D) the asterisk represents a significant difference between samples grown at 50 µmol photons m^{-2} s^{-1} and 200 µmol photons m^{-2} s^{-1} for a given nutrient growth condition ($P < 0.05$, unpaired Student's *t* test).

Table 3-6: Primary metabolites determined by gas chromatography coupled with mass spectrometry (GC-MS) at the end of the day on the fourth day of culture (log phase).

Conditions	Sucrose	Maltose	Citrate	Isocitrate	Fumarate	Malate	Glutamate	Ornithine	Aspartate	Arginine	Proline	Leucine	Isoleucine
N50	0.00073	0.00303	0.03380	0.00686	0.02180	0.02090	0.61390	0.00138	0.01041	0.00062	0.02420	0.07320	0.02140
A50	0.00000	0.00388	0.02240	0.00827	0.00132	0.00027	0.18820	0.00079	0.00406	0.00058	0.00738	0.01260	0.00279
U50	0.00000	0.00284	0.00864	0.00798	0.00474	0.00198	0.11770	0.00037	0.00295	0.00045	0.00628	0.02390	0.00633
N50CO_2	0.00082	0.00143	0.00922	0.00868	0.01980	0.01040	0.39200	0.00072	0.02304	0.00038	0.01340	0.02880	0.01020
A50CO_2	0.00000	0.00157	0.00759	0.00296	0.00360	0.00195	0.09100	0.00034	0.00174	0.00027	0.00410	0.00597	0.00140
N200	0.00000	0.00015	0.00332	0.00000	0.00000	0.00000	0.00991	0.00009	0.00310	0.00008	0.00269	0.01710	0.00696
A200	0.00000	0.00014	0.00000	0.00000	0.00000	0.00000	0.00000	0.00006	0.00000	0.00000	0.00187	0.01060	0.00392
U200	0.00000	0.00011	0.00013	0.00000	0.00000	0.00000	0.00000	0.00000	0.00000	0.00022	0.00172	0.00694	0.00310
N200CO_2	0.00000	0.00094	0.01120	0.00000	0.00863	0.00678	0.13540	0.00058	0.01181	0.00056	0.01400	0.05360	0.02270
A200CO_2	0.00000	0.00078	0.00186	0.00097	0.00288	0.00130	0.00000	0.00043	0.00560	0.00047	0.00982	0.03380	0.01040
Conditions	**Valine**	**Alanine**	**Glycine**	**Serine**	**Tyrosine**	**Lysine**	**Tryptophan**	**Phenylalanine**	**Glycolate**	**Glycerate**	**Nicotinate**	**Nicotinamide**	**Alpha-tocopherol**
N50	0.11860	0.01300	0.02890	0.04390	0.02570	0.00558	0.00368	0.00935	0.00148	0.00137	0.00098	0.02990	0.03080
A50	0.01420	0.00198	0.00444	0.01680	0.00928	0.00437	0.00124	0.00211	0.00044	0.00056	0.00065	0.01110	0.02370
U50	0.01990	0.00174	0.00404	0.01430	0.00914	0.00336	0.00128	0.00263	0.00126	0.00141	0.00051	0.01170	0.01890
N50CO_2	0.04980	0.00817	0.01130	0.02310	0.01150	0.00229	0.00122	0.00427	0.00289	0.00330	0.00147	0.01850	0.02060
A50CO_2	0.00661	0.00041	0.00396	0.01080	0.00448	0.00250	0.00066	0.00100	0.00087	0.00098	0.00079	0.01070	0.01410
N200	0.01310	0.00027	0.00163	0.00290	0.00247	0.00055	0.00134	0.00208	0.00050	0.00017	0.00035	0.00112	0.01210
A200	0.00650	0.00000	0.00000	0.00103	0.00085	0.00017	0.00093	0.00142	0.00009	0.00000	0.00025	0.00038	0.01710
U200	0.00529	0.00000	0.00012	0.00116	0.00070	0.00011	0.00085	0.00095	0.00014	0.00009	0.00019	0.00027	0.01260
N200CO_2	0.05980	0.01710	0.01070	0.01910	0.01640	0.00190	0.00459	0.00791	0.00085	0.00071	0.00040	0.00331	0.01410
A200CO_2	0.04120	0.02550	0.00825	0.01300	0.01490	0.00152	0.00225	0.00368	0.00031	0.00008	0.00028	0.00247	0.01020

Primary metabolites levels (relative units to internal palatinose standard) at the end of the day of the fourth day of culture (log phase) of *Synechocystis* cells grown under different nitrogen sources (A- ammonium; N- nitrate; U- urea), light intensities (50- 50 µmol photons m^{-2} s^{-1}; 200- 200 µmol photons m^{-2} s^{-1}) and with or without CO_2 supplementation.

Table 3-7: Primary metabolites determined by gas chromatography coupled with mass spectrometry (GC-MS) at the end of the night on the fourth day of culture (log phase).

Conditions	Sucrose	Maltose	Citrate	Isocitrate	Fumarate	Malate	Glutamate	Ornithine	Aspartate	Arginine	Proline	Leucine	Isoleucine
N50	0.00039	0.00484	0.02240	0.00833	0.06350	0.05560	0.47370	0.00179	0.00763	0.00065	0.01040	0.04340	0.01660
A50	0.00000	0.00766	0.01290	0.00615	0.01770	0.01450	0.41900	0.00165	0.00482	0.00067	0.00802	0.01940	0.00755
U50	0.00000	0.00206	0.00949	0.00917	0.01470	0.01280	0.21960	0.00095	0.00199	0.00059	0.00476	0.01380	0.00582
N50CO_2	0.00040	0.00046	0.01320	0.00434	0.03890	0.02730	0.12950	0.00034	0.00181	0.00016	0.00456	0.01950	0.00755
A50CO_2	0.00000	0.00088	0.00382	0.00191	0.01230	0.00888	0.13520	0.00044	0.00078	0.00027	0.00299	0.00904	0.00373
N200	0.00000	0.00026	0.01510	0.00052	0.01510	0.01590	0.06170	0.00053	0.00501	0.00060	0.00719	0.02370	0.00889
A200	0.00000	0.00040	0.00885	0.00262	0.01200	0.01240	0.16360	0.00079	0.00983	0.00061	0.00631	0.02640	0.01260
U200	0.00000	0.00058	0.00949	0.00406	0.01240	0.01390	0.12210	0.00078	0.01419	0.00047	0.00530	0.02530	0.01220
N200CO_2	0.00000	0.00057	0.01090	0.00000	0.01770	0.01680	0.09630	0.00092	0.00895	0.00094	0.00575	0.03020	0.01160
A200CO_2	0.00000	0.00092	0.00802	0.00665	0.00880	0.00634	0.05710	0.00143	0.09364	0.00147	0.00379	0.04120	0.02010
Conditions	**Valine**	**Alanine**	**Glycine**	**Serine**	**Tyrosine**	**Lysine**	**Tryptophan**	**Phenylalanine**	**Glycolate**	**Glycerate**	**Nicotinate**	**Nicotinamide**	**Alpha-tocopherol**
N50	0.03250	0.02940	0.01390	0.03890	0.00899	0.01660	0.00287	0.00666	0.00177	0.01170	0.00116	0.04070	0.04550
A50	0.01470	0.00500	0.00462	0.03780	0.00549	0.01590	0.00179	0.00337	0.00109	0.00714	0.00054	0.01330	0.02350
U50	0.00832	0.00627	0.00365	0.01150	0.00465	0.00821	0.00144	0.00257	0.00064	0.00393	0.00043	0.01310	0.01960
N50CO_2	0.01870	0.00566	0.00442	0.01420	0.00439	0.00231	0.00202	0.00323	0.00188	0.00126	0.00062	0.00694	0.03130
A50CO_2	0.00737	0.00248	0.00320	0.00921	0.00339	0.00417	0.00157	0.00183	0.00040	0.00155	0.00041	0.00754	0.02140
N200	0.02260	0.01040	0.00363	0.01260	0.00943	0.00593	0.00326	0.00363	0.00029	0.00016	0.00006	0.00417	0.01520
A200	0.02470	0.00766	0.00491	0.01710	0.01450	0.00685	0.00517	0.00485	0.00032	0.00050	0.00006	0.00444	0.02370
U200	0.02450	0.00928	0.00553	0.01610	0.01330	0.00726	0.00557	0.00502	0.00030	0.00036	0.00006	0.00485	0.01370
N200CO_2	0.02700	0.01870	0.00449	0.01500	0.01560	0.00610	0.00621	0.00502	0.00028	0.00043	0.00005	0.00448	0.01560
A200CO_2	0.03740	0.02910	0.00717	0.02930	0.01710	0.00752	0.00340	0.00634	0.00147	0.00097	0.00002	0.00297	0.00990

Primary metabolites levels (relative units to internal palatinose standard) at the end of the night of the fourth day of culture (log phase) of *Synechocystis* cells grown under different nitrogen sources (A- ammonium; N- nitrate; U- urea), light intensities (50- 50 µmol photons m^{-2} s^{-1}; 200- 200 µmol photons m^{-2} s^{-1}) and with or without CO_2 supplementation.

In order to obtain insights into the carbon-nitrogen (C/N) balance and cellular redox status of the cells grown in the ten contrasting growth conditions, we determined *ntcA* and *pII* expression (Figure 3.4). The relative expression levels of both genes showed no significant variations in response to the nitrogen source and CO_2 concentrations. On the other hand, their levels of expression at ED were negatively affected by the increase of the light intensity (Figure 3.4). In addition, *ntcA* and *pII* exhibit a significant reduction in their expressions at EN for all treatments (Figure 3.4).

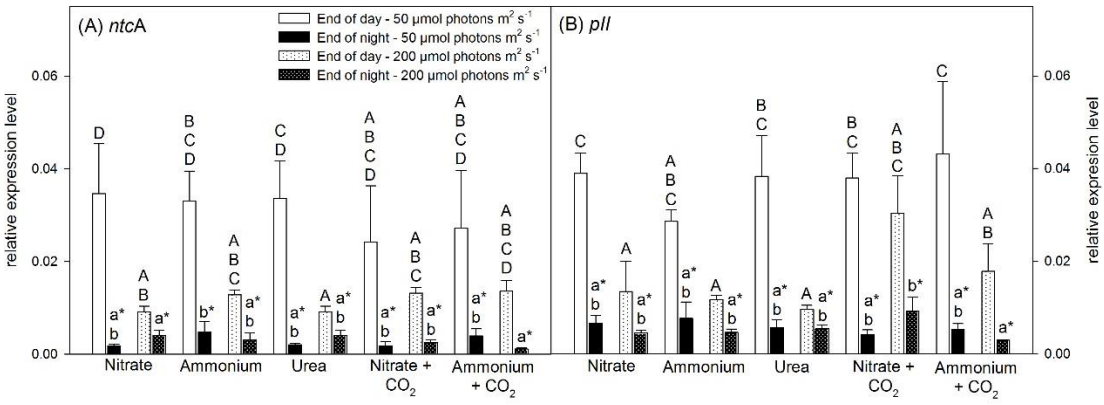

Figure 3-4: Relative expression levels of *ntcA* and *pII*.
Expression levels at the end of the day and end of the night of the fourth day of culture (log phase). Statistics are as described for Figure 3.3.

3.2.3 Metabolic and physiological traits during the stationary phase

For most growth conditions, photosynthetic rates decreased by 50-60% three days after the onset of the stationary phase (Table 3.8), thus allowing the maintenance of a significant production of photoassimilates. Moreover, cells cultured in the presence of nitrate and ammonium (not supplemented with CO_2), under HL, kept similar rates of photosynthesis with those observed in log phase (Table 3.8).

Table 3-8: Photosynthetic rate in stationary phase.

Culture	Photosynthetic rate	
	ML	**HL**
Nitrate	$2.28 \times 10^{-10} \pm 3.74 \times 10^{-11}$ **a**	$5.82 \times 10^{-10} \pm 6.33 \times 10^{-11}$ **b**
Ammonium	$2.75 \times 10^{-10} \pm 2.41 \times 10^{-11}$ **a**	$5.55 \times 10^{-10} \pm 5.23 \times 10^{-11}$ **b**
Urea	$2.23 \times 10^{-10} \pm 9.63 \times 10^{-12}$ **a**	$3.70 \times 10^{-10} \pm 1.11 \times 10^{-10}$ **a**
Nitrate + CO_2	$3.15 \times 10^{-10} \pm 7.82 \times 10^{-12}$ **a**	$6.09 \times 10^{-10} \pm 1.10 \times 10^{-11}$ **b**
Ammonium + CO_2	$2.59 \times 10^{-10} \pm 1.36 \times 10^{-11}$ **a**	$3.02 \times 10^{-10} \pm 6.66 \times 10^{-11}$ **a**

Photosynthetic rate (µmol oxygen L^{-1} s^{-1} $Cell^{-1}$) determined three days after the onset of the stationary phase at 50 µmol photons m^{-2} s^{-1} (**ML**) and 200 µmol photons m^{-2} s^{-1} (**HL**), with or without addition of CO_2. Values represent means ± standard deviation (n = 3). Statistics are as described for Table 3.1.

Biomass of cultures under ML exhibited a lower variation than at HL (Table 3.9). The levels of chlorophyll and phycocyanin were similar in almost all of the growth conditions (Figure 3.5A and B). Higher contents of total soluble sugars were observed for all cells grown under HL, especially for those grown in presence of nitrate plus CO_2 and ammonium (Figure 3.5C). This makes sense as these growth conditions were the ones in which photosynthetic rates remained high in stationary phase (Table 3.8). By contrast, higher sucrose levels were determined under ML (Figure 3.5E; Tables 3.10 and 3.11). The highest levels of glycogen were observed in cultures grown in the presence of nitrate under ML. Glycogen degradation was significant for most of the growth conditions under HL (Figure 3.5F). As the photosynthetic rates were two times higher for some growth conditions without a proportional increase of total soluble sugars and glycogen cellular contents (Figure 3.5C and F), we next analysed total soluble sugars in the culture medium. The highest levels of sugars in the medium were measured for the three growth conditions where photosynthetic rates were maintained (Figure 3.5D; Table 3.8), suggesting that photosynthetic rates were higher than necessary for the growth demand and that the excess of photosynthate production was released into the medium. Total soluble amino acids content was also increased in cells grown under HL, independently of the nutrient treatments (Figure 3.5G). In good agreement with this, glutamate levels were lower in these growth conditions (Figure 3.5H; Tables 3.10 and 3.11). In addition, all treatments displayed similar protein contents (Figure 3.5I), whilst light intensity negatively affected cyanophycin accumulation (Figure 3.5J).

Table 3-9: Cellular dry weight in stationary phase.

Culture	Cellular dry weight	
	ML	**HL**
Nitrate	$1.27 \times 10^{-9} \pm 7.16 \times 10^{-11}$ **bc**	$1.69 \times 10^{-9} \pm 4.42 \times 10^{-11}$ **d**
Ammonium	$1.38 \times 10^{-9} \pm 3.80 \times 10^{-11}$ **bc**	$1.23 \times 10^{-9} \pm 1.10 \times 10^{-10}$ **b**
Urea	$1.24 \times 10^{-9} \pm 6.40 \times 10^{-11}$ **b**	$9.66 \times 10^{-10} \pm 8.14 \times 10^{-11}$ **a**
Nitrate + CO_2	$1.44 \times 10^{-9} \pm 3.46 \times 10^{-11}$ **c**	$1.79 \times 10^{-9} \pm 6.20 \times 10^{-11}$ **d**
Ammonium + CO_2	$1.21 \times 10^{-9} \pm 2.13 \times 10^{-11}$ **b**	$9.89 \times 10^{-10} \pm 7.82 \times 10^{-11}$ **a**

Cellular dry weight (mg dry weight $cell^{-1}$) determined three days after the onset of the stationary phase at 50 µmol photons m^{-2} s^{-1} (**ML**) and 200 µmol photons m^{-2} s^{-1} (**HL**), with or without addition of CO_2. Values represent the mean ± standard deviation (n = 3). Statistics are as described for Table 3.1.

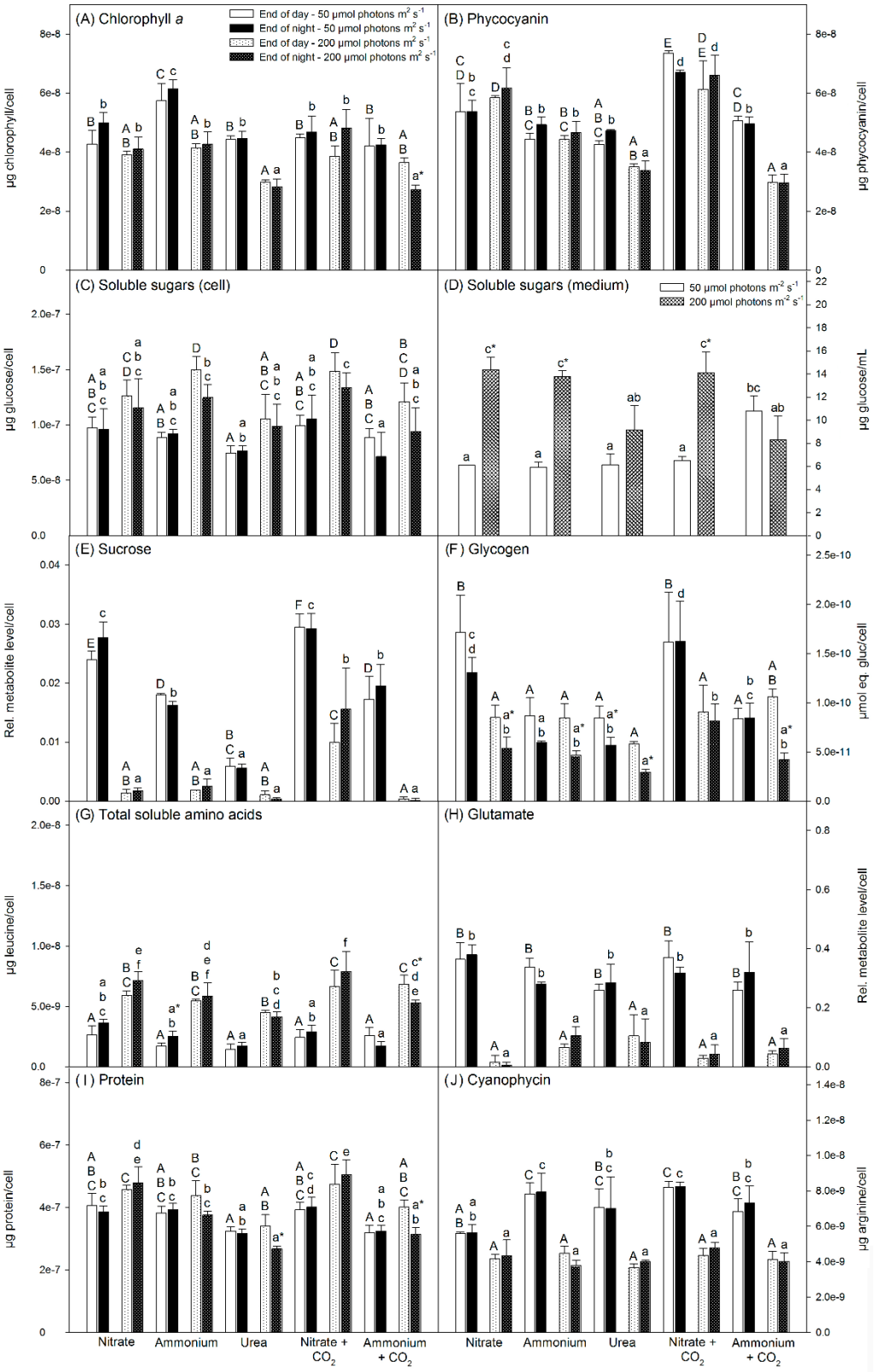

Figure 3-5: Pigments and metabolites determined three days after the onset of stationary phase Chlorophyll *a* (A), phycocyanin (B), total soluble sugars (cell) (C), total soluble sugars (medium) (D), sucrose (E), glycogen (F), total soluble amino acids (G), Glutamate (H), proteins (I) and cyanophycin (J). Sucrose and glutamate were determined by GC-MS and are expressed in relative units to internal palatinose standard. Values represent the mean ± standard deviation (n = 3). Statistics are as described for Figure 3.3.

Table 3-10: Primary metabolites determined by gas chromatography coupled with mass spectrometry (GC-MS) at the end of the day of the third day after the onset of the stationary phase.

Conditions	Sucrose	Maltose	Citrate	Isocitrate	Fumarate	Malate	Glutamate	Ornithine	Aspartate	Arginine	Proline	Leucine	Isoleucine
N50	0.02396	0.00513	0.00789	0.00013	0.01098	0.00956	0.36372	0.00334	0.01442	0.00338	0.02392	0.03033	0.01136
A50	0.01802	0.00527	0.06098	0.02547	0.01325	0.00786	0.33762	0.00348	0.01534	0.00168	0.01007	0.02859	0.00677
U50	0.00591	0.00313	0.04761	0.01045	0.01356	0.01447	0.25917	0.00293	0.01028	0.00171	0.00669	0.05306	0.01358
N50CO_2	0.02947	0.00623	0.05504	0.01112	0.03860	0.03516	0.36931	0.01056	0.03613	0.00821	0.01243	0.08159	0.03209
A50CO_2	0.01723	0.00353	0.03371	0.01397	0.02467	0.01920	0.25900	0.00582	0.02977	0.00351	0.00700	0.05675	0.01804
N200	0.00134	0.00154	0.00514	0.00000	0.01309	0.00758	0.01620	0.00403	0.01433	0.00203	0.03384	0.06063	0.02819
A200	0.00184	0.00209	0.01035	0.00069	0.01126	0.00737	0.06497	0.00571	0.01483	0.00291	0.01961	0.06292	0.02204
U200	0.00105	0.00215	0.02618	0.00610	0.01936	0.01885	0.10424	0.00558	0.04176	0.00293	0.02814	0.09939	0.03967
N200CO_2	0.00997	0.00482	0.01624	0.00227	0.03661	0.03598	0.02876	0.04240	0.04264	0.01884	0.05626	0.16936	0.05792
A200CO_2	0.00039	0.00098	0.00578	0.00126	0.01109	0.00792	0.04367	0.00332	0.02910	0.00129	0.01419	0.07569	0.02735
Conditions	**Valine**	**Alanine**	**Glycine**	**Serine**	**Tyrosine**	**Lysine**	**Tryptophan**	**Phenylalanine**	**Glycolate**	**Glycerate**	**Nicotinate**	**Nicotinamide**	**Alpha-tocopherol**
N50	0.02634	0.01166	0.00588	0.01528	0.01965	0.00652	0.00424	0.00797	0.00101	0.00066	0.00156	0.01821	0.02429
A50	0.02464	0.01997	0.00655	0.02156	0.02472	0.00939	0.00383	0.00619	0.00139	0.00295	0.00153	0.02310	0.02691
U50	0.04260	0.02426	0.00820	0.02674	0.03150	0.01478	0.00757	0.01111	0.00135	0.00178	0.00140	0.02398	0.03717
N50CO_2	0.12786	0.05268	0.02280	0.05792	0.05198	0.01317	0.01146	0.01639	0.00186	0.00214	0.00124	0.03053	0.02780
A50CO_2	0.06911	0.03635	0.01197	0.03774	0.03493	0.01085	0.00684	0.01045	0.00279	0.00426	0.00109	0.02453	0.01956
N200	0.05494	0.08628	0.01264	0.01697	0.02646	0.00877	0.00521	0.01469	0.00353	0.00100	0.00535	0.01621	0.05041
A200	0.03531	0.06946	0.00882	0.02765	0.03419	0.02365	0.00585	0.01381	0.00151	0.00100	0.00236	0.01039	0.03462
U200	0.09503	0.09362	0.02170	0.04247	0.04941	0.01707	0.01009	0.01779	0.00095	0.00080	0.00123	0.01781	0.01686
N200CO_2	0.16174	0.28319	0.06331	0.07305	0.10765	0.04994	0.01426	0.02561	0.00292	0.00267	0.00537	0.05632	0.03649
A200CO_2	0.04261	0.07764	0.01447	0.02839	0.02657	0.01187	0.00527	0.01468	0.00404	0.00827	0.00215	0.01605	0.01835

Primary metabolites levels (relative units to internal palatinose standard) at the end of the day of the third day after the onset of the stationary phase of *Synechocystis* cells grown under different nitrogen sources (A- ammonium; N- nitrate; U- urea), light intensities (50- 50 µmol photons m^{-2} s^{-1}; 200- 200 µmol photons m^{-2} s^{-1}) and with or without CO_2 supplementation.

Table 3-11: Primary metabolites determined by gas chromatography coupled with mass spectrometry (GC-MS) at the end of the night of the third day after the onset of the stationary phase.

Conditions	Sucrose	Maltose	Citrate	Isocitrate	Fumarate	Malate	Glutamate	Ornithine	Aspartate	Arginine	Proline	Leucine	Isoleucine
N50	0.02775	0.00482	0.03019	0.03173	0.03707	0.03668	0.37929	0.01425	0.19482	0.00557	0.00930	0.05275	0.02950
A50	0.01624	0.00035	0.01299	0.00169	0.00868	0.00524	0.28011	0.00243	0.00398	0.00175	0.00532	0.02677	0.00773
U50	0.00559	0.00029	0.02254	0.01296	0.04519	0.02876	0.28420	0.00300	0.01225	0.00209	0.00251	0.03939	0.01203
N50CO_2	0.02923	0.00232	0.08726	0.01478	0.07896	0.08010	0.31710	0.01690	0.02846	0.00563	0.00657	0.06129	0.02988
A50CO_2	0.01951	0.00035	0.02467	0.01755	0.04886	0.03783	0.32038	0.00491	0.01368	0.00212	0.00231	0.03608	0.01137
N200	0.00179	0.00000	0.00520	0.00000	0.02458	0.02009	0.00590	0.00392	0.01813	0.00239	0.02764	0.04750	0.02241
A200	0.00254	0.00000	0.00929	0.00213	0.01729	0.01347	0.10558	0.00830	0.02096	0.00396	0.01857	0.04437	0.01676
U200	0.00034	0.00000	0.00719	0.00081	0.01746	0.01604	0.08336	0.00256	0.02677	0.00112	0.01509	0.05075	0.02421
N200CO_2	0.01555	0.00404	0.01582	0.00454	0.05867	0.06871	0.04167	0.04237	0.08189	0.01822	0.02765	0.08811	0.04301
A200CO_2	0.00014	0.00000	0.00607	0.00066	0.01955	0.01573	0.06289	0.00235	0.02520	0.00177	0.01225	0.05905	0.02298
Conditions	**Valine**	**Alanine**	**Glycine**	**Serine**	**Tyrosine**	**Lysine**	**Tryptophan**	**Phenylalanine**	**Glycolate**	**Glycerate**	**Nicotinate**	**Nicotinamide**	**Alpha-tocopherol**
N50	0.07117	0.08820	0.02197	0.08153	0.04313	0.01672	0.01443	0.01329	0.00135	0.00184	0.00096	0.03722	0.02834
A50	0.01342	0.00921	0.00577	0.02252	0.02373	0.00894	0.00645	0.00640	0.00097	0.00636	0.00039	0.00902	0.02829
U50	0.01847	0.04656	0.00536	0.02760	0.02551	0.01523	0.00709	0.00945	0.00114	0.01211	0.00055	0.01901	0.02804
N50CO_2	0.06403	0.10650	0.01814	0.07381	0.05003	0.02490	0.01627	0.01762	0.00134	0.00180	0.00075	0.03684	0.02963
A50CO_2	0.01778	0.05814	0.00613	0.03565	0.02599	0.01901	0.00722	0.00828	0.00140	0.01279	0.00067	0.02467	0.02583
N200	0.03417	0.06976	0.00964	0.01792	0.02493	0.01239	0.00441	0.01235	0.00174	0.00148	0.00408	0.01439	0.03967
A200	0.02909	0.06465	0.00877	0.03216	0.03525	0.03384	0.00667	0.01102	0.00131	0.00189	0.00101	0.01066	0.03738
U200	0.04043	0.06201	0.01446	0.02897	0.02645	0.01224	0.00696	0.01127	0.00109	0.00105	0.00088	0.00910	0.01830
N200CO_2	0.08651	0.23959	0.05270	0.08842	0.10578	0.05512	0.01394	0.01937	0.00241	0.00301	0.00384	0.06577	0.03905
A200CO_2	0.03457	0.07104	0.01054	0.02949	0.02177	0.01907	0.00467	0.01303	0.00236	0.01235	0.00095	0.01286	0.02729

Primary metabolites levels (relative units to internal palatinose standard) at the end of the night of the third day after the onset of the stationary phase of *Synechocystis* cells grown under different nitrogen sources (A- ammonium; N- nitrate; U- urea), light intensities (50- 50 µmol photons m^{-2} s^{-1}; 200- 200 µmol photons m^{-2} s^{-1}) and with or without CO_2 supplementation.

3.2.4 The decrease in division rates seem to be unrelated to nutrient limitation, quorum sensing or self-shading

To evaluate the possible influence of nutrient depletion and/or quorum sensing, we transferred cells from a whole culture which had reached stationary phase to fresh medium (Figure 2.1). Cell density did not increase significantly (Tables 3.12 and 3.13). In order to assess if the old medium obtained from the culture which had reached stationary phase was suboptimal for growth, we grew a 3 mL inoculum from the same resuspended pellet in the old medium (Figure 2.1). After four days of culture cell density increased 11 to 22 times, with the division rates being statistically similar to the rates observed when an inoculum of the same density was grown on fresh medium (Tables 3.12 and 3.13). Besides, the whole growth cycle observed using the old medium appeared very similar to the one observed in fresh medium, and only when we attempted to re-use the medium for a third growth cycle we could observe a sharp decrease in division rates. High daily cell division rates were restored by addition of fresh nutrients to the medium, but not by addition of water (Figure 3.6). Thus, the slow growth rates at stationary phase seems likely not due to a nutrient limitation, as our metabolic data suggested, nor to quorum sensing as the growth of an inoculum would have been impaired in old medium due to the presence of a signal molecule, though we cannot exclude the possibility that this molecule had been highly unstable.

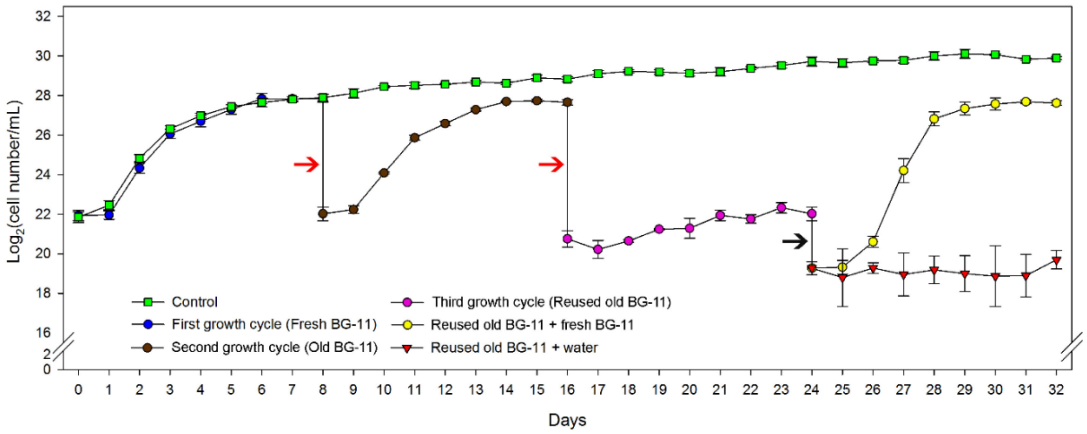

Figure 3-6: *Synechocystis* growth on fresh and reused BG-11.
Growth cycles of *Synechocystis* on fresh BG-11 (blue circles), old BG-11 (brown circle) and reused old BG-11 (pink circles). Red arrows show when the entire culture was centrifuged and the supernatant was filtered and used to grow an inoculum, obtained from the resuspended pellet, during additional eight days. Black arrow shows when cultures with reused old BG-11 were divided in two parts and supplemented in a proportion of 1:1 with fresh BG-11 (yellow circles) or water (red triangles). As a control, cultures were maintained growing as a batch for the entire period of 32 days (green squares).

Table 3-12: Cell density of an inoculum grown on filtered medium from a previous culture that had reached stationary phase (condition 1) or whole-cell culture that had reached stationary phase and was regrown without dilution on fresh medium (condition 2). All treatments were performed under 50 µmol photons m^{-2} s^{-1}.

Culture		Condition 1			Condition 2		
		Day 0	**Day 4**	**Ratio (D_4/D_0)**	**Day 0**	**Day 4**	**Ratio (D_4/D_0)**
Nitrate	Control	$6.0 \times 10^6 \pm 7.1 \times 10^4$	$6.5 \times 10^7 \pm 5.9 \times 10^6$	10.9 ± 1.1	$1.5 \times 10^8 \pm 1.2 \times 10^7$	$2.1 \times 10^8 \pm 2.9 \times 10^7$	1.4 ± 0.1
	Treatment	$4.3 \times 10^6 \pm 6.4 \times 10^5$	$5.7 \times 10^7 \pm 1.8 \times 10^7$	13.3 ± 3.6	$2.3 \times 10^8 \pm 6.8 \times 10^6$	$2.7 \times 10^8 \pm 5.3 \times 10^7$	1.2 ± 0.2
Ammonium	Control	$5.6 \times 10^6 \pm 6.4 \times 10^5$	$9.3 \times 10^7 \pm 1.3 \times 10^7$	16.7 ± 0.4	$1.9 \times 10^8 \pm 5.7 \times 10^6$	$2.1 \times 10^8 \pm 2.1 \times 10^7$	1.1 ± 0.1
	Treatment	$3.1 \times 10^6 \pm 6.8 \times 10^5$	$5.2 \times 10^7 \pm 1.8 \times 10^6$	17.4 ± 3.4	$1.5 \times 10^8 \pm 2.3 \times 10^7$	$2.7 \times 10^8 \pm 7.3 \times 10^6$	1.8 ± 0.4*****
Urea	Control	$6.6 \times 10^6 \pm 3.6 \times 10^5$	$1.3 \times 10^8 \pm 5.3 \times 10^6$	18.9 ± 0.4	$1.9 \times 10^8 \pm 2.5 \times 10^7$	$2.5 \times 10^8 \pm 9.0 \times 10^6$	1.3 ± 0.1
	Treatment	$3.8 \times 10^6 \pm 6.2 \times 10^5$	$8.5 \times 10^7 \pm 1.2 \times 10^7$	22.9 ± 6.1	$2.3 \times 10^8 \pm 2.9 \times 10^7$	$3.1 \times 10^8 \pm 4.7 \times 10^7$	1.4 ± 0.3
Nitrate + CO_2	Control	$4.0 \times 10^6 \pm 2.1 \times 10^5$	$7.8 \times 10^7 \pm 2.8 \times 10^6$	19.5 ± 0.4	$1.6 \times 10^8 \pm 4.8 \times 10^6$	$2.2 \times 10^8 \pm 1.1 \times 10^7$	1.3 ± 0.1
	Treatment	$4.6 \times 10^6 \pm 6.4 \times 10^5$	$6.6 \times 10^7 \pm 9.4 \times 10^6$	14.6 ± 3.5	$2.2 \times 10^8 \pm 3.6 \times 10^7$	$2.9 \times 10^8 \pm 2.9 \times 10^7$	1.3 ± 0.3
Ammonium + CO_2	Control	$5.5 \times 10^6 \pm 1.5 \times 10^6$	$1.1 \times 10^8 \pm 1.2 \times 10^7$	20.5 ± 4.2	$1.9 \times 10^8 \pm 1.2 \times 10^7$	$2.3 \times 10^8 \pm 1.7 \times 10^7$	1.2 ± 0.1
	Treatment	$2.8 \times 10^6 \pm 6.4 \times 10^5$	$4.0 \times 10^7 \pm 4.0 \times 10^6$	14.7 ± 2.0	$2.0 \times 10^8 \pm 1.9 \times 10^7$	$2.9 \times 10^8 \pm 2.1 \times 10^7$	1.5 ± 0.2

Cell number (cell number mL^{-1}) under 50 µmol photons m^{-2} s^{-1}, with or without addition of CO_2. Control data were obtained on growth curves shown on figure 3.1 between the first four days of culturing (condition 1) and the last four days of culturing (condition 2). Values represent the mean ± standard deviation (n = 3). The asterisk represents a significant difference between control and treatment for the same growth condition ($P < 0.05$, unpaired Student's *t* test).

Table 3-13: Cell density of an inoculum grown on filtered medium from a previous culture that had reached stationary phase (condition 1) or whole-cell culture that had reached stationary phase and was regrown without dilution on fresh medium (condition 2). All treatments were performed under 200 µmol photons m^{-2} s^{-1}.

Culture		Condition 1			Condition 2		
		Day 0	Day 4	Ratio (D_4/D_0)	Day 0	Day 4	Ratio (D_4/D_0)
Nitrate	Control	$3.9 \times 10^6 \pm 8.5 \times 10^5$	$7.8 \times 10^7 \pm 2.4 \times 10^7$	19.7 ± 1.8	$1.8 \times 10^8 \pm 1.5 \times 10^7$	$2.1 \times 10^8 \pm 3.0 \times 10^7$	1.1 ± 0.1
	Treatment	$2.8 \times 10^6 \pm 4.7 \times 10^5$	$3.8 \times 10^7 \pm 4.9 \times 10^6$	14.4 ± 5.4	$1.1 \times 10^8 \pm 5.8 \times 10^6$	$1.3 \times 10^8 \pm 2.0 \times 10^7$	1.2 ± 0.2
Ammonium	Control	$5.7 \times 10^6 \pm 1.2 \times 10^6$	$8.6 \times 10^7 \pm 7.1 \times 10^6$	15.5 ± 1.9	$1.9 \times 10^8 \pm 3.0 \times 10^7$	$2.5 \times 10^8 \pm 3.1 \times 10^7$	1.3 ± 0.1
	Treatment	$4.5 \times 10^6 \pm 6.5 \times 10^5$	$5.3 \times 10^7 \pm 6.4 \times 10^6$	11.9 ± 1.8	$1.7 \times 10^8 \pm 2.7 \times 10^7$	$2.4 \times 10^8 \pm 3.6 \times 10^7$	1.4 ± 0.3
Urea	Control	$6.3 \times 10^6 \pm 1.3 \times 10^6$	$1.3 \times 10^8 \pm 1.8 \times 10^7$	20.4 ± 1.3	$1.3 \times 10^8 \pm 1.8 \times 10^7$	$2.3 \times 10^8 \pm 2.3 \times 10^7$	1.8 ± 0.1
	Treatment	$4.8 \times 10^6 \pm 8.6 \times 10^5$	$8.5 \times 10^7 \pm 7.1 \times 10^6$	17.8 ± 1.9	$1.2 \times 10^8 \pm 1.1 \times 10^7$	$1.9 \times 10^8 \pm 2.9 \times 10^7$	1.6 ± 0.2
Nitrate + CO_2	Control	$5.1 \times 10^6 \pm 1.4 \times 10^6$	$8.2 \times 10^7 \pm 1.1 \times 10^7$	16.7 ± 2.3	$1.8 \times 10^8 \pm 1.2 \times 10^7$	$2.2 \times 10^8 \pm 1.1 \times 10^7$	1.2 ± 0.1
	Treatment	$3.9 \times 10^6 \pm 7.2 \times 10^5$	$7.1 \times 10^7 \pm 7.3 \times 10^6$	18.2 ± 0.4	$8.5 \times 10^7 \pm 6.2 \times 10^6$	$1.2 \times 10^8 \pm 2.4 \times 10^7$	1.4 ± 0.2
Ammonium + CO_2	Control	$6.2 \times 10^6 \pm 4.5 \times 10^5$	$1.1 \times 10^8 \pm 1.5 \times 10^7$	17.5 ± 1.1	$1.1 \times 10^8 \pm 1.5 \times 10^7$	$1.9 \times 10^8 \pm 1.3 \times 10^7$	1.8 ± 0.1
	Treatment	$4.9 \times 10^6 \pm 1.2 \times 10^6$	$9.1 \times 10^7 \pm 3.1 \times 10^7$	19.0 ± 6.6	$1.0 \times 10^8 \pm 9.5 \times 10^6$	$1.7 \times 10^8 \pm 1.2 \times 10^7$	1.7 ± 0.1

Cell number (cell number mL^{-1}) under 200 µmol photons m^{-2} s^{-1}, with or without addition of CO_2. Control data were obtained on growth curves shown on figure 3.1 between the first four days of culturing (condition 1) and the last four days of culturing (condition 2). Values represent the mean ± standard deviation (n = 3). The asterisk represents a significant difference between control and treatment for the same growth condition ($P < 0.05$, unpaired Student's *t* test).

To confirm the absence of quorum sensing in our culture conditions and also test the possibility of an effect of light intensity and/or quality due to the high cell density of the culture, we next inoculated cells into a microtube fixed at the bottom of a flask containing a culture which had reached stationary phase (Figure 2.1). Importantly we allowed the exchange of medium between the culture and the cells within the microtube by sealing a filter of 0.45 µm at the entrance of the microtube. After four days of culture under ML, cell density in the microtubes reached 60% of what was achieved by an inoculum in presence of fresh medium (Table 3.14), so the cells divided only one time less. Moreover, when cells were grown under HL, we did not observe any difference with a fresh culture (Table 3.14). This indicates that quorum sensing is not responsible for the decrease in growth rates and for the onset of stationary phase in *Synechocystis*. Moreover, self-shading had a very moderate effect under ML, and probably no effect under HL.

Table 3-14: Cell density of an inoculum grown in microtubes fixed at the bottom of flasks containing BG11 fresh medium (control) or a culture that had reached stationary phase (treatment).

Condition	**ML**		
	Day 0	**Day 4**	**Ratio (Day 4:Day 0)**
Control	$5.69x10^{6} \pm 7.63x10^{5}$	$4.31x10^{7} \pm 6.07x10^{6}$*	7.58 ± 0.39
Treatment	$5.23x10^{6} \pm 8.19x10^{5}$	$2.43x10^{7} \pm 2.86x10^{6}$*	4.67 ± 0.33
Condition	**HL**		
	Day 0	**Day 4**	**Ratio (Day 4:Day 0)**
Control	$3.40x10^{6} \pm 8.61x10^{5}$	$3.81x10^{7} \pm 1.36x10^{7}$*	11.00 ± 1.23
Treatment	$3.12x10^{6} \pm 2.89x10^{5}$	$3.40x10^{7} \pm 7.90x10^{6}$*	10.83 ± 1.62

Cell number (cell number mL^{-1}) is shown for urea cultures grown under 50 µmol photons m^{-2} s^{-1} (**ML**) and 200 µmol photons m^{-2} s^{-1} (**HL**). Values represent the means ± standard deviation (n = 3). The asterisk represents significant difference between means for the same growth condition ($P < 0.05$, paired Student's *t* test).

Given that nutrient limitation, quorum sensing and self-shading may not explain the gradual decrease of growth and the onset of stationary phase, we considered whether a regulation triggered by cell-cell interaction could be involved in this process. For this purpose, experiments were performed with cultures grown on urea under HL, to avoid the moderate self-shading effect observed under ML. In order to test this hypothesis, we started cultures using inocula at different cell densities. Cultures initiated with higher cell density showed slower division rates during the second and third days of culturing, and

all cultures exhibited a gradual decrease in their division rates from the fourth day (Figure 3.7A and B).

In order to evaluate how fast the rate of cell division responded to an increase in cell density, we used centrifugation to artificially increase by a factor of 10 the density of log-phase cultures. This treatment led to a 58% and 77% decrease in growth rates after 24 and 48 h, respectively. Cultures submitted to the same centrifugation process, but resuspended without being concentrated, did not present any alteration in their growth rate, dividing as fast as cultures which had not been centrifuged (Figure 3.7C and D).

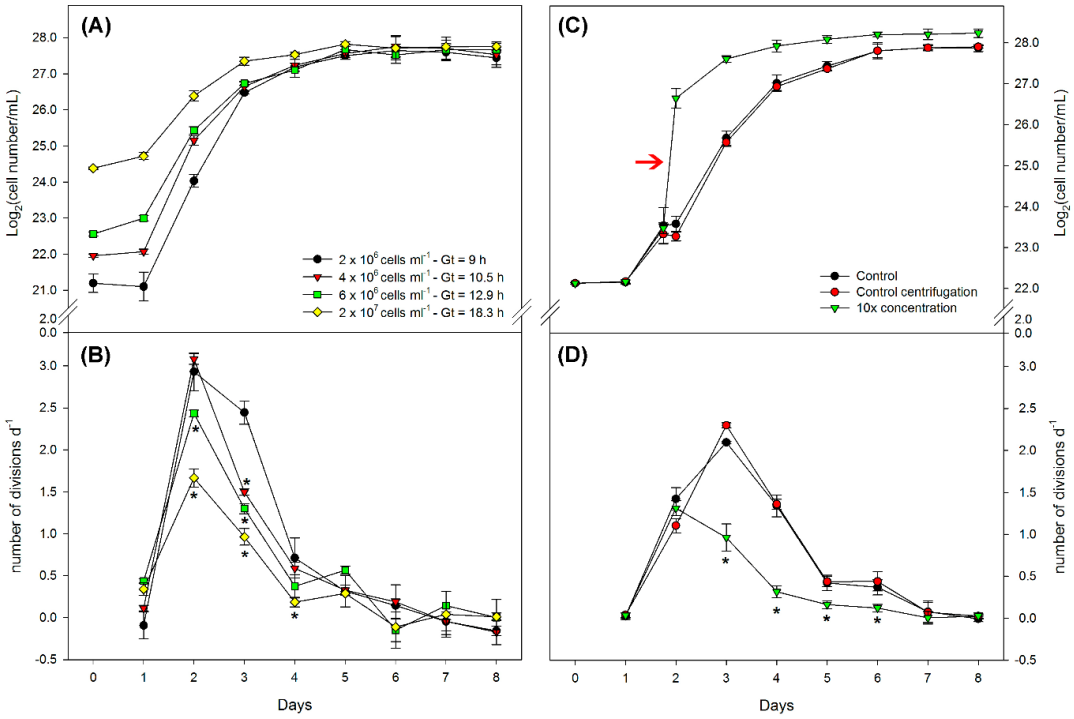

Figure 3-7: Experimental setups to test the effect of cell density on *Synechocystis* growth. Effects of different initial cell densities on growth cycle (**A**) and daily number of divisions (**B**): 2 x 10^6 (black), 4 x 10^6 (red), 6 x 10^6 (green) and 2 x 10^7 (yellow) cells mL^{-1}. Effects of an artificial increase of cell density on growth cycle (**C**) and daily number of divisions (**D**). Red arrow in **C** indicates an artificial increase of cell density. Control cultures (black) were not disturbed during their growth; control centrifugation cultures (red) were submitted to the same pipetting, centrifugation and growth conditions of 10x concentration, but not concentrated after centrifugation; 10x concentration cultures (green) were artificially concentrated after centrifugation. The asterisk represents significant difference from 2 x 10^6 cells mL^{-1} (**B**) or control (**D**) ($P < 0.05$, paired Student's *t* test).

In order to determine whether cell density is quantitatively controlling the rate of cell division, we grew *Synechocystis* in a fed-batch system at two different dilution rates. Cultures started with low cell density (4 x 10^6 cells mL^{-1}) and submitted to a dilution rate of 0.5 time increase in density during the first four days (Figure 3.8A and B). When cultures reached a density of 7 x 10^7 cells mL^{-1}, growth and dilution rate were counterbalanced and the culture density stayed stable, with cells dividing around 0.46 to

0.66 time per day for seven days (Figure 3.8A and B). Next, we increased the dilution rate to 2 times per day. The cells divided faster than the dilution rate during the first two days till the culture reached a density of 3.5 x 10^7 cells mL^{-1} when cell division rate and dilution rate were counterbalanced. During the following days, the cells divided fast with 1.7 to 2.2 divisions per day (Figure 3.8A and B).

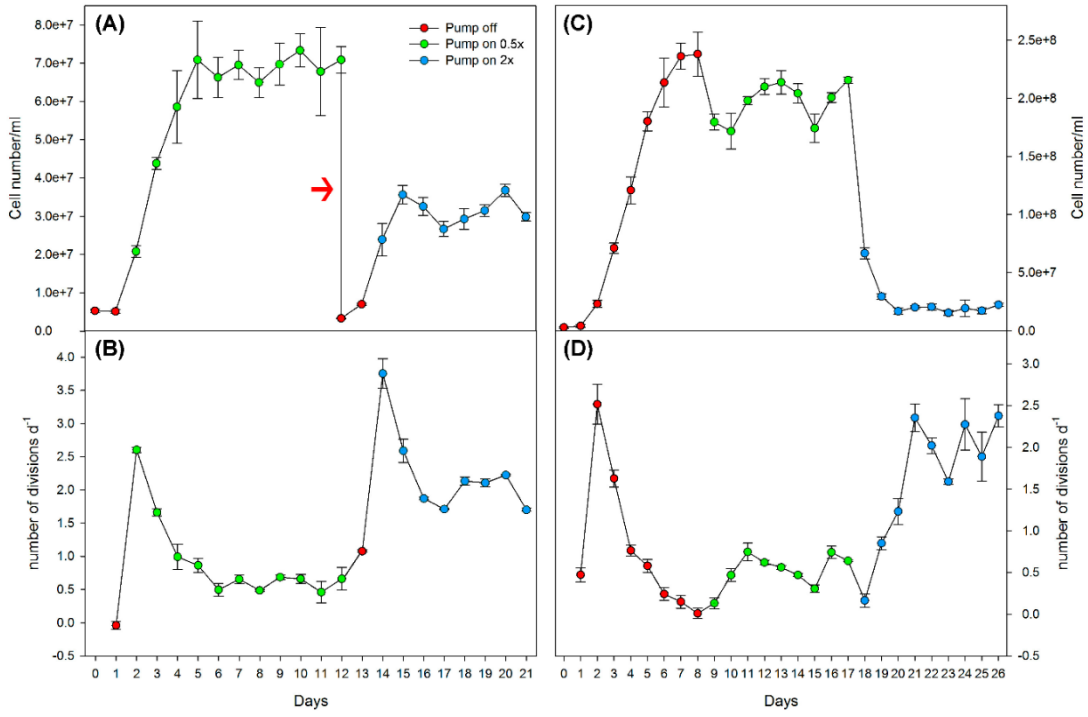

Figure 3-8: *Synechocystis* growth on fed-batch conditions.
Growth cycle and daily number of divisions are shown for cultures grown in fed-batch condition starting at low cell density (**A** and **B**) and high cell density (**C** and **D**). Red arrow (**A)** indicates that cultures were diluted to the same initial density of day 0.

Next, we investigated the effect of the same dilution rates on cultures which had reached stationary phase. At a dilution rate of 0.5 time per day, cultures divided slower than the dilution rate on the first day, leading to a decrease of the cell density. Then, cell division rates entered in balance with dilution, dividing 0.46 to 0.74 per day during the following six days (Figure 3.8C and D). When we applied a dilution rate of 2 times per day, we observed a gradual increase in cell division rates, which counterbalanced the dilution rate on the third day of growth at a cell density around 2 x 10^7 cells mL^{-1}, with cells dividing 1.6 to 2.3 times per day for the next six days (Figure 3.8C and D). In summary, cell division rates appeared to be directly related to the cell density of the cultures.

3.3 Discussion

3.3.1 Growth rates are only partially controlled by the metabolic capacity and mostly by the cell division machinery

We built a Spearman's rank correlation matrix to identify potential metabolic and physiological traits which could be linked to growth and biomass (Figure 3.9; Supplemental Figure 3.1 and 3.2). Gt and biomass were significantly and positively correlated (r_s = 0.71; Figure 3.9), meaning that cells dividing fast do accumulate less biomass than cells dividing slowly. Photosynthesis did not correlate with growth and biomass. However, photosynthetic rates were positively correlated with amino acids levels at both ED and EN, and with soluble sugars pools and glycogen at EN (Figure 3.9). The absence of correlation between Gt and photosynthetic rate indicates that photosynthesis and growth were unrelated on the fourth day of culture, so three days in the log phase for most of the culture conditions studied. This suggests that instead of dividing, the cells stored photoassimilates (Figures 3.9 and 3.10). In agreement, Gt correlates positively with proteins and sucrose at ED and EN, and with glycogen, soluble sugars, citrate and malate at EN. Additionally, we observed a strong negative correlation between cell number with protein and total soluble sugars, both at ED and EN (Figure 3.9). Thus, the gradual decrease in the division rate observed in our batch cultures (Figure 3.1) does not appear to be due to a metabolic limitation, but to a progressive decrease in the ability of cells to divide. Altogether, we observe uncoupling of Gt and photosynthetic rate, a progressive increase in both the C- and N- reserves, and finally the release of soluble sugars in the growth medium. The release of sugars into the medium can be seen as a strategy to avoid a possible inhibition of photosynthesis by negative sugar feedback (Stitt et al., 1991; Oswald et al., 2001).

CO_2 supplementation did not promote increments in photosynthesis. Importantly, photosynthesis in this study is defined as O_2 release, which is related to the capacity to produce ATP and NADPH, and not to CO_2 assimilation. Therefore, we cannot exclude a higher Calvin-Benson cycle activity in the presence of higher CO_2 levels due to an inhibition of the photorespiratory pathway. However, this is highly unlikely because we did not notice significant changes in cellular contents of glycine and serine (Figure 3.10; Tables 3.6 and 3.7).

	Day				Night			
	Gt	Biomass	*A*	Cell number	Gt	Biomass	*A*	Cell number
Gt								
Biomass	**0.71**				**0.71**			
A	0.33	0.04			0.33	0.04		
Cell number	**-0.93**	-0.56	-0.35		**-0.93**	-0.56	-0.35	
Chlorophyll *a*	0.56	**0.72**	0.04	-0.43	0.54	**0.75**	-0.03	-0.35
Phycocyanin	0.36	0.53	0.27	-0.33	0.12	0.05	0.37	-0.18
Proteins	**0.85**	0.56	0.52	**-0.90**	**0.94**	0.59	0.41	**-0.88**
Total amino acids	0.33	-0.09	**0.72**	-0.42	0.36	0.12	**0.75**	-0.41
Cyanophycin	0.16	-0.21	0.25	-0.31	0.50	0.24	0.55	-0.55
Glycogen	-0.27	-0.37	-0.26	0.13	**0.70**	0.21	**0.73**	**-0.71**
% degraded glycogen					**-0.90**	**-0.84**	-0.14	**0.84**
Total soluble sugars (cell)	0.56	0.26	0.38	**-0.72**	**0.66**	0.21	**0.73**	**-0.71**
Sucrose	**0.68**	**0.63**	0.08	-0.52	**0.68**	**0.63**	0.08	-0.52
Total soluble sugars (medium)					0.27	-0.01	0.26	-0.42
Maltose	0.18	0.52	-0.45	-0.20	-0.39	0.03	-0.43	0.28
Citrate	0.38	0.59	-0.16	-0.48	**0.64**	0.44	0.27	**-0.75**
Isocitrate	0.25	0.46	-0.43	-0.10	-0.21	0.08	-0.38	0.24
Glutamate	0.56	**0.72**	-0.03	-0.56	0.20	0.47	0.15	-0.13
Ornithine	0.38	0.44	-0.27	-0.48	-0.25	-0.18	-0.09	0.01
Aspartate	0.50	0.38	-0.19	-0.57	-0.38	**-0.68**	0.37	0.19
Arginine	-0.01	0.22	-0.31	-0.18	-0.20	-0.44	-0.07	-0.10
Fumarate	0.48	**0.80**	-0.14	-0.42	0.59	0.60	0.20	**-0.65**
Malate	0.48	**0.80**	-0.14	-0.42	**0.67**	0.56	0.42	**-0.73**
Proline	0.41	0.49	-0.24	-0.50	0.35	0.04	0.56	-0.55
Leucine	0.36	0.31	-0.09	-0.50	0.14	-0.16	0.43	-0.35
Isoleucine	0.38	0.24	0.08	-0.52	-0.07	-0.42	0.39	-0.14
Valine	0.43	0.50	-0.22	-0.53	0.05	-0.27	0.35	-0.26
Alanine	0.09	0.14	-0.43	-0.23	0.07	-0.12	0.27	-0.31
Glycine	0.38	0.50	-0.27	-0.45	-0.16	-0.32	0.35	0.01
Serine	0.42	0.60	-0.22	-0.47	-0.01	-0.30	0.31	-0.20
Tyrosine	0.31	0.39	-0.28	-0.44	-0.27	**-0.65**	0.30	0.05
Lysine	0.24	0.60	-0.41	-0.26	-0.36	-0.20	-0.03	0.16
Tryptophan	0.20	0.09	-0.09	-0.45	-0.07	-0.45	0.62	-0.08
Phenylalanine	0.45	0.45	-0.14	-0.55	-0.07	-0.31	0.43	-0.18
Glycolate	0.54	**0.89**	-0.30	-0.43	0.22	0.32	-0.38	-0.13
Glycerate	0.41	**0.84**	-0.30	-0.26	0.10	0.47	-0.36	-0.07
Nicotinate	0.58	**0.82**	-0.31	-0.48	0.45	**0.67**	0.07	-0.31
Nicotinamide	0.44	**0.76**	-0.36	-0.38	0.13	0.58	-0.04	-0.08
Alpha-tocopherol	0.45	**0.63**	0.15	-0.37	**0.71**	**0.71**	0.28	-0.56
ntcA	0.16	0.58	-0.45	-0.14	-0.42	-0.22	0.20	0.49
pII	0.31	**0.81**	-0.44	-0.22	-0.10	0.19	0.24	-0.03

Figure 3-9: Spearman's rank coefficient of correlation among parameters determined on the fourth day of culture (log phase)

Correlations between Gt, biomass, photosynthetic rate (*A*), and cell number, and metabolites and gene expression levels determined at the end of the day and end of the night on the fourth day of culture. Total soluble sugars (medium) was determined only at the end of the night. Significant correlations at 5% probability are highlighted in green (positive) and red (negative). Additional correlations between all growth, physiologic, metabolic and molecular traits are present in Supplemental Figures 3.1 and 3.2.

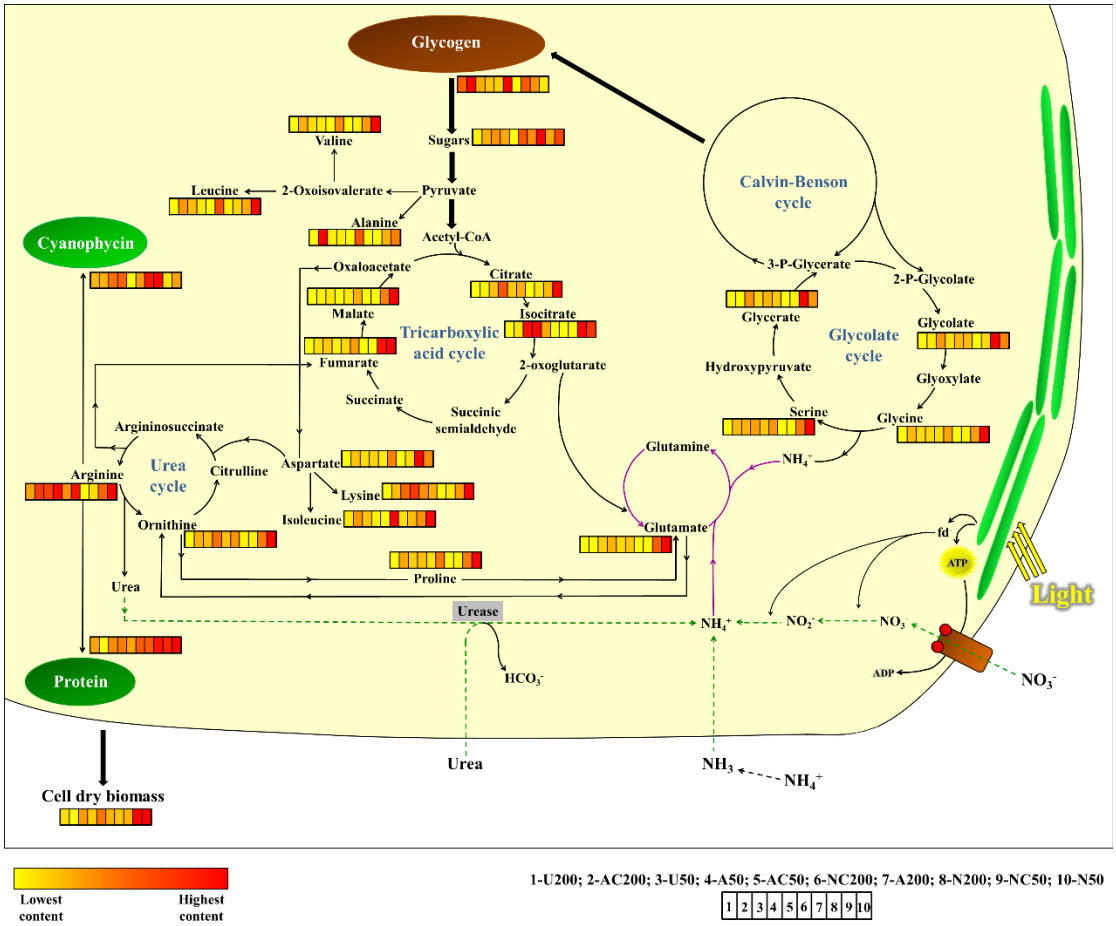

Figure 3-10: Heat map of metabolites levels.
Culture conditions are ordered based on growth rates, from the fastest (left) to the slowest (right). A, Ammonium; C, CO_2; N, Nitrate; U, Urea; 50, 50 µmol photons m^{-2} s^{-1}; 200, 200 µmol photons m^{-2} s^{-1}.

An increase in light intensity only increased photosynthetic rates for cultures grown in the presence of ammonium and urea. In fact, HL treatment mostly led to a decrease in the amount of chlorophyll and phycocyanin (Table 3.4; Figure 3.3). The lower pigment content observed under HL might lead to a lower redox state of the ETC (Alfonso et al., 2000), which might be a strategy to avoid production of reactive oxygen species and inhibition of photosynthesis (Hihara et al., 2001; Muramatsu et al., 2009), particularly when photoassimilates cannot be used for cell division. Interestingly, Kopečná et al. (2012) showed that even with a lower cellular chlorophyll content under HL, the rate of chlorophyll synthesis was higher than at lower light intensity. This was explained by a reduction of the half-life of chlorophyll molecules and a greater demand for chlorophylls as a result of faster growth rates.

pII and *ntcA* are major proteins involved in sensing C/N balance in cyanobacteria (Flores and Herrero, 2005). The expression levels of *ntcA* were not affected by nitrogen sources, as previously described (Alfonso et al., 2001). *pII* and *ntcA* transcript levels were

positively correlated (r_s = 0.83; Figure 3.11), which was expected because *ntcA* controls *pII* expression (García-Domínguez and Florencio, 1997; Lee et al., 1999). *ntcA* and *pII* transcript levels correlated negatively with total amino acids levels, and positively with chlorophyll, citrate, isocitrate, fumarate, malate and glutamate, in agreement with their role in sensing C/N balance (Figure 3.11). *pII* expression correlated positively with biomass (r_s = 0.83; Figure 3.9), but not with Gt. It is likely explained by the positive correlation between Gt and biomass, showing that cells dividing slowly accumulate more biomass, and in particular Carbon rich compounds. Thus, cells dividing slowly were not metabolically limited, however, another factor clearly limits their growth.

	Day		Night	
	ntcA	***pII***	***ntca***	***pII***
ntcA				
pII	**0.83**		0.50	
Chlorophyll *a*	**0.70**	0.60	0.03	0.12
Citrate	**0.73**	**0.67**	-0.38	0.26
Isocitrate	**0.73**	0.55	-0.13	-0.01
Fumarate	**0.66**	**0.79**	-0.08	0.51
Malate	**0.66**	**0.79**	-0.21	0.38
Glutamate	**0.72**	**0.66**	0.39	0.53
Total amino acids	**-0.67**	-0.58	-0.16	0.16

Figure 3-11: Spearman's rank coefficient of correlation of *ntcA* and *pII*
Correlation analysis between the relative expression levels of *ntcA* and *pII* with chlorophyll *a*, citrate, isocitrate, fumarate, malate, glutamate, and total amino acids levels determined at the end of the day and end of the night on the fourth day of culture (log phase). Significant correlations at 5% probability are highlighted in green (positive) and red (negative).

When *Synechocystis* was grown in the presence of urea, it displayed fast division rates, one of the shortest growth cycles, and lower metabolite contents (Figures 3.1 and 3.10; Table 3.1), suggesting that urea may be a promising alternative to nitrate and ammonium for growing cyanobacteria species of biotechnological interest. In this condition, cells displayed higher photosynthetic rates when cultured under HL, although it did not lead to increased growth rates (Tables 3.1 and 3.4). These data reinforce our observations that growth and photosynthesis are not directly linked. Moreover, even with a fast growth rate and lower reserves, cells may still present sink limitations to support the rate of photoassimilates synthesis, since the cellular levels of soluble sugars and their concentrations in the medium were similar to those observed under the other nine treatments (Figure 3.3C and D).

Altogether, our metabolic and physiological data indicate the absence of a metabolic limitation of growth at log phase. The photosynthetic rates observed were high enough to support the synthesis of sugars and amino acids required for growth, which instead of being used for it were redirected for the synthesis of storage proteins. Indeed, at day four of culture, the protein content was positively correlated to Gt and negatively with the number of cells (Figure 3.9), suggesting that a major fraction of proteins were

used as nitrogen storage. Moreover, a significant amount of sugars were released to the growth medium, instead of being used by the cellular metabolism.

3.3.2 Is stationary phase reached because of metabolic/ nutrient limitation?

Cultures grown under the different growth conditions reached stationary phase with similar cell densities (Table 3.2) despite varying durations of culture due to slightly different division rates (Figure 3.1; Table 3.1). This suggests that a non-metabolic factor is responsible for the onset of stationary phase. In order to provide further support for the above hypothesis, we investigated the role of metabolism, nutrients, quorum sensing and self-shading in the onset of stationary phase.

At stationary phase, the rate of photosynthesis remained high compared to those observed at log phase, decreasing by 50-60% under ML and being largely unaffected under HL (Table 3.4). The decrease under ML is likely explained by self-shading, and this difference between HL and ML led to dramatic differences in the metabolic profiles of cells grown under ML and HL. The rate of photosynthesis correlated negatively with glutamate at both ED and EN, and positively with total soluble sugars (in cells and culture medium), proteins, total soluble amino acids as well as the levels of some individual amino acids, such as leucine, isoleucine, alanine, glycine and phenylalanine at ED; and proline at both ED and EN (Figure 3.12). Total soluble amino acids correlated negatively with chlorophyll, cyanophycin, citrate, isocitrate and glutamate, and positively with total soluble sugars (in cells and culture medium), proteins and proline (Figure 3.12). The negative correlations of amino acids with citrate, isocitrate and glutamate suggested that these metabolites had been used mainly as a source of carbon skeleton for amino acids synthesis. Additionally, the correlations of total amino acids and soluble sugars with proteins (r_s = 0.7 and 0.79, respectively) and cyanophycin (r_s = -0.82 and -0.62, respectively) indicate that protein synthesis was the main sink of these metabolites. Moreover, positive correlations between arginine, proteins and biomass, at this stage, were observed (Figure 3.12; Supplemental Figures 3.3 and 3.4).

As the photoassimilates were not used for growth, we observed an accumulation of soluble sugars, concomitant to an accumulation of amino acids, and enhanced export of sugars to the culture medium (Figure 3.12). Because of the higher export of sugars to the medium under HL than ML, the levels of sucrose in cells under HL were much lower than under ML (Figure 3.5E).

	Day			Night		
	Biomass	*A*	Total amino acids	Biomass	*A*	Total amino acids
Biomass						
A	0.36			0.36		
Total amino acids	-0.02	**0.68**		0.30	**0.88**	
Cell number				-0.28	-0.21	-0.41
Chlorophyll	0.37	-0.55	**-0.83**	0.61	-0.22	-0.24
Phycocyanin	**0.82**	0.02	-0.21	**0.90**	0.20	0.12
Proteins	0.59	**0.71**	**0.70**	**0.96**	0.47	0.39
Cyanophycin	0.36	-0.50	**-0.82**	0.41	-0.49	**-0.67**
Glycogen	0.50	-0.10	0.10	0.55	-0.30	-0.35
Total soluble sugars (cell)	0.14	**0.88**	**0.85**	0.48	**0.88**	**0.87**
Sucrose	0.49	-0.35	-0.61	0.44	-0.36	-0.45
Total soluble sugars (medium)				0.15	**0.78**	**0.71**
Maltose	0.45	-0.27	-0.62	0.55	-0.17	-0.09
Citrate	0.04	-0.37	**-0.82**	0.21	-0.50	-0.56
Isocitrate	-0.12	-0.38	**-0.67**	0.09	-0.54	-0.52
Glutamate	-0.04	**-0.68**	**-0.81**	-0.19	**-0.78**	**-0.77**
Ornithine	0.33	0.62	0.19	0.58	0.30	0.26
Aspartate	-0.05	0.44	0.28	0.15	0.31	0.49
Arginine	0.35	0.28	0.02	**0.67**	0.32	0.37
Fumarate	0.26	0.22	-0.28	0.41	-0.04	-0.12
Malate	0.14	-0.02	-0.14	0.41	-0.01	-0.08
Proline	0.32	**0.78**	**0.75**	0.31	**0.88**	**0.98**
Leucine	-0.01	**0.72**	0.59	0.27	0.45	0.58
Isoleucine	0.14	**0.78**	0.58	0.31	0.44	0.54
Valine	0.16	0.53	0.31	0.28	0.39	0.55
Alanine	0.04	**0.85**	**0.73**	0.43	0.48	0.62
Glycine	0.14	**0.68**	0.49	0.28	0.45	0.59
Serine	-0.05	0.42	0.20	0.15	0.07	0.16
Tyrosine	0.03	0.47	0.13	0.36	0.30	0.24
Lysine	-0.10	0.45	0.20	0.19	0.36	0.41
Tryptophan	0.05	0.33	0.05	0.21	-0.24	-0.28
Phenylalanine	0.16	**0.76**	0.54	0.42	0.44	0.59
Glycolate	0.28	0.43	0.60	0.30	0.37	0.56
Glycerate	-0.07	-0.09	0.05	-0.22	-0.49	-0.42
Nicotinate	0.54	0.59	**0.66**	0.32	**0.72**	**0.92**
Nicotinamide	0.48	-0.13	-0.42	0.49	-0.03	0.08
Alpha-tocopherol	**0.75**	0.27	-0.08	**0.84**	0.58	0.60

Figure 3-12: Spearman's rank coefficient of correlation among parameters determined three days after the onset of the stationary phase

Correlation between biomass, photosynthetic rate (*A*) and total amino acids, and metabolites levels determined at the end of the day and end of the night in cells three days after the onset of the stationary phase. Total soluble sugars (medium) was determined only at the end of the night. Significant correlations at 5% probability are highlighted in green (positive) and red (negative). Additional correlations between all growth, physiologic and metabolic traits are present in Supplemental Figures 3.3 and 3.4.

Sucrose is described as a compatible solute, with no net charge, and it is proposed that it can be accumulated without interfering in the cellular homeostasis (Brown, 1976; Mackay et al., 1984; Mikkat et al., 1997; Miao et al., 2003; Hagemann, 2011). Our data suggest that sucrose might, however, have an effect on cellular homeostasis, and in particular photosynthesis, possibly by sugar feedback inhibition (Stitt et al., 1991; Oswald et al., 2001). Indeed, in contrast to ML, cells grown under HL could maintain a high level of photosynthesis while exporting larger amount of sucrose in the medium and accumulating a much lower amount of sucrose within their cells. Altogether, the correlations suggest that stationary phase was not achieved due to a limitation in the availability of building blocks and/or energy necessary for maintaining cell division.

Considering that the metabolism is not controlling the rate of cell division, we tested whether already known factors were responsible such as: (*i*) nutrient starvation (Lazazzera, 2000; Berla and Pakrasi, 2012), (*ii*) quorum sensing (Sharif et al., 2008), and (*iii*) reduction of light quality and intensity available to the cells due to high cell density (self-shading) (Raven and Kübler, 2002; Ort et al., 2011; Lea-Smith et al., 2014).

Nutrient deficiency could not account for the gradual decrease of cell division rate because (1) a whole culture which had reached stationary phase did not re-start its growth when transferred to a fresh medium; and (2) when we grew an inoculum into the medium obtained from a culture at stationary phase, the inoculum could grow at the same rate as in fresh medium, and an inhibition of growth was observed only if we attempted to re-use the medium a third time (Figure 3.6; Tables 3.12 and 3.13). For the same reason, low cell viability could not account for the decrease in cell division. Our conclusion differs from that of Schuurmans et al. (2017) who concluded that the transition to stationary phase is caused by nutrient limitation. However, the authors artificially stopped growth by bubbling cultures with nitrogen gas (N_2), which deprived cells from CO_2 and O_2, and indeed led to carbon starvation and growth arrest. However, it does not mean a culture not deprived of CO_2 and O_2 would reach stationary phase for the same reason.

Quorum sensing is unlikely responsible because (1) an inoculum could grow normally on a medium obtained from a culture which had reached stationary phase (Tables 3.12 and 3.13); and (2) an inoculum in a microtube fixed at bottom of a culture which had reached stationary phase could grow almost normally under ML, and normally under HL (Table 3.14). This second observation also led us to conclude that light intensity and quality had a minor impact on the onset of stationary phase. Moreover, cell density reached at stationary phase was the same for 9 out of the 10 growth conditions we tested,

thus independent from the two contrasting light intensities we applied (Figure 3.1; Table 3.2). Schuurmans et al. (2017) showed that a gradual increase of light intensity can lead cells to divide faster and avoid a linear phase. Based on this observation, the authors affirmed that the decrease of cell division from log to linear phase is solely caused by light limitation (self-shading). The authors used 30 µmol photons m^{-2} s^{-1} and indeed cells might have been light limited, thus leading to lower CO_2 assimilation and limitation of photoassimilates available for growth. Moreover, the authors stopped their experiment after 72 h by bubbling N_2 which led to acute carbon starvation and growth arrest, while in our study we observed delayed growth due to cell density after 72-96 h of growth. Based on our results, we suggest that cells can continue growing after 72 h and then will exhibit a gradual decrease in their growth rates, reaching linear phase before the onset of stationary phase, irrespective of the light intensity.

Our results indicate that cell density may affect negatively the growth rates of cultures at relatively high densities as an artificial increase of density by 10 times led to a decrease in the daily growth rate by 58% after 24 h ($p<0.001$), and 77% after 48 h ($p<0.0001$; Figure 3.7C and D). Moreover, cell density seems to be involved in the control of the growth rates as demonstrated by fed-batch data. Indeed, we could stabilise cell division over several days by maintaining cells at two given densities, applying different dilution rates. Interestingly, a dilution rate of 0.5 time per day led to a division rate of 0.5 time per day, while a dilution rate of 2 times per day, led to two divisions per day (Figure 3.8B and D), which is close to the maximal division rates we observed in our batch cultures and in line with Kim et al. (2011). Moreover, when applying a dilution rate of 2 times, we first observed higher division rates (around four divisions per day), which is close to those reported by Hihara et al. (2001) and Zavřel et al. (2015). This fast growth rate led to an increase in the density of the culture before the division rates stabilise and quantitatively counterbalance the daily dilution applied. Altogether, these data suggest that cell density is involved in the control of the division rates in *Synechocystis*.

It is important to highlight that the observations in fed-batch cultures are not an effect of fresh nutrients on growth since previous data indicate that medium from a culture at stationary phase contain enough nutrients to support a second entire growth cycle with similar growth rates (Figure 3.6). Even though self-shading showed moderate effect at ML (Table 3.14), we propose that a cell-cell interaction process (Belas, 2014; Ellison and Brun, 2015), is involved in the control of cell division rate, and that this mechanism may be responsible for the gradual decrease in daily growth rates until the onset of stationary

phase when cells are cultured in batch. At stationary phase, cells can still divide at very slow rates and reach higher densities. Cultures maintained for 24 days after the onset of stationary phase reached cell densities around 1.2 x 10^9 cell mL^{-1} (Figure 3.6). However, during this period, cells only divided 3.5 times.

Even though our data suggest that a mechanism involving cell-cell interaction is possibly involved in the control of division rates of *Synechocystis* when grown planktonically, this regulation seems absent when cells are grown on agar. Indeed, *Synechocystis* normally forms dense colonies on agar, exhibiting log growth and fast doubling times of approximately 8 h (Law et al., 2000; Lamb et al., 2014). This observation suggests that *Synechocystis* growth regulation differs when cultured on agar surface or in liquid. Data from the literature show that heterotrophic bacteria exhibit different gene expression patterns in biofilm and in planktonic growth (Imanaka et al., 2010; He and Ahn, 2011; Romero-Lastra et al., 2017). Among the genes that are upregulated under biofilm conditions some encode proteins located in the outer membrane, cell envelope and involved in transport or binding (Romero-Lastra et al., 2017). Furthermore, a significant number of the genes differentially expressed encode for proteins of unknown functions (Imanaka et al., 2010). Compared to heterotrophic bacteria, there is little information about biofilm formation in cyanobacteria (Parnasa et al., 2016). However recent studies have shown that *Synechocystis* and *Synechococcus elongatus* PCC 7942 also exhibit variations in gene expression pattern when grown on solid surface or in liquid (Nakasugi and Neilan, 2005; Schatz et al., 2013; Agostoni et al., 2016). Interestingly, the *Synechocystis* strain used in the present study, which is not identified as "glucose tolerant", grew well in liquid BG11 supplemented with glucose concentrations from 0.2 mM to 20 mM (Figure 3.13). Moreover, as observed by Williams (1988), colonies of the strain could not grow on agar containing more than 0.2 mM glucose (Figure 3.13). It is thus possible that *Synechocystis* exhibits variations in its regulation of growth when grown on solid or liquid medium and that the control of growth via cell-cell interaction we observed in liquid medium does not occur on solid medium.

This process of cell-cell interaction might be a strategy to avoid competition for nutrients and light, thus starvation and death. If cells keep a constant rate of cell division they would become limited by light and nutrients due to depletion of the nutrients in the environment and self-shading. Thus, they would die due to starvation, since their cellular reserves are finite. Hence, a natural selection of individuals able to sense a gradual increase in density and regulate their division rates accordingly may have occurred.

Besides, cells which did not have this mechanism and exhibited an unrestricted growth would be probably more susceptible to environmental variations as they would likely have less reserves to buffer environmental variations. Our conclusions therefore significantly vary from what is usually observed in non-photosynthetic bacteria, where starvation and quorum sensing are responsible for the onset of stationary phase (Lazazzera, 2000; Shiloach and Fass, 2005).

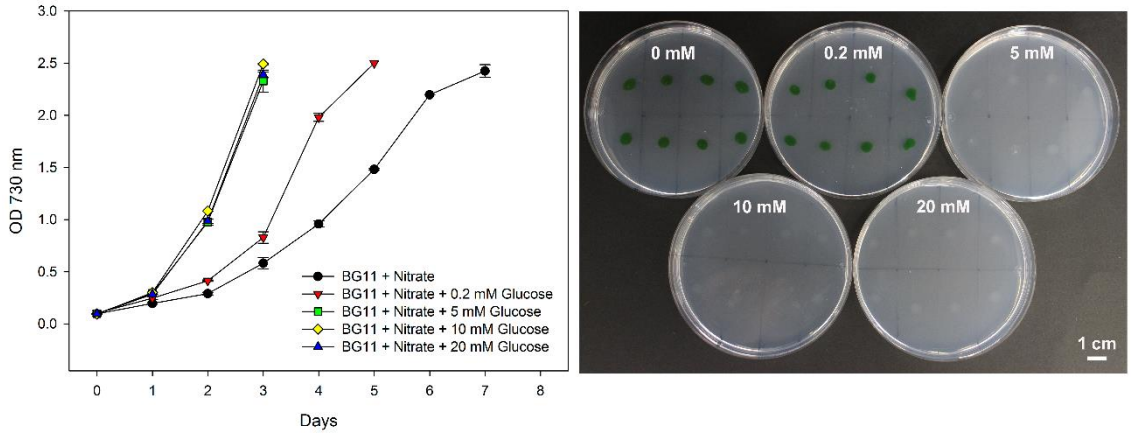

Figure 3-13: Glucose tolerance test with *Synechocystis* sp. PCC 6803.
Synechocystis was cultured in mixotrophic conditions in liquid (left) and agar (right) BG-11 supplemented with nitrate and different glucose concentrations.

3.4 Conclusion

Our data suggest that cell-cell interaction is possibly affecting growth, and promoting a gradual decrease of the division rate during the log phase. As a consequence, the photoassimilates start to be stored instead of used for growth, leading to a decoupling between growth and photosynthesis. This storage of metabolites decreases the cellular sink capacity, and cells start to export sugars to the medium as an alternative to avoid an inhibition of photosynthesis by negative feedback. As the growth rates in batch cultures seem to be primarily regulated by cell density, dilutions are necessary to maintain fast division rates for a long period. Our conclusions have not only biotechnological implications, but also suggest that studies investigating major drivers of the metabolic control of growth should be performed with care at culture densities where a possible growth inhibition by cell density do not occur, ideally in fed-batch or continuous cultures in order to control precisely cell densities and then cell division rates. Another outcome of this study is that urea is a valuable nitrogen source, as we could get high division rates and short growth cycles. This nitrogen source can be an alternative to grow some cyanobacteria as an economically viable biomass production since urea is cheaper than

ammonium and nitrate, its transport does not require metabolic energy, and during its assimilation there is a release of CO_2 into to the cell.

3.5 Supplemental material

Supplemental table 1: Primers used in this chapter

Gene	Primer name	Sequence	Forward/Reverse
ntcA	RS007	AGTGTTTCGACGCTTAGGCA	Forward
	RS008	CTTAACAGCCCCCTTGAGCA	Reverse
pII	RS009	TCGACGAAGGACAGGTTGAC	Forward
	RS010	CCACCGGGCTGATGAAGATT	Reverse
rnpB	RS013	CAAACTTGCTGGGTAACGCC	Forward
	RS014	GGGCGGTATTTTTCTGTGGC	Reverse
ftsZ	RS015	ACTTTTGCCAGCCCTAGTCC	Forward
	RS016	CCCACTGGCAATCATACGGT	Reverse

	Gt	Biomass	*A*	Cell number	Chlorophyll a	Phycocyanin	Proteins	Total amino acids	Cyanophycin	Glycogen	Total soluble sugars (cell)	Sucrose	Maltose	Citrate	Isocitrate	Glutamate	Ornithine	Aspartate	Arginine	Fumarate	Malate	Proline	Leucine	Isoleucine	Valine	Alanine	Glycine
Gt																											
Biomass	0.71																										
A	0.33	0.04																									
Cell number	-0.93	-0.56	-0.35																								
Chlorophyll a	0.56	0.72	0.04	-0.43																							
Phycocyanin	0.36	0.53	0.27	-0.33	0.38																						
Proteins	0.85	0.56	0.52	-0.90	0.45	0.28																					
Total amino acids	0.33	-0.09	0.72	-0.42	-0.27	-0.05	0.61																				
Cyanophycin	0.16	-0.21	0.25	-0.31	-0.04	0.24	0.43	0.41																			
Glycogen	-0.27	-0.37	-0.26	0.13	-0.71	-0.64	-0.13	0.35	-0.15																		
Total soluble sugars (cell)	0.56	0.26	0.38	-0.72	0.08	0.33	0.82	0.59	0.77	0.01																	
Sucrose	0.68	0.63	0.08	-0.52	0.63	-0.19	0.52	0.03	-0.35	-0.14	0.03																
Maltose	0.18	0.52	-0.45	-0.20	0.70	0.21	0.15	-0.55	-0.02	-0.35	0.07	0.24															
Citrate	0.38	0.59	-0.16	-0.48	0.60	0.10	0.48	-0.13	-0.03	-0.07	0.31	0.41	0.85														
Isocitrate	0.25	0.46	-0.43	-0.10	0.76	-0.18	0.14	-0.46	-0.18	-0.30	-0.17	0.63	0.76	0.62													
Glutamate	0.56	0.72	-0.03	-0.56	0.76	0.08	0.59	-0.08	-0.10	-0.21	0.28	0.67	0.79	0.94	0.73												
Ornithine	0.38	0.44	-0.27	-0.48	0.54	-0.12	0.38	-0.27	-0.07	-0.05	0.22	0.52	0.81	0.90	0.67	0.88											
Aspartate	0.50	0.38	-0.19	-0.57	0.20	-0.37	0.47	0.08	-0.18	0.38	0.28	0.64	0.40	0.69	0.43	0.71	0.82										
Arginine	-0.01	0.22	-0.31	-0.18	0.28	-0.15	0.13	-0.33	-0.10	0.08	0.13	0.19	0.76	0.84	0.46	0.72	0.89	0.65									
Fumarate	0.48	0.80	-0.14	-0.42	0.49	0.08	0.39	-0.21	-0.39	-0.04	0.15	0.67	0.58	0.73	0.51	0.81	0.73	0.73	0.63								
Malate	0.48	0.80	-0.14	-0.42	0.49	0.08	0.39	-0.21	-0.39	-0.04	0.15	0.67	0.58	0.73	0.51	0.81	0.73	0.73	0.63	1.00							
Proline	0.41	0.49	-0.24	-0.50	0.31	-0.13	0.38	-0.18	-0.19	0.15	0.27	0.52	0.61	0.81	0.44	0.79	0.92	0.91	0.84	0.86	0.86						
Leucine	0.36	0.31	-0.09	-0.50	0.03	-0.22	0.48	0.10	0.08	0.33	0.53	0.41	0.30	0.56	0.17	0.55	0.70	0.83	0.67	0.70	0.70	0.87					
Isoleucine	0.38	0.24	0.08	-0.52	-0.19	-0.22	0.49	0.32	0.05	0.47	0.55	0.35	-0.02	0.33	-0.10	0.34	0.45	0.75	0.43	0.59	0.59	0.72	0.94				
Valine	0.43	0.50	-0.22	-0.53	0.25	-0.14	0.45	-0.08	-0.09	0.22	0.39	0.52	0.54	0.76	0.39	0.74	0.85	0.91	0.78	0.86	0.86	0.98	0.94	0.82			
Alanine	0.09	0.14	-0.43	-0.23	-0.04	-0.38	0.05	-0.28	-0.26	0.40	0.08	0.30	0.43	0.57	0.28	0.49	0.78	0.84	0.80	0.65	0.65	0.91	0.83	0.71	0.88		
Glycine	0.38	0.50	-0.27	-0.45	0.37	-0.22	0.36	-0.20	-0.30	0.18	0.16	0.63	0.61	0.81	0.54	0.81	0.92	0.92	0.83	0.87	0.87	0.98	0.83	0.67	0.95	0.88	
Serine	0.42	0.60	-0.22	-0.47	0.52	-0.13	0.44	-0.16	-0.21	0.07	0.22	0.63	0.73	0.92	0.65	0.93	0.94	0.87	0.84	0.88	0.88	0.94	0.76	0.56	0.92	0.77	0.96
Tyrosine	0.31	0.39	-0.28	-0.44	0.21	-0.14	0.30	-0.22	-0.16	0.19	0.26	0.41	0.59	0.76	0.36	0.70	0.89	0.87	0.87	0.80	0.80	0.99	0.88	0.73	0.96	0.94	0.95
Lysine	0.24	0.60	-0.41	-0.26	0.72	0.27	0.21	-0.54	-0.04	-0.37	0.12	0.30	0.99	0.87	0.73	0.81	0.82	0.42	0.77	0.66	0.66	0.66	0.37	0.07	0.60	0.46	0.66
Tryptophan	0.20	0.09	-0.09	-0.45	-0.20	-0.13	0.43	0.22	0.33	0.45	0.67	0.03	0.22	0.49	-0.09	0.35	0.55	0.66	0.62	0.43	0.43	0.71	0.90	0.87	0.79	0.73	0.62
Phenylalanine	0.45	0.45	-0.14	-0.55	0.22	-0.16	0.50	-0.01	0.01	0.20	0.47	0.52	0.48	0.71	0.36	0.72	0.83	0.89	0.75	0.81	0.81	0.95	0.96	0.85	0.99	0.86	0.92
Glycolate	0.54	0.89	-0.30	-0.43	0.64	0.18	0.43	-0.21	-0.32	-0.07	0.14	0.68	0.64	0.71	0.65	0.79	0.61	0.60	0.43	0.87	0.87	0.65	0.47	0.33	0.67	0.40	0.71
Glycerate	0.41	0.84	-0.30	-0.26	0.66	0.13	0.33	-0.24	-0.35	-0.10	0.03	0.63	0.67	0.71	0.73	0.79	0.56	0.50	0.42	0.81	0.81	0.55	0.33	0.18	0.56	0.29	0.62
Nicotinate	0.58	0.82	-0.31	-0.48	0.82	0.21	0.38	-0.37	-0.30	-0.30	0.03	0.68	0.81	0.79	0.80	0.87	0.76	0.59	0.52	0.77	0.77	0.66	0.32	0.12	0.60	0.40	0.71
Nicotinamide	0.44	0.76	-0.36	-0.38	0.77	0.13	0.36	-0.43	-0.18	-0.28	0.13	0.63	0.88	0.84	0.83	0.90	0.84	0.61	0.68	0.84	0.84	0.76	0.52	0.26	0.73	0.52	0.79
Alpha-tocopherol	0.45	0.63	0.15	-0.37	0.87	0.28	0.47	-0.18	0.07	-0.64	0.21	0.51	0.75	0.72	0.72	0.84	0.66	0.30	0.50	0.57	0.57	0.47	0.22	-0.01	0.41	0.13	0.47
ntcA	0.16	0.58	-0.45	-0.14	0.70	0.26	0.09	-0.67	-0.08	-0.45	0.03	0.30	0.94	0.73	0.73	0.72	0.75	0.33	0.71	0.66	0.66	0.61	0.36	0.05	0.56	0.45	0.61
pII	0.31	0.81	-0.44	-0.22	0.60	0.42	0.10	-0.58	-0.38	-0.28	-0.05	0.35	0.78	0.67	0.55	0.66	0.59	0.37	0.52	0.79	0.79	0.60	0.28	0.10	0.55	0.41	0.60

Supplemental Figure 3.1: Spearman's rank coefficient of correlation between all growth, physiologic, metabolic and molecular traits determined at the end of the day on the fourth day of culture (log phase). Significant correlations at 5% probability are highlighted in green (positive) and red (negative). Continue on page 73.

Continuing from page 72.

Serine	Tyrosine	Lysine	Tryptophan	Phenylalanine	Glycolate	Glycerate	Nicotinate	Nicotinamide	Alpha-tocopherol	*ntcA*	*pII*	
												Gt
												Biomass
												A
												Cell number
												Chlorophyll a
												Phycocyanin
												Proteins
												Total amino acids
												Cyanophycin
												Glycogen
												Total soluble sugars (cell)
												Sucrose
												Maltose
												Citrate
												Isocitrate
												Glutamate
												Ornithine
												Aspartate
												Arginine
												Fumarate
												Malate
												Proline
												Leucine
												Isoleucine
												Valine
												Alanine
												Glycine
												Serine
0.89												Tyrosine
0.77	0.64											Lysine
0.56	0.76	0.27										Tryptophan
0.88	0.94	0.54	0.82									Phenylalanine
0.78	0.56	0.70	0.24	0.60								Glycolate
0.75	0.45	0.71	0.10	0.49	0.96							Glycerate
0.79	0.58	0.83	0.09	0.53	0.89	0.87						Nicotinate
0.88	0.70	0.92	0.28	0.68	0.88	0.87	0.93					Nicotinamide
0.64	0.38	0.76	0.02	0.42	0.54	0.61	0.71	0.77				Alpha-tocopherol
0.70	0.60	0.96	0.21	0.52	0.66	0.67	0.77	0.90	0.74			*ntcA*
0.66	0.56	0.83	0.13	0.45	0.84	0.82	0.85	0.84	0.54	0.83		*pII*

	Gt	Biomass	*A*	Cell number	Chlorophyll a	Phycocyanin	Proteins	Total amino acids	Cyanophycin	Glycogen	% degraded glycogen	Total soluble sugars (cell)	Sucrose	Total soluble sugars (media)	Maltose	Citrate	Isocitrate	Glutamate	Ornithine	Aspartate	Arginine	Fumarate	Malate	Proline	Leucine	Isoleucine	Valine	Alanine
Gt																												
Biomass	0.71																											
A	0.33	0.04																										
Cell number	-0.93	-0.56	-0.35																									
Chlorophyll a	0.54	0.75	-0.03	-0.35																								
Phycocyanin	0.12	0.05	0.37	-0.18	-0.01																							
Proteins	0.94	0.59	0.41	-0.88	0.54	-0.02																						
Total amino acids	0.36	0.12	0.75	-0.41	-0.20	0.05	0.49																					
Cyanophycin	0.50	0.24	0.55	-0.55	0.25	0.19	0.62	0.52																				
Glycogen	0.70	0.66	0.02	-0.72	0.21	-0.24	0.55	0.25	0.16																			
% degraded glycogen	-0.90	-0.84	-0.14	0.84	-0.49	-0.12	-0.76	-0.28	-0.33	-0.85																		
Total soluble sugars (cell)	0.66	0.21	0.73	-0.71	0.20	0.10	0.78	0.73	0.73	0.36	-0.48																	
Sucrose	0.68	0.52	-0.14	-0.08	0.24	0.63	-0.14	-0.24	-0.30	0.19	-0.41	-0.30																
Total soluble sugars (media)	0.27	-0.01	0.26	-0.42	-0.24	-0.20	0.27	0.47	0.21	0.59	-0.37	0.61	-0.19															
Maltose	-0.39	0.03	-0.43	0.28	0.27	0.05	-0.44	-0.68	-0.20	-0.20	0.28	-0.49	0.24	-0.35														
Citrate	0.64	0.44	0.27	-0.75	0.48	-0.18	0.77	0.41	0.54	0.50	-0.53	0.72	-0.24	0.43	0.01													
Isocitrate	-0.21	0.08	-0.38	0.24	0.47	-0.30	-0.20	-0.61	0.04	-0.05	0.15	-0.19	-0.08	-0.03	0.72	0.12												
Glutamate	0.20	0.47	0.15	-0.13	0.76	0.38	0.20	-0.25	0.39	-0.16	-0.13	0.07	0.30	-0.47	0.58	0.26	0.50											
Ornithine	-0.25	-0.18	-0.09	0.01	-0.03	0.08	-0.24	-0.32	0.31	-0.08	0.25	-0.08	-0.14	-0.01	0.75	0.19	0.59	0.42										
Aspartate	-0.38	-0.68	0.37	0.19	-0.72	-0.04	-0.35	0.21	0.13	-0.13	0.44	0.18	-0.46	0.47	-0.10	-0.19	-0.02	-0.41	0.38									
Arginine	-0.20	-0.44	-0.07	-0.10	-0.52	0.04	-0.21	-0.13	0.21	0.02	0.25	-0.07	-0.30	0.13	0.31	0.03	0.08	-0.13	0.77	0.61								
Fumarate	0.59	0.60	0.20	-0.65	0.58	-0.17	0.66	0.25	0.31	0.50	-0.51	0.44	-0.04	0.11	0.19	0.88	0.08	0.40	0.17	-0.38	-0.04							
Malate	0.67	0.56	0.42	-0.73	0.47	-0.18	0.76	0.49	0.42	0.59	-0.58	0.66	-0.14	0.35	-0.05	0.92	-0.04	0.25	0.05	-0.20	-0.07	0.95						
Proline	0.35	0.04	0.56	-0.55	0.18	0.33	0.49	0.42	0.76	0.02	-0.14	0.70	-0.24	0.21	0.12	0.71	0.03	0.44	0.52	0.19	0.38	0.54	0.59					
Leucine	0.14	-0.16	0.43	-0.35	-0.38	-0.02	0.08	0.27	0.33	0.43	-0.13	0.42	-0.24	0.66	-0.05	0.21	0.04	-0.21	0.47	0.79	0.64	0.07	0.25	0.37				
Isoleucine	-0.07	-0.42	0.39	-0.14	-0.47	0.07	-0.10	0.14	0.27	0.15	0.12	0.35	-0.30	0.60	-0.01	0.04	0.13	-0.21	0.50	0.90	0.65	-0.17	0.01	0.35	0.94			
Valine	0.05	-0.27	0.35	-0.26	-0.48	-0.08	-0.01	0.21	0.25	0.38	-0.04	0.33	-0.30	0.65	-0.08	0.12	0.03	-0.32	0.44	0.84	0.67	-0.04	0.14	0.27	0.99	0.95		
Alanine	0.07	-0.12	0.27	-0.31	-0.42	-0.14	0.04	0.36	0.35	0.50	-0.16	0.41	-0.24	0.79	-0.04	0.30	0.08	-0.31	0.47	0.72	0.60	0.08	0.26	0.35	0.92	0.83	0.90	
Glycine	-0.16	-0.32	0.35	0.01	-0.18	0.02	-0.19	-0.10	0.16	0.02	0.24	0.20	-0.24	0.36	0.35	0.08	0.43	0.13	0.65	0.76	0.54	0.01	0.09	0.36	0.81	0.88	0.79	0.64
Serine	-0.01	-0.30	0.31	-0.20	-0.05	0.16	-0.01	-0.16	0.26	-0.03	0.18	0.26	-0.24	0.21	0.42	0.26	0.37	0.27	0.73	0.59	0.65	0.20	0.21	0.59	0.70	0.77	0.67	0.49
Tyrosine	-0.27	-0.65	0.30	0.05	-0.81	-0.09	-0.24	0.28	0.19	-0.02	0.35	0.16	-0.52	0.43	-0.22	-0.15	-0.20	-0.53	0.35	0.94	0.73	-0.33	-0.16	0.19	0.78	0.83	0.84	0.73
Lysine	-0.36	-0.20	-0.03	0.16	0.08	0.09	-0.30	-0.31	0.30	-0.25	0.36	-0.04	-0.14	-0.02	0.78	0.18	0.71	0.53	0.94	0.35	0.55	0.12	0.02	0.52	0.33	0.43	0.30	0.36
Tryptophan	-0.07	-0.45	0.62	-0.08	-0.71	-0.02	-0.03	0.59	0.14	0.08	0.18	0.36	-0.41	0.45	-0.48	-0.05	-0.50	-0.54	-0.01	0.82	0.41	-0.14	0.09	0.19	0.72	0.70	0.75	0.61
Phenylalanine	-0.07	-0.31	0.43	-0.18	-0.43	0.02	-0.09	0.24	0.22	0.25	0.07	0.37	-0.24	0.66	0.08	0.19	0.12	-0.19	0.53	0.85	0.61	0.04	0.20	0.41	0.95	0.95	0.94	0.89
Glycolate	0.22	0.32	-0.38	-0.13	0.64	-0.22	0.12	-0.68	-0.15	0.26	-0.24	-0.12	0.14	-0.01	0.50	0.19	0.76	0.41	0.25	-0.26	-0.09	0.25	0.13	-0.12	0.02	0.03	0.01	-0.09
Glycerate	0.10	0.47	-0.36	-0.07	0.70	0.14	-0.01	-0.67	0.02	0.05	-0.16	-0.30	0.41	-0.42	0.82	0.15	0.71	0.81	0.53	-0.45	0.04	0.36	0.12	0.12	-0.18	-0.20	-0.24	-0.24
Nicotinate	0.45	0.67	0.07	-0.31	0.96	0.13	0.44	-0.24	0.22	0.13	-0.39	0.19	0.30	-0.26	0.42	0.47	0.50	0.85	0.12	-0.61	-0.42	0.60	0.48	0.28	-0.28	-0.35	-0.39	-0.37
Nicotinamide	0.13	0.58	-0.04	-0.08	0.77	0.19	0.12	-0.28	0.08	-0.02	-0.16	-0.09	0.41	-0.42	0.70	0.35	0.49	0.88	0.33	-0.56	-0.24	0.59	0.39	0.28	-0.32	-0.39	-0.43	-0.33
Alpha-tocopherol	0.71	0.71	0.28	-0.56	0.84	0.30	0.64	-0.08	0.43	0.27	-0.58	0.33	0.30	-0.25	0.15	0.42	0.22	0.78	0.07	-0.49	-0.25	0.56	0.49	0.36	-0.07	-0.18	-0.18	-0.26
ntcA	-0.42	-0.22	0.20	0.49	0.03	0.36	-0.37	-0.16	-0.26	-0.73	0.56	-0.37	0.14	-0.77	0.27	-0.38	-0.13	0.39	-0.02	-0.12	-0.16	-0.08	-0.21	-0.01	-0.42	-0.31	-0.43	-0.61
pII	-0.10	0.19	0.24	-0.03	0.12	0.21	-0.03	0.16	0.25	-0.14	0.13	-0.05	0.08	-0.39	0.48	0.26	-0.01	0.53	0.49	-0.09	0.27	0.51	0.38	0.50	-0.01	-0.13	-0.09	0.01

Supplemental Figure 3.2: Spearman's rank coefficient of correlation between all growth, physiologic, metabolic and molecular traits determined at the end of the night on the fourth day of culture (log phase). Significant correlations at 5% probability are highlighted in green (positive) and red (negative). Continue on page 75.

Continuing from page 74.

Glycine	Serine	Tyrosine	Lysine	Tryptophan	Phenylalanine	Glycolate	Glycerate	Nicotinate	Nicotinamide	Alpha-tocopherol	*ntcA*	*pII*	
													Gt
													Biomass
													A
													Cell number
													Chlorophyll a
													Phycocyanin
													Proteins
													Total amino acids
													Cyanophycin
													Glycogen
													% degraded glycogen
													Total soluble sugars (cell)
													Sucrose
													Total soluble sugars (media)
													Maltose
													Citrate
													Isocitrate
													Glutamate
													Ornithine
													Aspartate
													Arginine
													Fumarate
													Malate
													Proline
													Leucine
													Isoleucine
													Valine
													Alanine
													Glycine
0.90													**Serine**
0.59	0.48												**Tyrosine**
0.65	**0.68**	0.21											**Lysine**
0.48	0.35	**0.85**	-0.10										**Tryptophan**
0.88	**0.76**	**0.77**	0.47	**0.71**									**Phenylalanine**
0.31	0.35	-0.39	0.27	-0.53	-0.01								**Glycolate**
0.15	0.28	-0.54	0.54	**-0.71**	-0.18	**0.73**							**Glycerate**
0.01	0.14	**-0.75**	0.24	**-0.64**	-0.28	**0.65**	**0.77**						**Nicotinate**
0.01	0.13	**-0.68**	0.44	-0.62	-0.25	0.44	**0.83**	**0.87**					**Nicotinamide**
0.04	0.21	-0.53	0.07	-0.38	-0.19	0.52	**0.64**	**0.87**	**0.65**				**Alpha-tocopherol**
-0.03	0.04	-0.21	0.09	-0.04	-0.28	-0.20	0.15	0.18	0.38	0.12			***ntcA***
0.08	0.20	-0.05	0.47	0.01	0.05	-0.27	0.33	0.25	0.61	0.21	0.50		***pII***

	Biomass	A	Total amino acids	Cell number	Chlorophyll	Phycocyanin	Proteins	Cyanophycin	Glycogen	Total soluble sugars (cell)	Sucrose	Maltose	Citrate	Isocitrate	Glutamate	Ornithine	Aspartate	Arginine	Fumarate	Malate	Proline	Leucine	Isoleucine	Valine
Biomass																								
A	0.36																							
Total amino acids	-0.02	**0.68**																						
Cell number	-0.28	-0.21	-0.42																					
Chlorophyll	0.37	-0.55	**-0.83**	0.09																				
Phycocyanin	**0.82**	0.02	-0.21	-0.26	0.55																			
Proteins	0.59	**0.71**	**0.70**	-0.49	-0.31	0.35																		
Cyanophycin	0.36	-0.50	**-0.82**	0.24	**0.96**	0.54	-0.36																	
Glycogen	0.50	-0.10	0.10	**-0.64**	0.31	**0.66**	0.44	0.27																
Total soluble sugars (cell)	0.14	**0.88**	**0.85**	-0.21	**-0.66**	-0.10	**0.79**	-0.62	-0.01															
Sucrose	0.49	-0.35	-0.61	0.14	**0.81**	**0.77**	-0.12	**0.84**	0.47	-0.45														
Maltose	0.45	-0.27	-0.62	0.13	**0.72**	**0.65**	-0.18	**0.77**	0.41	-0.48	**0.94**													
Citrate	0.04	-0.37	**-0.82**	0.42	**0.66**	0.08	**-0.64**	**0.75**	-0.14	**-0.65**	0.56	**0.71**												
Isocitrate	-0.12	-0.38	**-0.67**	0.37	0.50	-0.07	**-0.73**	0.61	-0.21	**-0.65**	0.42	0.56	**0.93**											
Glutamate	-0.04	**-0.68**	**-0.81**	0.18	**0.77**	0.36	-0.53	**0.77**	0.31	**-0.71**	**0.77**	**0.77**	**0.67**	0.53										
Ornithine	0.33	0.62	0.19	0.31	-0.12	0.28	0.25	0.07	-0.12	0.45	0.30	0.33	0.18	0.18	-0.12									
Aspartate	-0.05	0.44	0.28	0.10	-0.37	-0.09	0.01	-0.19	-0.04	0.28	0.05	0.26	0.24	0.36	-0.07	**0.72**								
Arginine	0.35	0.28	0.02	0.42	-0.02	0.48	0.16	0.15	0.09	0.20	0.52	0.52	0.14	0.07	0.15	**0.82**	0.58							
Fumarate	0.26	0.22	-0.28	0.45	0.12	0.19	-0.27	0.32	-0.21	-0.12	0.32	0.47	0.62	0.62	0.14	**0.70**	**0.64**	0.62						
Malate	0.14	-0.02	-0.14	0.37	-0.03	0.22	-0.24	0.18	0.10	-0.19	0.37	0.50	0.41	0.44	0.24	0.52	**0.68**	**0.73**	**0.79**					
Proline	0.32	**0.78**	**0.75**	-0.36	**-0.65**	0.13	**0.79**	**-0.68**	0.13	**0.77**	-0.30	-0.24	**-0.64**	**-0.68**	-0.59	0.35	0.30	0.32	-0.10	-0.01				
Leucine	-0.01	**0.72**	0.59	0.04	**-0.67**	-0.19	0.33	-0.50	-0.08	**0.67**	-0.36	-0.21	-0.19	-0.15	-0.44	0.60	**0.73**	0.45	0.48	0.48	0.55			
Isoleucine	0.14	**0.78**	0.58	-0.02	**-0.66**	-0.05	0.38	-0.52	-0.09	**0.66**	-0.35	-0.21	-0.24	-0.21	-0.50	0.61	**0.66**	0.48	0.52	0.47	**0.64**	**0.96**		
Valine	0.16	0.53	0.31	0.20	-0.44	0.09	0.09	-0.24	-0.10	0.35	-0.08	0.03	0.02	0.09	-0.28	**0.70**	**0.72**	**0.66**	**0.77**	**0.76**	0.36	**0.84**	**0.89**	
Alanine	0.04	**0.85**	**0.73**	-0.08	**-0.82**	-0.30	0.44	**-0.72**	-0.27	**0.76**	-0.62	-0.49	-0.39	-0.31	**-0.78**	0.47	0.54	0.21	0.31	0.20	**0.68**	**0.88**	**0.92**	**0.72**
Glycine	0.14	**0.68**	0.49	-0.04	-0.54	-0.03	0.25	-0.36	-0.02	0.53	-0.25	-0.10	-0.07	0.02	-0.41	**0.64**	**0.76**	0.45	**0.64**	0.58	0.44	**0.94**	**0.95**	**0.93**
Serine	-0.05	0.42	0.20	0.33	-0.33	-0.16	-0.07	-0.09	-0.15	0.28	-0.03	0.14	0.30	0.38	-0.12	**0.71**	**0.88**	0.56	**0.78**	**0.75**	0.12	**0.83**	**0.75**	**0.84**
Tyrosine	0.03	0.47	0.13	0.50	-0.30	-0.10	-0.03	-0.05	-0.27	0.32	-0.01	0.13	0.28	0.30	-0.14	**0.77**	**0.76**	**0.66**	**0.83**	**0.72**	0.15	**0.82**	**0.77**	**0.87**
Lysine	-0.10	0.45	0.20	0.49	-0.37	-0.44	0.10	-0.20	-0.36	0.43	-0.28	-0.13	0.18	0.12	-0.28	0.44	0.49	0.28	0.47	0.35	0.16	**0.71**	0.59	0.49
Tryptophan	0.05	0.33	0.05	0.52	-0.27	-0.07	-0.05	-0.04	-0.19	0.21	-0.01	0.13	0.26	0.22	-0.08	0.60	0.62	**0.64**	**0.79**	**0.78**	0.13	**0.78**	**0.75**	**0.85**
Phenylalanine	0.16	**0.76**	0.54	-0.03	**-0.64**	-0.07	0.39	-0.50	-0.07	**0.64**	-0.37	-0.22	-0.22	-0.24	-0.49	0.53	0.59	0.42	0.49	0.44	0.62	**0.95**	**0.99**	**0.85**
Glycolate	0.28	0.43	0.60	-0.39	-0.27	0.13	0.42	-0.20	0.22	0.45	-0.26	-0.37	-0.42	-0.20	-0.60	0.22	0.13	-0.05	0.04	-0.03	0.16	0.30	0.33	0.33
Glycerate	-0.07	-0.09	0.05	-0.07	0.09	-0.16	-0.24	0.21	0.07	-0.14	-0.01	0.02	0.28	0.55	-0.09	0.10	0.32	-0.18	0.26	0.20	-0.45	0.04	-0.05	0.13
Nicotinate	0.54	0.59	**0.66**	-0.48	-0.28	0.18	**0.93**	-0.36	0.36	**0.68**	-0.26	-0.32	-0.62	**-0.68**	**-0.64**	0.02	-0.18	-0.10	-0.38	-0.37	**0.64**	0.18	0.21	-0.08
Nicotinamide	0.48	-0.13	-0.42	0.33	0.39	0.50	-0.21	0.55	0.20	-0.39	**0.66**	**0.75**	0.61	0.59	0.37	0.47	0.43	**0.65**	**0.79**	**0.85**	-0.19	0.12	0.15	0.50
Alpha-tocopherol	**0.75**	0.27	-0.08	0.03	0.28	0.44	0.45	0.26	0.09	0.16	0.12	0.01	-0.07	-0.26	-0.25	0.07	-0.47	0.04	0.10	-0.16	0.12	-0.09	0.04	0.01

Supplemental Figure 3.3: Spearman's rank coefficient of correlation between all growth, physiologic and metabolic traits determined at the end of the day in cells three days after the onset of the stationary phase. Significant correlations at 5% probability are highlighted in green (positive) and red (negative). Continue on page 77.

Continuing from page 76.

Alanine	Glycine	Serine	Tyrosine	Lysine	Tryptophan	Phenylalanine	Glycolate	Glycerate	Nicotinate	Nicotinamide	Alpha-tocopherol	
												Biomass
												A
												Total amino acids
												Cell number
												Chlorophyll
												Phycocyanin
												Proteins
												Cyanophycin
												Glycogen
												Total soluble sugars (cell)
												Sucrose
												Maltose
												Citrate
												Isocitrate
												Glutamate
												Ornithine
												Aspartate
												Arginine
												Fumarate
												Malate
												Proline
												Leucine
												Isoleucine
												Valine
0.84												Alanine
0.60	**0.85**											Glycine
0.61	**0.82**	**0.95**										Serine
0.59	0.56	**0.73**	**0.79**									Tyrosine
0.55	**0.77**	**0.88**	**0.95**	**0.78**								Lysine
0.90	**0.93**	**0.71**	**0.75**	0.62	**0.76**							Tryptophan
0.43	0.45	0.21	0.13	-0.03	0.03	0.28						Phenylalanine
0.02	0.22	0.38	0.19	0.09	0.07	-0.10	0.61					Glycolate
0.38	0.10	-0.19	-0.16	0.12	-0.16	0.25	0.48	-0.08				Glycerate
-0.09	0.30	0.49	0.50	0.15	0.55	0.14	-0.02	0.27	-0.27			Nicotinate
0.07	-0.03	-0.21	-0.01	0.10	0.08	0.12	0.24	-0.18	0.55	0.16		Nicotinamide
												Alpha-tocopherol

	Biomass	*A*	Total amino acids	Chlorophyll	Phycocyanin	Proteins	Cyanophycin	Glycogen	Total soluble sugars (cell)	Sucrose	Total soluble sugars (media)	Maltose	Citrate	Isocitrate	Glutamate	Ornithine	Aspartate	Arginine	Fumarate	Malate	Proline	Leucine	Isoleucine	Valine
Biomass																								
A	0.36																							
Total amino acids	0.30	**0.88**																						
Chlorophyll	0.61	-0.22	-0.24																					
Phycocyanin	**0.90**	0.20	0.12	0.54																				
Proteins	**0.96**	0.47	0.39	0.58	**0.90**																			
Cyanophycin	0.41	-0.49	**-0.67**	0.60	0.59	0.35																		
Glycogen	0.55	-0.30	-0.35	**0.70**	**0.76**	0.56	**0.81**																	
Total soluble sugars (cell)	0.48	**0.88**	**0.87**	0.03	0.32	0.55	-0.47	-0.10																
Sucrose	0.44	-0.36	-0.45	**0.76**	**0.65**	0.47	**0.81**	**0.96**	-0.15															
Total soluble sugars (media)	0.15	**0.78**	**0.71**	-0.50	0.08	0.26	-0.54	-0.30	0.60	-0.41														
Maltose	0.55	-0.17	-0.09	**0.81**	0.62	0.55	0.57	**0.84**	0.09	**0.81**	-0.36													
Citrate	0.21	-0.50	-0.56	0.62	0.42	0.19	**0.72**	**0.88**	-0.25	**0.92**	-0.47	**0.75**												
Isocitrate	0.09	-0.54	-0.52	0.55	0.28	0.09	0.55	**0.81**	-0.27	**0.84**	-0.37	**0.70**	**0.95**											
Glutamate	-0.19	**-0.78**	**-0.77**	0.44	0.08	-0.19	0.59	**0.65**	-0.56	**0.76**	**-0.65**	0.47	**0.84**	**0.87**										
Ornithine	0.58	0.30	0.26	0.45	**0.64**	**0.64**	0.19	**0.67**	0.55	0.62	0.30	**0.65**	0.60	0.61	0.22									
Aspartate	0.15	0.31	0.49	0.08	0.22	0.20	-0.21	0.25	0.56	0.18	0.13	0.52	0.26	0.27	0.02	0.60								
Arginine	**0.67**	0.32	0.37	0.42	**0.71**	**0.72**	0.16	**0.65**	0.59	0.54	0.31	0.62	0.49	0.49	0.10	**0.94**	0.59							
Fumarate	0.41	-0.04	-0.12	0.15	0.58	0.36	0.49	**0.68**	0.05	0.54	0.15	0.51	**0.65**	0.59	0.26	**0.67**	0.39	**0.66**						
Malate	0.41	-0.01	-0.08	0.20	0.60	0.38	0.47	**0.72**	0.12	0.60	0.15	0.59	**0.68**	**0.64**	0.31	**0.75**	0.50	**0.68**	**0.98**					
Proline	0.31	**0.88**	**0.98**	-0.20	0.09	0.37	**-0.70**	-0.39	**0.90**	-0.48	**0.67**	-0.10	-0.56	-0.53	**-0.78**	0.26	0.49	0.33	-0.14	-0.09				
Leucine	0.27	0.45	0.58	-0.07	0.28	0.27	-0.18	0.14	0.61	-0.01	0.24	0.36	0.09	0.02	-0.27	0.48	**0.88**	0.56	0.49	0.52	0.56			
Isoleucine	0.31	0.44	0.54	0.04	0.33	0.31	-0.15	0.21	**0.65**	0.10	0.21	0.46	0.19	0.13	-0.18	0.59	**0.94**	0.60	0.50	0.58	0.56	**0.96**		
Valine	0.28	0.39	0.55	0.07	0.30	0.28	-0.20	0.20	0.62	0.09	0.19	0.49	0.18	0.15	-0.15	0.58	**0.96**	0.59	0.45	0.54	0.58	**0.94**	**0.99**	
Alanine	0.43	0.48	0.62	0.05	0.48	0.48	-0.12	0.32	**0.67**	0.16	0.32	0.47	0.18	0.14	-0.19	**0.66**	**0.88**	**0.77**	0.54	0.58	0.58	**0.94**	**0.92**	**0.90**
Glycine	0.28	0.45	0.59	0.09	0.33	0.35	-0.16	0.25	0.62	0.15	0.21	0.54	0.16	0.14	-0.14	0.58	**0.96**	0.58	0.39	0.50	0.58	**0.90**	**0.95**	**0.96**
Serine	0.15	0.07	0.16	0.32	0.25	0.24	0.12	0.58	0.28	0.53	0.05	**0.70**	**0.64**	**0.68**	0.36	**0.77**	**0.76**	**0.72**	0.60	**0.66**	0.10	0.61	**0.65**	**0.66**
Tyrosine	0.36	0.30	0.24	0.41	0.39	0.41	0.07	0.52	0.56	0.53	0.19	0.62	0.59	0.59	0.24	**0.92**	**0.72**	**0.77**	0.56	**0.67**	0.28	0.55	**0.70**	**0.68**
Lysine	0.19	0.36	0.41	0.02	0.18	0.27	-0.14	0.26	0.49	0.16	0.41	0.25	0.27	0.31	-0.04	**0.66**	0.50	**0.75**	0.50	0.45	0.32	0.59	0.50	0.47
Tryptophan	0.21	-0.24	-0.28	0.50	0.38	0.20	0.49	**0.77**	0.03	**0.78**	-0.25	**0.76**	**0.92**	**0.88**	**0.65**	**0.75**	0.56	0.60	**0.73**	**0.81**	-0.26	0.39	0.52	0.50
Phenylalanine	0.42	0.44	0.59	0.04	0.44	0.42	-0.12	0.26	**0.65**	0.10	0.25	0.46	0.15	0.09	-0.22	0.59	**0.89**	**0.68**	0.54	0.58	0.58	**0.98**	**0.96**	**0.95**
Glycolate	0.30	0.37	0.56	-0.25	0.32	0.36	-0.16	0.15	0.32	-0.09	0.58	0.17	-0.10	-0.03	-0.36	0.36	0.43	0.54	0.50	0.45	0.43	0.59	0.47	0.48
Glycerate	-0.22	-0.49	-0.42	0.03	-0.25	-0.24	0.27	0.12	-0.62	0.07	-0.20	-0.01	0.16	0.24	0.24	-0.25	-0.45	-0.15	0.09	-0.05	-0.54	-0.35	-0.50	-0.49
Nicotinate	0.32	**0.72**	**0.92**	-0.24	0.22	0.41	**-0.64**	-0.19	**0.81**	-0.32	**0.73**	-0.02	-0.41	-0.30	-0.58	0.42	0.55	0.53	0.05	0.10	**0.89**	0.55	0.55	0.59
Nicotinamide	0.49	-0.03	0.08	0.32	0.60	0.47	0.33	**0.72**	0.19	0.56	0.14	**0.70**	**0.64**	**0.66**	0.27	**0.79**	0.59	**0.82**	**0.89**	**0.90**	0.04	0.56	0.60	0.61
Alpha-tocopherol	**0.84**	0.58	0.60	0.36	**0.71**	**0.87**	-0.04	0.26	**0.75**	0.16	0.42	0.27	-0.05	-0.09	-0.36	0.59	0.22	**0.73**	0.18	0.18	0.60	0.31	0.32	0.31

Supplemental Figure 3.4: Spearman's rank coefficient of correlation between all growth, physiologic and metabolic traits determined at the end of the night in cells three days after the onset of the stationary phase. Significant correlations at 5% probability are highlighted in green (positive) and red (negative). Continue on page 79.

Continuing from page 78.

Alanine	Glycine	Serine	Tyrosine	Lysine	Tryptophan	Phenylalanine	Glycolate	Glycerate	Nicotinate	Nicotinamide	Alpha-tocopherol	
												Biomass
												A
												Total amino acids
												Chlorophyll
												Phycocyanin
												Proteins
												Cyanophycin
												Glycogen
												Total soluble sugars (cell)
												Sucrose
												Total soluble sugars (media)
												Maltose
												Citrate
												Isocitrate
												Glutamate
												Ornithine
												Aspartate
												Arginine
												Fumarate
												Malate
												Proline
												Leucine
												Isoleucine
												Valine
												Alanine
0.90												Glycine
0.70	**0.70**											Serine
0.62	**0.67**	**0.81**										Tyrosine
0.68	0.45	**0.76**	0.59									Lysine
0.43	0.48	**0.81**	**0.82**	0.42								Tryptophan
0.98	**0.92**	0.62	0.60	0.58	0.43							Phenylalanine
0.70	0.50	0.44	0.15	0.60	0.04	0.62						Glycolate
-0.32	-0.48	0.08	-0.38	0.20	-0.05	-0.39	0.20					Glycerate
0.67	0.59	0.24	0.32	0.43	-0.15	0.62	**0.65**	-0.44				Nicotinate
0.68	0.56	**0.76**	**0.66**	0.58	**0.75**	**0.66**	0.62	0.07	0.30			Nicotinamide
0.52	0.30	0.13	0.36	0.38	-0.01	0.45	0.37	-0.35	**0.66**	0.35		Alpha-tocopherol

Chapter 4: Changes in Culture Conditions or the Absence of Pili do not Reduce the Negative Effect of Cell-Cell Interaction on *Synechocystis* Growth but do Affect DNA Cell Levels

4.1 Introduction

Cyanobacteria are the unique known prokaryotic organisms able to perform oxygenic photosynthesis (Govindjee and Shevela, 2011). These microorganisms present very simple metabolic needs (nutrients, light, CO_2 and water) and high photosynthetic efficiency (Parmar et al., 2011; Ruffing, 2011). The large metabolic diversity and plasticity presented by the different species of cyanobacteria make them good candidates for production of food supplement (Lu et al., 2011), pigments (Sekar and Chandramohan, 2008), biomolecules (Frommeyer et al., 2014), secondary metabolites (Nunnery et al., 2010) and biofuels (Wijffels et al., 2013). For this reason, large-scale production of cyanobacteria biomass may be an alternative to replace fossil fuels, and decrease the demand for arable lands and water for crop production (Ducat et al., 2011; Machado and Atsumi, 2012), thus reducing deforestation. However, the major issue faced by cyanobacteria cultivators is the lower growth rates and biomass productivity exhibited by cyanobacteria when cultured in batch conditions using low-cost open raceway ponds (Williams and Laurens, 2010; Granata, 2017). As a photosynthetic organism, cyanobacteria growth cycle is characterized by an exponential growth phase followed by a linear phase in which the growth rates and biomass productivity gradually decrease until the onset of stationary phase (Schuurmans et al., 2017). This issue can be circumvented by using closed systems such as photoreactors where cultures are continuously diluted (Zavřel et al., 2015). However, it tremendously increases production costs due to the increase in the demand for nutrient supply and energy for mixing and harvesting, thus threatening the economic viability of this activity (Schenk et al., 2008; Brennan and Owende, 2010; Straka and Rittmann, 2017). Hence, the industrial production of cyanobacteria biomass requires not only the use of low-cost sources of nutrients and facilities but also the identification of the limiting factors that affect negatively cyanobacteria growth and biomass productivity.

Compared to heterotrophic bacteria, very little is known about the mechanisms and regulations involved in cell division and DNA replication in cyanobacteria (Marbouty et al., 2009b). Recent investigations identified proteins that compose or are related to the cell division machinery and cell wall synthesis of cyanobacteria, describing their possible functions, targets and interactions (Mazouni et al., 2004; Leganés et al., 2005; Miyagishima et al., 2005; Marbouty et al., 2009a; Marbouty et al., 2009b; Marbouty et al., 2009c). Most cyanobacteria present multiple copies of a single circular chromosome (Cassier-Chauvat et al., 2016), and, curiously, different from well-known bacterial

species (i.e. *Escherichia coli* and *Bacillus subtilis*), cell division in cyanobacteria seems not to require sequential replication of these copies to allow cytokinesis (Schneider et al., 2007). The regulation of DNA replication in cyanobacteria is not a well-understood process and differs among cyanobacteria strains. In *Synechococcus elongatus* PCC 7942, as observed for heterotrophic bacteria, DnaA is responsible for the initiation of DNA replication by recruiting the replication machinery to the origin region of replication (*oriC*). However, this protein is non-essential in *Synechocystis* sp. PCC 6803 (hereafter termed *Synechocystis*) and *Anabaena* sp. PCC 7120, suggesting that these strains present multiple replication origins (Ohbayashi et al., 2016).

The higher complexity of the regulation of cell division in cyanobacteria, compared to heterotrophic bacteria, can be explained by the presence of a gate control of cell division cycle by the circadian clock. Cyanobacteria is the unique bacterial phylum that presents a circadian clock that regulates cell division and other processes such as metabolic reactions and gene expression (Foster et al., 2007; Dörrich et al., 2014). The cyanobacterial circadian clock is characterised as a temperature insensitive system, as it is able to maintain periodic oscillations of 24 h regardless of changes in temperature (van Alphen and Hellingwerf, 2015). Thus, the impact of temperature on division rates may be related only to its effect on the velocity of metabolic reactions. On the other hand, the circadian clock is sensitive to variations in light and dark periods, being reset by light. Hence, the regulatory role of light availability/intensity on cell division is not only driven by the amount of resources assimilated via photosynthesis, but also by of its capacity to reset the circadian gate of cell division (Pando and van Oudenaarden, 2010; Yang et al., 2010). Whether cell division is controlled by the clock, very surprisingly DNA replication is not under clock control. Replication shows constant rate during light periods and is mostly affected by the cellular energy status (Mori et al., 1996; Ohbayashi et al., 2013), with strains presenting reduced replication rate during dark periods (Ohbayashi et al., 2017). Additionally, in batch culture conditions, *Synechococcus elongatus* PCC 7942 exhibits high DNA replication rate and cellular content during the lag phase (first 18 hours of the growth cycle). After this point, DNA content gradually decreases, probably as result of decreased replication rates, reaching stable levels after 48 hours of growth (Watanabe et al., 2015).

The use of cyanobacteria for biotechnology applications requires a better understanding of the cell cycle and the main factors responsible for the changes in growth performance. Previous analyses showed that the gradual decrease in growth rates

observed in *Synechocystis* cultures was not caused by limitations of metabolism, medium nutrients and quorum sensing (Chapter 3). Moreover, cellular self-shading only showed a negative effect on the growth of cells cultured under moderate light intensity (50 µmol photons m^{-2} s^{-1}) and no effect was observed when cells were cultured under high light intensity (200 µmol photons m^{-2} s^{-1}). Thus, we suggested that these factors were not the main responsible for the decreases in cell division rates, and likely a cell-cell interaction mechanism could be associated with the control of cell density in *Synechocystis* (Esteves-Ferreira et al., 2017b). In this chapter, we investigated whether: (*i*) modifications in growth conditions could circumvent the growth inhibition triggered by cell-cell interaction mechanism; (*ii*) the regulation of cell division is related to the capacity of cells to replicate DNA; and (*iii*) pili, the cellular appendages present on *Synechocystis* cell wall, present some sensorial function which could be related to cell-cell interaction. Our data indicate that changes in culture conditions can decrease the length of lag phase, leading the cells to leave this stage of the growth cycle sooner and start exponential growth. However, none of the conditions could prolong the duration of the log phase or increase the cell density in the linear or stationary phase. Moreover, the low division rates observed in the late stages of the growth cycle are possibly associated with a lower capacity to replicate DNA. Finally, analysis using pili mutants revealed that these appendages do not present a sensorial function related to cell-cell interaction, and might be only related to cell motility and DNA uptake capacity.

4.2 Results

4.2.1 Cell density at stationary phase is not affected by changes in the culture conditions

Since changes in light intensity, nitrogen sources and CO_2 levels did not affect cell density at stationary phase, due to a possible negative effect of a cell-cell interaction mechanism on growth, we tested whether changes in other parameters such as mixing speed, temperature and photoperiod could allow cultures to reach higher densities at stationary phase. To perform these analyses *Synechocystis* was cultured on BG-11 medium with urea as the nitrogen source, a light intensity of 200 µmol photons m^{-2} s^{-1} and a starting cell density of 2 $x10^6$ cells per mL. This growth condition allowed the highest growth rates among the 10 conditions we tested previously (Chapter 3).

First, we evaluated whether decreasing by 50% the speed at which the cultures were mixed (from 120 rpm to 60 rpm) could affect the contact between cells and consequently

the cell density at stationary phase. Cells mixed at 120 rpm and 60 rpm presented a similar growth cycle (Figure 4.1A), although cells grown at 120 rpm displayed lower Gt during the logarithmic growth (Table 4.1). Moreover, cultures mixed at 120 rpm exhibited higher cell density at the end of days (ED) three and seven, but as cultures at 60 rpm showed higher division rates during these respective days, they displayed similar cell density on the next day and at stationary phase (Figure 4.1A and B; Table 4.1).

In a second attempt, we tested whether replacing the homogenization method from shaking to air bubbling could affect growth rate and/or cell density at stationary phase. Cultures grown with air bubbling exhibited variations in the growth cycle during the log phase (Figure 4.1C). Cell growth under constant shaking of 120 rpm entered earlier in the log phase, presenting higher cell division rate during the second day of culture and higher cell densities at ED two and three. However, cultures grown with air bubbling showed higher divisions rates from day three to four, exhibiting similar Gt and achieving stationary phase with comparable density as cultures at 120 rpm (Figure 4.1C and D; Table 4.1).

Table 4-1: Generation time and cell density at stationary phase of *Synechocystis* cultures grown under varying conditions

Period	Generation time	Cell density at stationary phase
Control	9.77 ± 1.02 **a**	$2.33 \times 10^8 \pm 3.73 \times 10^7$ **a**
60 rpm	12.78 ± 0.26 **b**	$2.56 \times 10^8 \pm 1.32 \times 10^7$ **a**
Air bubbling	9.60 ± 0.31 **a**	$2.49 \times 10^8 \pm 3.14 \times 10^7$ **a**
32° C	10.21 ± 0.29 **a**	$1.99 \times 10^8 \pm 5.10 \times 10^7$ **a**
Continuous light	10.20 ± 0.47 **a**	$2.05 \times 10^8 \pm 2.73 \times 10^7$ **a**

Generation time (hours) was calculated using a regression of the data within the logarithmic growth period. Cell density at stationary phase (cell mL^{-1}) refers to the highest density reached during the last three days of growth. The control means cultures grown on BG-11 supplemented with urea, at constant shaken at 120 rpm, the temperature of 26° C ± 1° C and 18h/6h day/night photoperiod. Values represent the mean ± standard deviation (n = 3). Means followed by the same letter do not differ by 5% of probability (Tukey's test).

Then we considered increases in temperature and/or the length of the light period, as they could allow higher metabolic activity, and thus potentially promote positive effects on growth. Thus, we evaluated whether those effects would be related only to early stages of the growth cycle or could also affect later stages (linear and stationary phase). Cells grown at 32° C presented a shorter lag phase, dividing 1.5 times during the first 24 h of the growth cycle and showing higher cell density at ED one and two (Figure 4.1E and F). Cultures grown under continuous light also exhibited a shorter lag phase, dividing

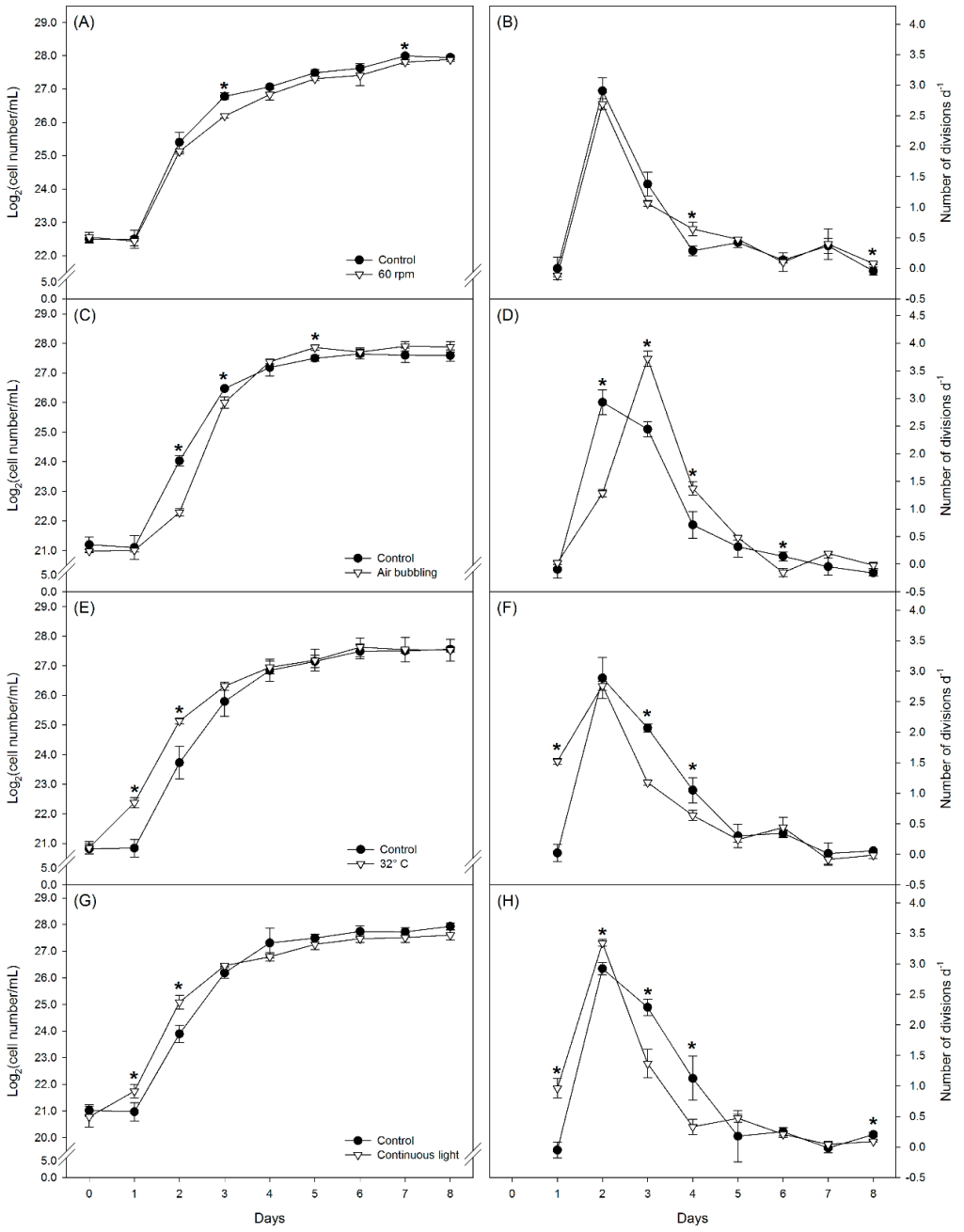

Figure 4-1: *Synechocystis* growth cycles in varying culture conditions
Growth curves represented on a Log(cell) basis (**A**, **C, E,** and **G**) and a daily number of division (**B**, **D, F,** and **H**) of *Synechocystis* grown on varying culture conditions. The control means cultures grown on BG-11 supplemented with urea, at constant shaken at 120 rpm, the temperature of 26° C ± 1° C and 18h/6h day/night photoperiod. Values represent the mean ± standard deviation (n = 3). The asterisk represents a significant difference between control and treatment ($P < 0.05$, unpaired Student's *t* test).

1 time during the first day of growth and keeping a higher division rate than cultures under a light/dark cycle until ED two (Figure 4.1G and H). On the other hand, cells cultured under a long day photoperiod (18 h of light and 6 h of dark) and 26° C initiate division during the second day of culture, showing higher division rates than cultures at 32° C or continuous light from the third until the fourth day (Figure 4.1E and H), and

presenting comparable Gt and cell density from ED three until the onset of stationary phase (Table 4.1).

4.2.2 The length of lag phase is mostly affected by temperature and not by light/dark photoperiods; both temperatures and periods having little impact on cell density at stationary phase

As cells grown under continuous light could start division during the first day of culture, and the cultures grown in an 18/6 photoperiod could not (Figure 4.1G and H), we speculated that cell division started in the last 6 h of this respective day because cell division cannot occur in the dark. Growth analysis performed hourly confirmed that *Synechocystis* do not divide during the dark periods when cells are cultured photoautotrophically (Figure 4.2A and B). On the other hand, it has been described that cell division is gated by the circadian clock (Mori et al., 1996; Mori and Johnson, 2001; van Alphen and Hellingwerf, 2015). Hence, resetting the clock earlier by applying non 24 hours periods might lead to faster division rates than those observed under continuous light where the clock is free running with periods of 23.3 h (Mori et al., 1996). Then, based on these two assumptions, we decided to investigate the effect of non 24 periods on cyanobacteria growth.

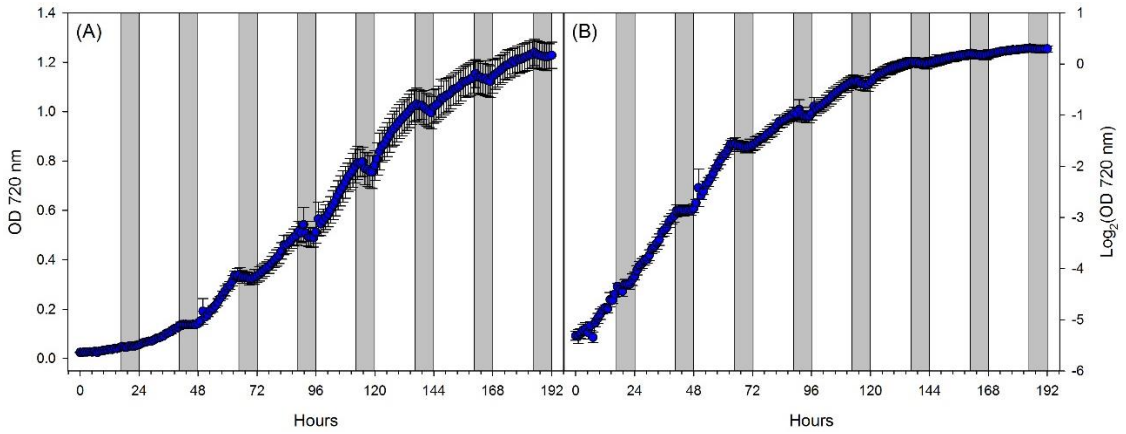

Figure 4-2: *Synechocystis* growth measured hourly.
Synechocystis growth curve on an OD basis (**A**) and a Log(OD) basis (**B**) shows that growth is restricted to light periods

All cultures submitted to different light/dark periods at 26° C presented lower division rates during the first 24 h of growth than cultures grown under continuous light ($P < 0.03$; Figure 4.3 A and B). However, their growth cycle and Gts were similar to those determined in cultures under continuous light or the 24 h long day photoperiod (Table 4.2). Curiously, when these light regimes were applied at a temperature of 32° C, all of

them led to faster division rates during the first day of growth than cells cultured under the usual long day light/dark photoperiod ($P < 0.03$). Moreover, cells submitted to 4.5/1.5 light/dark and 6/2 light/dark periods exhibited similar division rates to cells at continuous light, with cells at 6/2 light/dark dividing exactly at the same rate as cells grown under continuous light ($P < 0.99$; Figure 4.3C and D). However, when considering the growth during the log phase, all cultures grown at 32° C presented similar growth cycles and Gts, and the same observation was made at 26° C (Table 4.2). When comparing Gts of cultures at 26 and 32° C, very little differences were observed. The only cultures differing significantly being the 6/2 and 9/3 light/dark at 26° C, which grew faster than continuous light at 32° C.

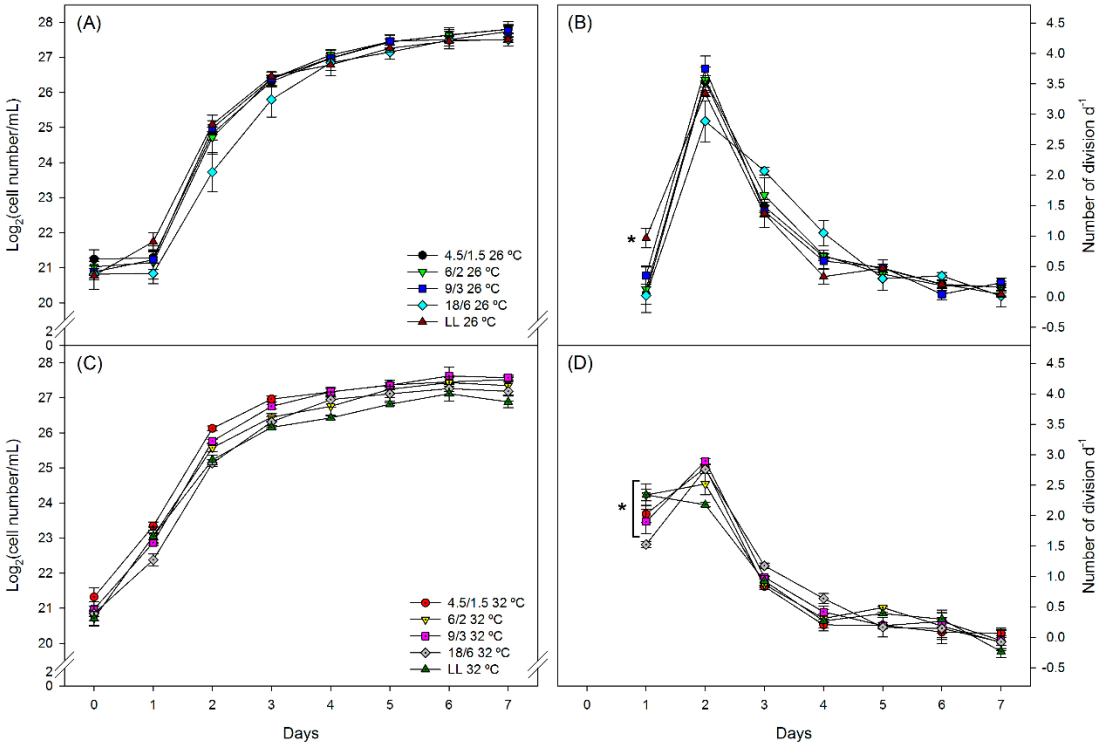

Figure 4-3: *Synechocystis* growth cycles at varying light/dark regimes.
Growth curves represented on a Log(cell) basis (**A** and **C**) and a daily number of division (**B** and **D**) of *Synechocystis* grown under different light/dark and temperature conditions. Values represent the mean ± standard deviation (n = 3). Statistics are as described in Figure 4.1.

The divergences observed in the length of the lag phase among cultures at 26° C and 32 °C led us to hypothesize that those variations might be due to a faster rate of DNA replication of cells grown at a higher temperature, which could allow them to initiate earlier cell division. Hence, we determined DNA level over the entire growth cycle of cells grown at both temperatures under continuous light, where shorter lag phase was

observed, 6/2 light/dark, which was the light/dark cycle with the shortest lag phase, and 18/6 light/dark, as the control.

Table 4-2: Generation time of *Synechocystis* grown under ten different culture conditions

Period	Generation time
18 h light/6 h dark 26° C	9.71 ± 0.62 **ab**
18 h light/6 h dark 32° C	9.79 ± 0.45 **ab**
4.5 h light/1.5 h dark 26° C	9.55 ± 0.04 **ab**
4.5 h light/1.5 h dark 32° C	9.99 ± 0.4 **ab**
6 h light/2 h dark 26° C	9.19 ± 0.6 **a**
6 h light/2 h dark 32° C	9.88 ± 0.27 **ab**
9 h light/3 h dark 26° C	9.30 ± 0.20 **a**
9 h light/3 h dark 32° C	10.02 ± 0.33 **ab**
Continuous light 26° C	9.73 ± 0.31 **ab**
Continuous light 32° C	10.63 ± 0.17 **b**

Generation time (hours) was calculated using a regression of the data within the logarithmic growth period. Values represent the mean ± standard deviation (n = 3). Statistics are as described in Table 4.1.

After 6 h of culture no growth was observed in any of the conditions, instead, cells increased their volume and DNA levels (Figure 4.4; Supplemental Table 4.1). Analyses performed after 18 h of growth showed that all cells growing at 32° C already started cell division independent of the light regime. Cells at 26° C only increased their volume, and those grown under 6/2 light/dark and continuous light were significantly bigger at 26° C than at 32° C. The DNA levels increased for all growth conditions, and during the interval from 6 to 18 h of culture, cells presented the highest replication levels of the whole growth cycle. Interestingly, cultures under 18/6 light/dark showed a positive effect of temperature on DNA levels, although this effect was not observed for the other two light regimes, which showed similar DNA levels regardless temperature (Figure 4.4; Supplemental Table 4.1).

Only cultures submitted to light/dark cycles (6/2 and 18/6) and a temperature of 26° C did not divide on the first day. Cultures under continuous light divided almost 1 time during the timeslot 18-24 h of culture, confirming our hypothesis that, for this condition, cell division started at the end of the first day and cultures at 18/6 light/dark could not initiate division because, at this point, they were blocked due to the absence of light. As a consequence of the lower division rates during the first 24 h of growth, cultures at 26°

C reached their biggest volume and DNA content at the end of this day. On the other hand, all cells from cultures at 32° C were decreasing in size, although DNA levels were not reducing for all of them (Figure 4.4; Supplemental Table 4.1).

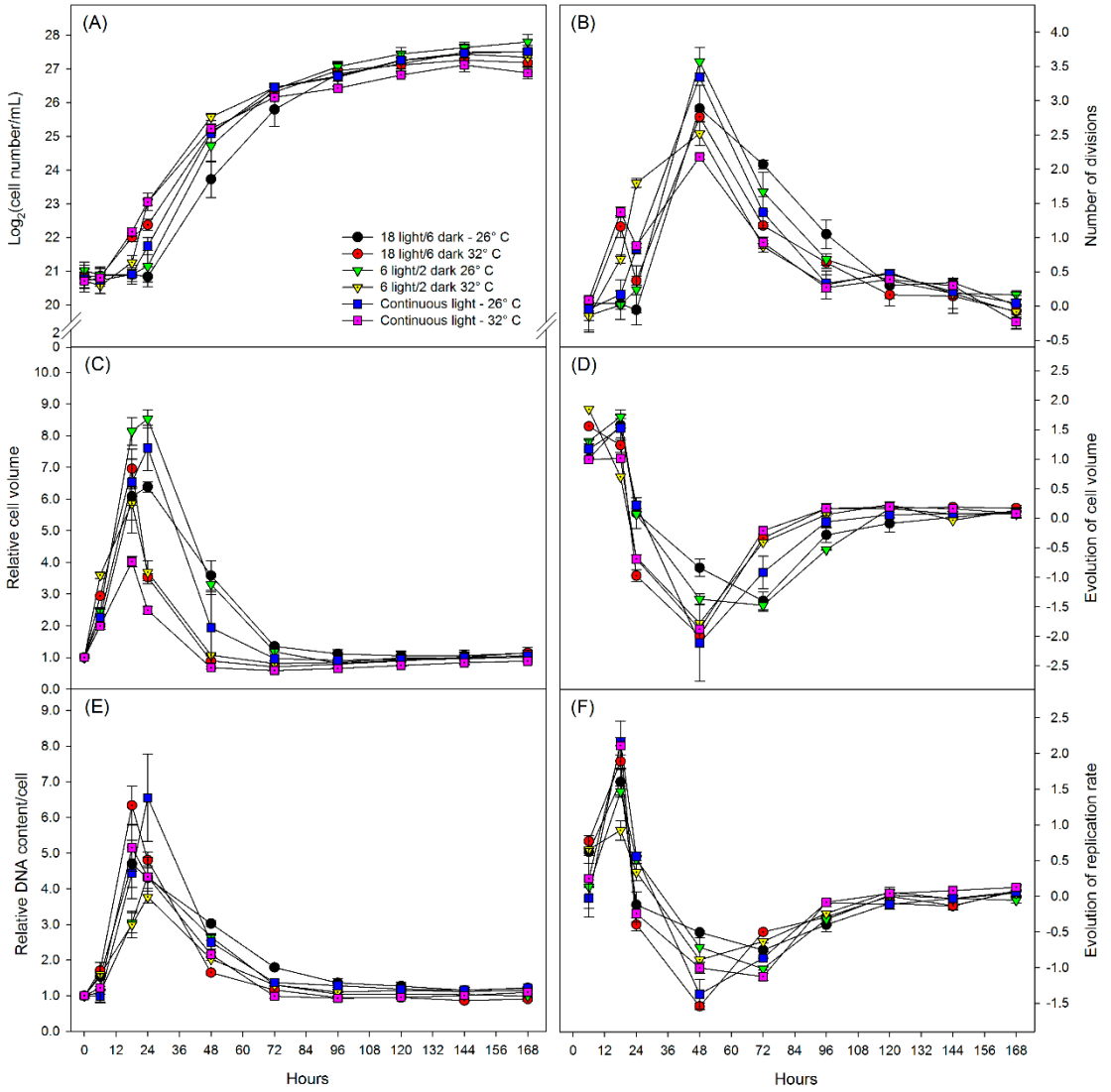

Figure 4-4: Evolution of cell volume and DNA content in *Synechocystis* cells
Synechocytis growth characterized on a Log(cell) basis (**A**), daily number of division (**B**), relative cell volume (**C**), evolution of cell volume (**D**), DNA content (**E**) and evolution of replication rate (**F**) in varying conditions of light and temperature. The cellular volume and DNA content are relative to time zero. Values represent the mean ± standard deviation (n = 3). Statistic is present in the Supplemental Table 4.1.

Cells at 26°C presented their highest division rates during the second day of the growth cycle. However, despite this high division rate, their volume and DNA levels were still higher than those of cells cultured at 32° C. In the third day of growth, the volume and DNA content of the cells had returned to their initial values when they were inoculated, for most of the growth conditions. These values then remained stable until the end of the growth cycle. Probably, as a result, all cultures showed after three days of

culture a progressive decrease in their growth rates until the onset of the stationary phase (Figure 4.4; Supplemental Table 4.1).

The DNA profiles of almost all cultures presented a spike-shape at time zero with a variable number of peaks, which means that the population was not homogeneous in terms of chromosome copy number per cell (Figure 4.5). The analysis performed after 6 h of growth revealed that the spike-shape gave space to profiles with only one peak, suggesting that at this stage the chromosome copy number was similar within the cell population. All cultures presented this DNA profile until 48 h of growth, and during this period the fluorescence emitted by the SYBR green/DNA complexes reached their maximum levels after 18 or 24 h, depending on the growth condition (Figure 4.5). At 48 h of growth, the signal was lower and continued decreasing by 72 h when some growth conditions started to show again a spike-shape DNA profile. The signal was similar to time zero after 96 h of growth. From this point, the fluorescence signal stayed stable until the end of the analysis and almost all growth condition presented a spike-shape DNA profile with two to three peaks (Figure 4.5). Curiously, only cells grown under continuous light and 32° C did not exhibit a spike-shape DNA profile during the growth cycle. For this condition, DNA profiles always presented one peak, with only the intensity of the fluorescence signal varying (Figure 4.5).

4.2.3 Effect of viscosity on growth rates and cell density

Since variations in growth temperatures and periods could not circumvent the gradual decrease in the growth rates during the growth cycle, we decided to increase the viscosity of the medium, with the hypothesis that it could reduce the frequency of cell-cell contacts and thus possibly decrease its negative effect on growth.

Analyses revealed that the *Synechocystis* strain used in this study could not grow mixotrophically at 200 µmols photons m^{-2} s^{-1} when supplemented with urea or ammonium (Supplemental Figure 4.1). In good agreement, during the acclimation process, cells did not grow on BG-11 plus urea and supplemented with dextran under 200 µmols photons m^{-2} s^{-1}. Moreover, no growth was observed when *Synechocystis* was inoculated on BG-11 containing 10% (m/v) of dextran, regardless the light intensity. Thus, the viscosity analyses were performed at 50 µmols photons m^{-2} s^{-1}, using BG-11 supplemented with 1%, 2.5% and 5% of dextran, which led to increases in viscosity from 3.74 to 46% (Table 4.3).

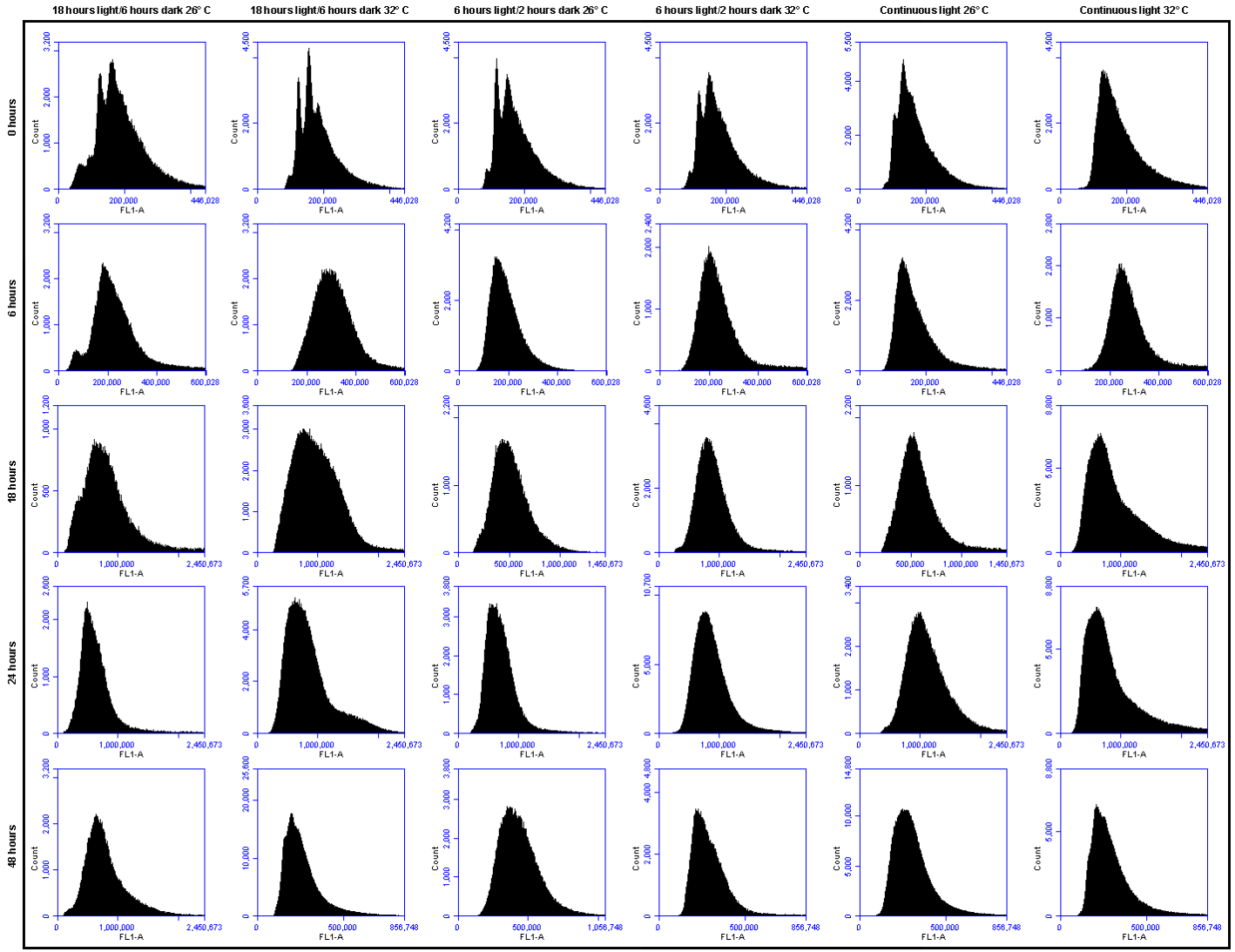

Figure 4-5: DNA content profiles of *Synechocystis*
Cells cultured in different light/dark regimes and temperature were harvested at the indicated time points for analysis by flow cytometry.

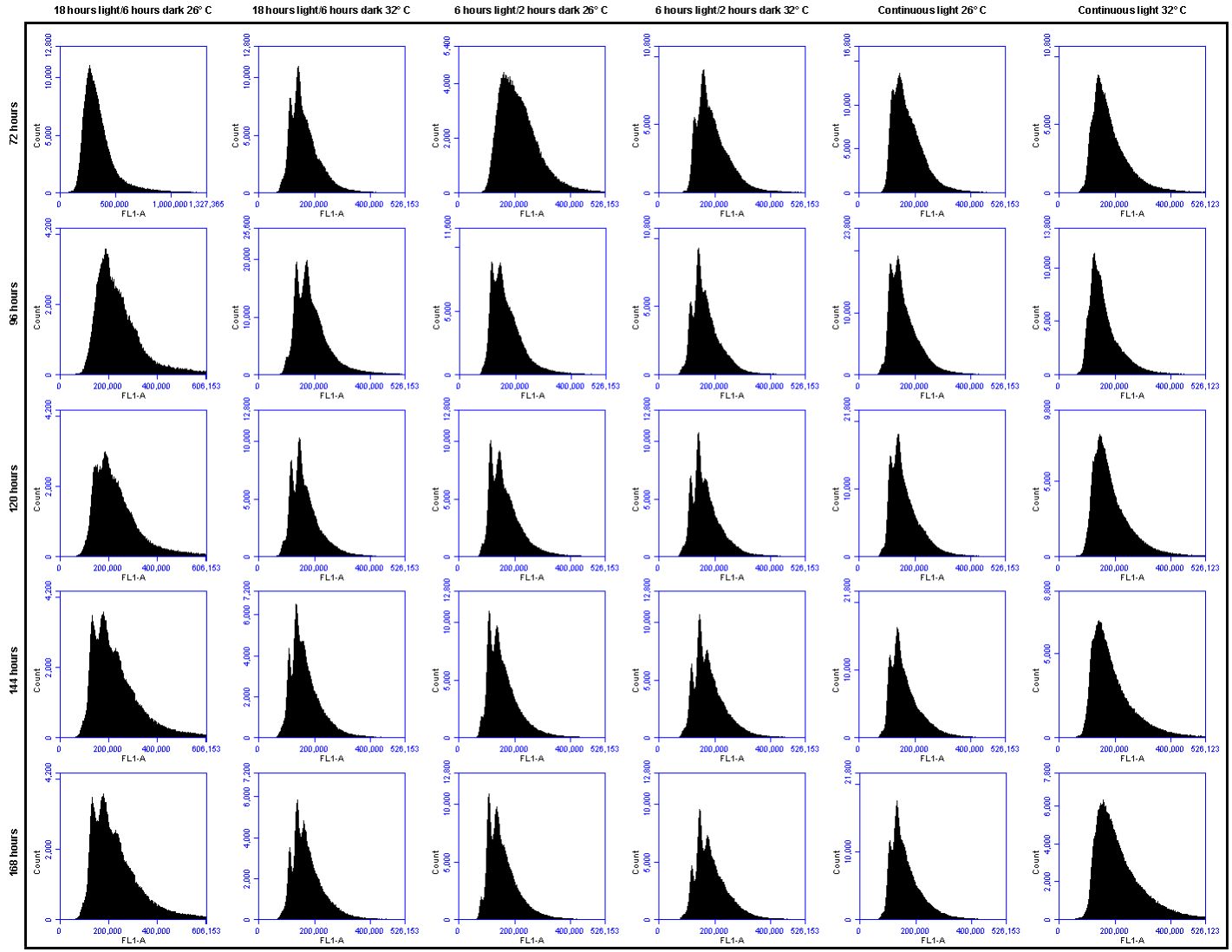

Figure 4-5: DNA content profiles of *Synechocystis*
Cells cultured in different light/dark regimes and temperature were harvested at the indicated time points for analysis by flow cytometry.

Table 4-3: The effect of dextran on the viscosity of BG-11 medium and generation time of S*ynechocystis*

Medium	Viscosity (cSt s^{-1})	Increase (%)	Gt (h)
BG-11 (control)	0.93	-	15.8 ± 0.7
BG-11 + 1% dextran	0.97*	3.74%	23.5 ± 1.0*
BG-11 + 2.5% dextran	1.13*	21.42%	15.7 ± 0.9
BG-11 + 5% dextran	1.36*	46.07%	36.9 ± 1.5*
BG-11 + 10% dextran	2.16*	130.07%	-

Viscosity in centistoke s^{-1} and generation time (Gt) in hours (h). Values represent the mean ± standard deviation (n = 3). The asterisk represents a significant difference between control (BG-11 supplemented with urea) and treatments (BG-11 supplemented with urea and different percentages (m/v) of dextran; $P < 0.05$, unpaired Student's *t* test).

Synechocystis presented variations in its growth cycle when grown under the different concentrations of dextran (Figure 4.6). Cells on 1% dextran presented higher Gt than control conditions, mostly due to a sharp decline in their division rates from the second to the third day of culture. Afterwards, cells showed a gradual decrease in their division rates until they enter in stationary phase, at a similar cell density as those observed for the control (Figure 4.6; Table 4.3). Curiously, cells on 2.5% dextran exhibited similar Gt (Table 4.3). These cultures showed slower division rates, compared to control and 1% dextran, during the first two days. However, the higher division rates exhibited during the third and fourth days lead them to reach a similar cell density to the control at day four, and, from this time point, cells on control conditions and 2.5% dextran maintained similar cell division rates until the onset of the stationary phase (Figure 4.6).

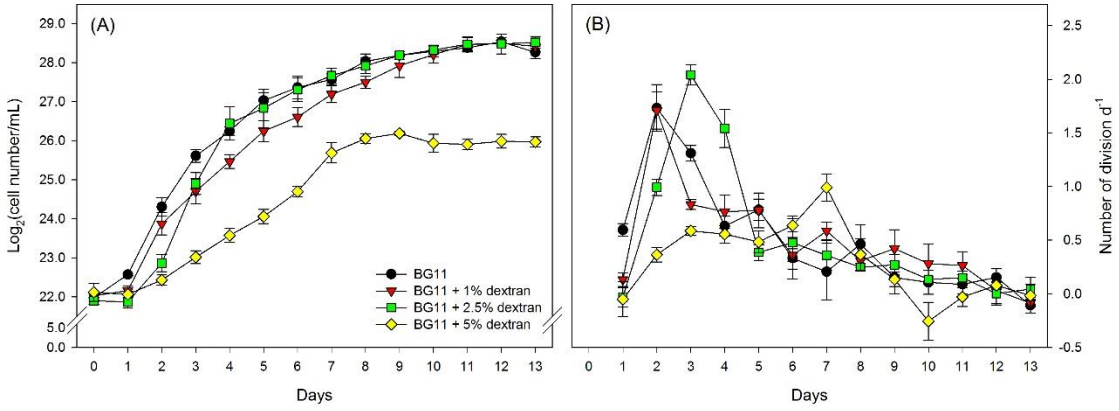

Figure 4-6: *Synechocystis* growth under different viscosity levels.
Growth curves represented on a Log(cell) basis (**A**) and daily number of division (**B**) of *Synechocystis* grown on BG-11 supplemented with urea (control) and different percentages (m/v) of dextran (treatment) under 50 µmols photons m^{-2} s^{-1}. Values represent the mean ± standard deviation (n = 3).

Cells on BG-11 supplemented with 5% dextran presented the slowest daily division rates during the first three days of culture, followed by constant growth and an apparent

start of a second log phase. However, after this sharp increase of growth rate at day seven, cells showed an acute decrease in the division rates and entered in stationary phase with a cell density 5.5 times lower than the control and the other two dextran treatments (Figure 4.6).

4.2.4 Pili structures are not involved in cell-cell interaction

Considering the importance of pili for motility and phototaxis in *Synechocystis* (Bhaya et al., 2000), we wondered whether it could also be involved in cell-cell interaction, allowing cells to sense density. Hence, in an attempt to investigate whether pili is involved in the process of growth control by cell-cell interaction we created mutants of *pilA1A2* and *sigF* that present only thin pili or no pili at all, respectively (Bhaya et al., 1999; Bhaya et al., 2000), and evaluated their growth performances.

PCR analysis confirmed that all copies of the chromosome in the cells of the *sigF* null mutant (Δ*sigF*) and *pilA1A2* null mutant (Δ*pilA1A2*) were carrying interrupted sequences of *sigF* or *pilA1A2*, respectively, containing the cassette that confers kanamycin resistance (Figure 4.7A and B). Real-time PCR analysis showed that the relative expression levels of *pilA1*, *pilA2*, and *sigF* in Δ*sigF* were very low compared to wild type (WT; Figure 4.7C). In Δ*pilA1A2*, *pilA1* levels were lower than the WT and similar to the levels observed in the Δ*sigF* mutant. The levels of *pilA2* were also lower than those determined in the WT, although higher than in Δ*sigF*. *sigF* levels were similar to the WT and consequently higher than in Δ*sigF* (Figure 4.7C).

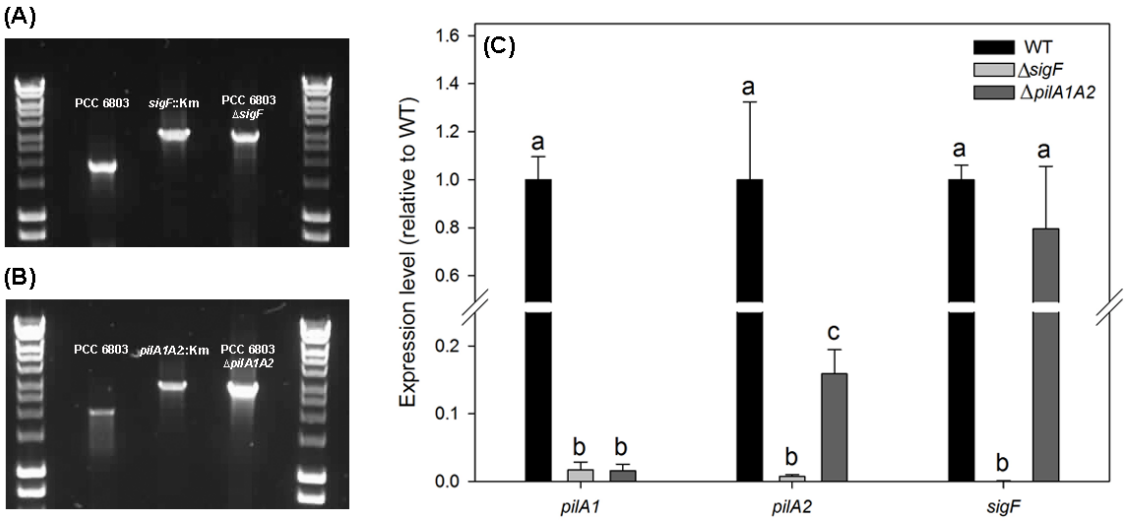

Figure 4-7: Mutations in the genes *sigF* and *pilA1A2* of *Synechocystis*
PCR analysis confirming the absence of wild type (WT) copies of *sigF* (**A**) and *pilA1A2* (**B**) in the Δ*sigF* and Δ*pilA1A2* mutants, respectively; Expression levels of *pilA1*, *pilA2*, and *sigF* in *Synechocystis* WT strain and pili mutants (**C**). Expression levels were calculated relative to the levels of the WT strain.

The growth of Δ*sigF* and Δ*pilA1A2* was evaluated on agar and liquid BG-11 using cells from three different colonies of each mutant. Directional motility assays demonstrated that different from the WT, the mutants did not present motility and phototaxis when grown under a unidirectional light source (Figure 4.8A). When grown planktonically, the cultures of both mutants were homogeneous and no cell agglomeration was observed macroscopically (Figure 4.8B). Microscopic analysis confirmed the absence of cell agglomeration (Figure 4.8C-E). Moreover, measurements showed that the cellular size of the mutants was similar to the WT strains (Table 4.4).

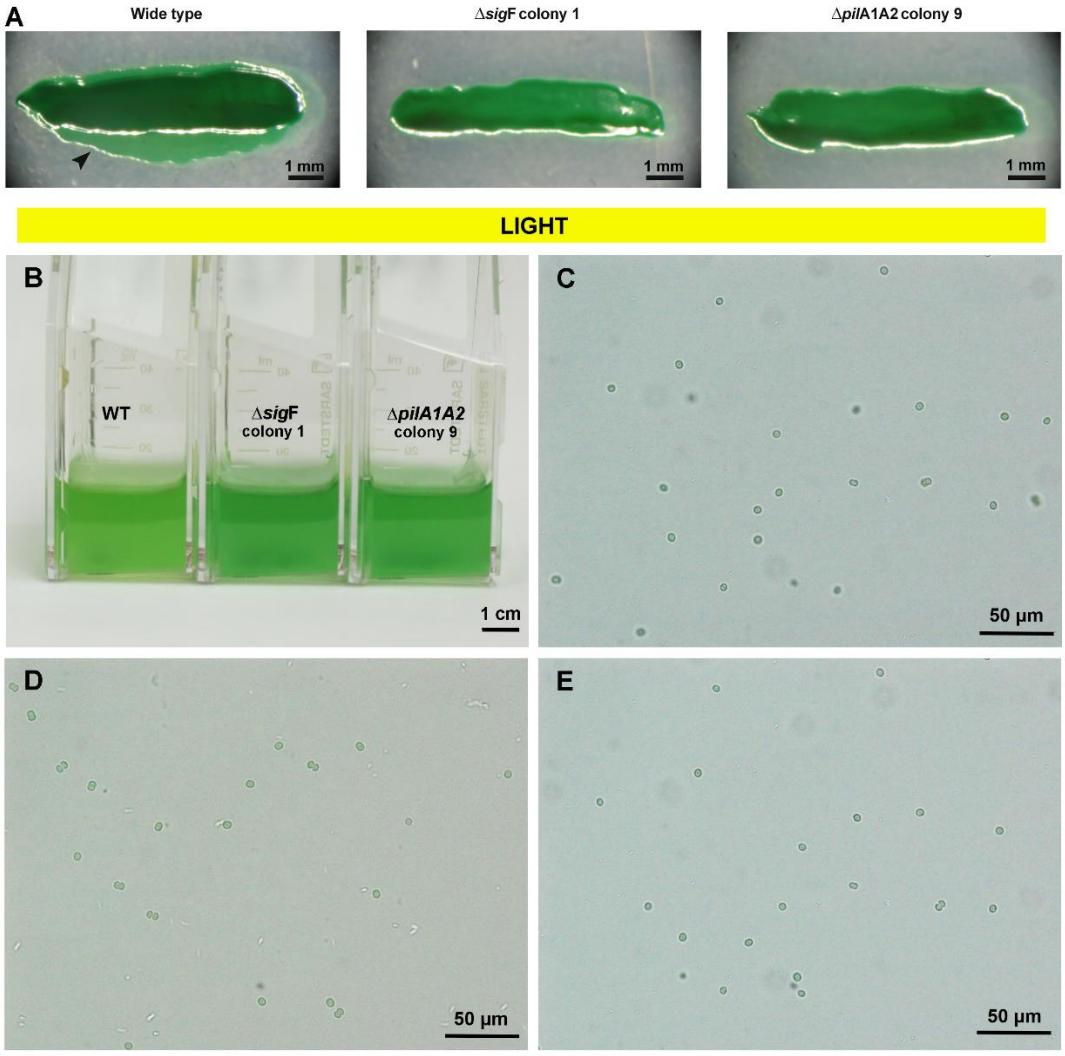

Figure 4-8: Macroscopic and microscopic characterization of *Synechocystis* wild type strain and pili mutants
Mobility assay under unidirectional light (**A**). The black arrow indicates colony growth in the direction of the light source. Liquid cultures of *Synechocystis* wild type (WT) strain and pili mutants (**B**). Photomicrographs of *Synechocystis* WT cells (**C**), Δ*sigF* (**D**) and and Δ*pilA1A2* (**E**) at 1,000 times magnification.

Cells from the three Δ*sigF* colonies presented similar growth cycle, Gt, and cell density at stationary phase compared to WT (Figure 4.9A and B; Table 4.4). On the other

hand, cells from Δ*pilA1A2* colonies exhibited a shorter lag phase than WT. However, after four days of growth, all cultures showed similar cell density and Gt. From this point, no significant differences in cell density among WT and mutants were observed until the onset of the stationary phase (Figure 4.9C and D; Table 4.4).

Table 4-4: Cell size, generation time, and density at stationary phase of *Synechocystis* wild type strains and pili mutants

Genotype		Cell size	Generation time	Cell density at stationary phase
Wild type (control)		4.85 ± 0.22 **ab**	23.51 ± 0.68 **ab**	1.77 x10^8 ± 1.55 x10^7 **a**
Δ*sigF*	Colony 1	4.82 ± 0.38 **ab**	22.81 ± 0.07 **ab**	1.91 x10^8 ± 7.53 x10^6 **a**
	Colony 2	5.03 ± 0.42 **b**	25.07 ± 0.97 **b**	1.92 x10^8 ± 2.07 x10^7 **a**
	Mixed colonies	4.52 ± 0.20 **ab**	22.30 ± 0.23 **ab**	1.79 x10^8 ± 3.21 x10^6 **a**
Δ*pilA1A2*	Colony 9	4.37 ± 0.31 **a**	22.86 ± 0.28 **ab**	1.80 x10^8 ± 3.09 x10^6 **a**
	Colony 13	4.45 ± 0.20 **a**	20.79 ± 0.88 **a**	1.90 x10^8 ± 3.24 x10^7 **a**
	Mixed colonies	4.72 ± 0.17 **ab**	22.04 ± 2.15 **a**	2.06 x10^8 ± 1.55 x10^7 **a**

Cell size (µm) was determined on the fourth day of culture. Generation time (hours) was calculated using a regression of the data within the logarithmic growth period. Cell density at stationary phase (cell.mL^{-1}) refers to the highest density reached during the last three days of growth. Values represent the mean ± standard deviation (n = 3). Statistics are as described in Table 4.1.

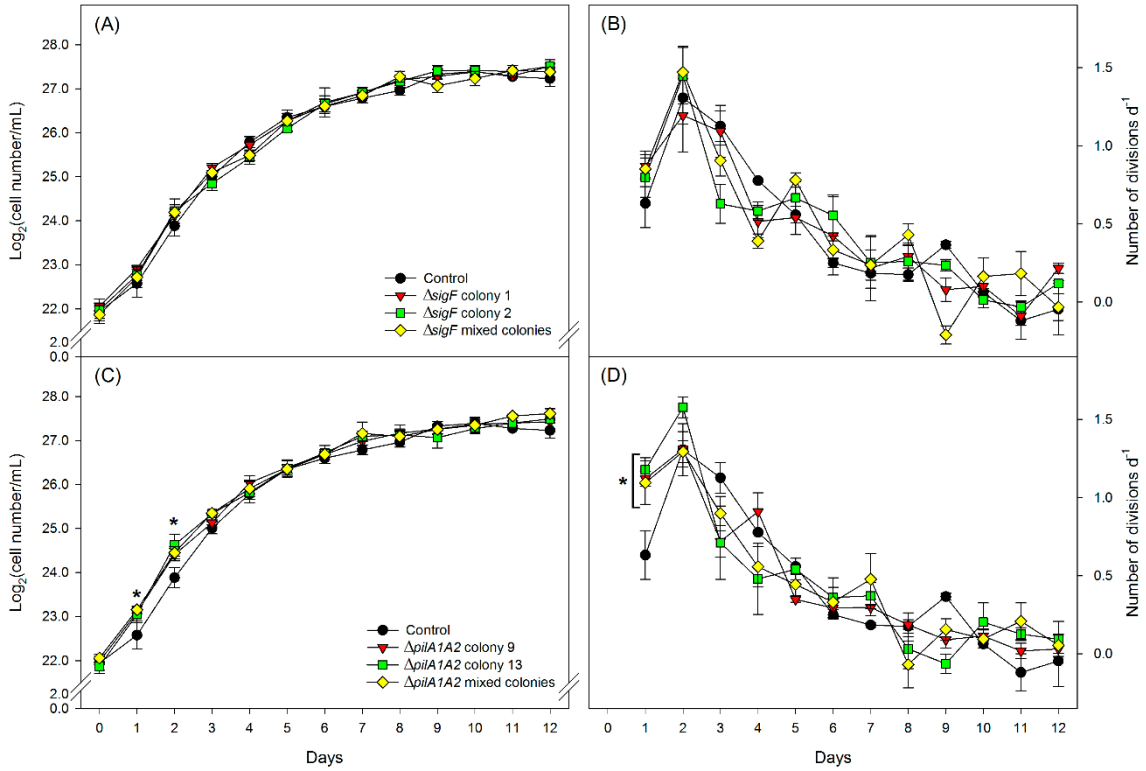

Figure 4-9: Growth cycle of *Synechocystis* wild type strain and pili mutants
Growth curves represented on a Log(cell) basis (**A** and **C**) and a daily number of division (**B** and **D**) of *Synechocystis* wild type strain and pili mutants. Values represent the mean ± standard deviation (n = 3). The asterisk represents a significant difference between *Synechocystis* wild type strain (control) and pili mutants ($P < 0.05$, unpaired Student's *t* test).

4.3 Discussion

Currently, the alternative to keep cyanobacteria dividing at very high rates is the use of dilution systems. As observed in chapter 3 (Esteves-Ferreira et al., 2017b), the use of this system allows to control density and reduce the negative effect of cell-cell interaction on growth rates. However, constant dilution increases the production costs due to a higher requirement of nutrients and harvesting steps (Brennan and Owende, 2010; Straka and Rittmann, 2017). Thus, in order to find economically viable solutions for this issue, we should aim at (1) the identification of growth conditions in which cells could keep fast division rates for periods longer than three to four days and/or (2) select genetic engineered strains less sensitive to increases of cell density. Applying these strategies would allow to maintain high growth rates in batch cultures such as open-ponds at a low cost, which would open the possibility to produce cyanobacteria biomass and a number of high-value products derived from it at a competitive price.

The similar Gt between cells submitted to the standard mixing speed of 120 rpm or agitation by bubbling air into the culture indicates that the mixing speed of 120 rpm allowed adequate aeration of the culture and provided enough levels of CO_2 and O_2 to support maximum growth rates (Figure 4.1C and D; Table 4.1). Thus, the higher Gt of cultures mixed at 60 rpm compared to those submitted to 120 rpm may indicate that the reduction of the mixing speed affected the aeration of the culture (Figure 4.1A and B; Table 4.1), decreasing the supply of CO_2 and O_2 in the medium and, consequently, slowing down growth. Mixing is a very important step of cyanobacteria biomass production as it prevents cell sedimentation (Grima et al., 1999) and stabilises growth by allowing CO_2 and O_2 exchanges between the liquid medium and the atmosphere (Eriksen, 2008; Brennan and Owende, 2010). Consequently, poor mixing can result in deficient aeration of the medium, affecting negatively growth and biomass productivity (Ugwu et al., 2008).

The highest number of divisions per day was observed in the second day of growth for most of the growth conditions (Figures 4.1, 4.3 and 4.4). During this day, cells divided from 2.7 to 3.7 times and the highest number of divisions were determined in the growth conditions that showed longer lag phase. Taking in account that *Synechocystis* do not divide during the dark period (Figure 4.2), cells under light/dark regimes could only divide during the 18 h of light, meaning that their Gts varied from 6.7 to 4.8 h. On the other hand, cells under continuous light could divide along the entire diurnal cycle and, thus, exhibited Gts from 7.8 to 5.29 h. These Gts, observed during the second day of

growth, are similar or even faster to those described by Zavřel et al. (2015) and Hihara et al. (2001), who reported Gts of 5.6 and 6 h, respectively, for *Synechocystis.* Additionally, these data also indicate that the positive effect of continuous light on cell division is restricted to the first day of culture, and similar growth performances and cell densities can be obtained using 25% less light energy input (Figures 4.1, 4.3 and 4.4).

Changes in growth conditions did not affect the final cell density of the cultures, and for most of the treatments, Gt was also similar (Figure 4.1; Table 4.1). The attempt of splitting the 6 h of dark into shorter periods to reset the circadian clock also did not lead to faster Gts or higher densities at stationary phase (Figure 4.3; Table 4.2). However, curiously, the combination of higher temperature and shorter periods led cells to divide earlier than those under the standard photoperiod (18 h light/6 h dark), i.e. during the first day of growth (Figure 4.3), suggesting that shorter periods may be able to reset the circadian clock and stimulate cell division in a temperature dependent way. Hence, since temperature does not affect cyanobacteria circadian oscillations (Pando and van Oudenaarden, 2010; van Alphen and Hellingwerf, 2015), this temperature dependent effect of shorter periods on cell division may be due to faster metabolic and/or physiological processes of cells grown at higher temperature.

The longer lag phase observed in cultures at 26° C indicate that cells in these conditions may need at least 18 h of light to start division. However, cells at 32° C do not need even half of this interval (Figure 4.4). Intriguingly, cells at 26° C had doubled their volume after 6 h of growth and were even bigger than cells at 32° C after 18 h, but no growth was observed during this period independent of the light regime. Moreover, in some of the growth conditions, DNA levels of cells grown at both temperatures were similar during the first 24 h of the growth cycle but only cells at 32° C could divide (Figure 4.4; Supplemental Table 4.1). Indeed, after 18 h of growth cells cultured under a 6/2 h light/dark period at 26° C had similar DNA levels and higher volume than cells under the same light regime at 32° C. However, from 18 to 24 h of growth, cultures at 26° C exhibited a very low division rate (0.24) compared to cultures at 32° C (1.8) (Figure 4.4; Supplemental Table 4.1). Thus, based in the information about the evolution of cell volume and DNA content over the growth cycle, is possible to infer that these factors are not coupled with cell division and, consequently, increases in cell volume or DNA levels do not trigger the initiation of cell division. Furthermore, since photosynthesis is the main provider of the ATP required for DNA synthesis (McHenry, 2011; Young et al., 2011; Knoop et al., 2013), and the unique provider of the carbon for cell membrane production

(Figure 1.3) (Knoop et al., 2013; Lea-Smith et al., 2016), the high content of DNA (4 to 6 times) and high cellular volume (6 to 8 times) in the first 24 h of growth indicate that the longer lag phase observed in cultures grown at 26° C was possibly not due to photosynthetic limitations that led to low supply of energy and photoassimilates. Therefore, we hypothesise that a signalling network may regulate the duration of the lag phase, and cells at 32° C could process this signal faster than cells at 26° C and initiate cell division. Importantly, this signal could be the same than the one involved with the gradual decrease of cell division and the onset of the stationary phase we described in chapter 3. Indeed, when cells are transferred to lower density, they may need time to erase the cell-cell interaction inhibitory signal to be able to start cell division.

Flow cytometry analysis also showed that at some stages of the growth cycle the population of *Synechocystis* cells presented variations in their chromosome copy number. The increase of the DNA levels during the first 18 to 24 h of growth, its gradual decrease until reach the initial levels after 72 h (Figure 4.4E-F) and the shape of the DNA content profiles are in good agreement with data reported by Watanabe et al. (2015) for *Synechococcus elongatus* PCC 7942. However, different from *Synechocystis*, this strain only started cell division after DNA content reaches maximum levels. This longer lag phase observed in *Synechococcus* is likely due to the lower light intensity this strain was cultured (40 µmol photons m^{-2} s^{-1}), and cells may be able to start dividing before DNA reach the maximal accumulation levels whether cultured in higher light intensities. Nevertheless, both strains presented a spike-shape profile before and after the logarithmic growth (Figure 4.5), which indicate the presence of two to three different populations of cells with different chromosome copy numbers, and a rounded-shape during the log phase, suggesting that most of the cells presented similar DNA levels during this stage.

Heterotrophic bacteria can monitor the environmental conditions through flagella movements. Hence, changes in medium viscosity that reduce or inhibit flagellar movements can trigger signalling pathways that regulate adjustments of cell morphology, from planktonic to biofilm forms, or even activate virulence (Belas and Suvanasuthi, 2005; Siryaporn et al., 2014). These responses of heterotrophic bacterial cells to changes in environmental viscosity led us to hypothesise that an increase of viscosity could also affect *Synechocystis* growth by decreasing cell-cell interaction, driving cells to exhibit a longer log phase and reach stationary phase with higher densities. However, increases in medium viscosity did not entail on maintenance of the logarithmic growth or delay the onset of the stationary phase. Small increments in viscosity (3.7% and 21.7%) prolonged

lag phase, and further increase (46%) affected negatively logarithmic growth and cell density at stationary phase, possibly by disturbing medium aeration, and consequently reducing CO_2 and O_2 availability (Ugwu et al., 2008).

The results obtained suggest that changes in growth conditions and medium properties are likely not going to allow decreasing cell-cell contacts significantly to prolong the log phase or postpone stationary phase. Thus, the alternative may be to identify the possible proteins or proteins complexes present in *Synechocystis* cell wall that are involved in the cell-cell interaction mechanism. *Synechocystis* possess two types of pili in its cell wall called thin and thick pili (Schuergers and Wilde, 2015). These structures are important for motility and phototaxis (Bhaya et al., 2000), transformation competency (Yoshihara et al., 2001), and iron uptake (Lamb et al., 2014). As no sensorial function is described for these structures, we wondered whether it could also be involved in cell-cell interaction and thus allow cells to sense density. Null mutants of *sigF* and *pilA1A2* were obtained after some rounds of segregation (Figure 4.7A and B), in agreement with their nonessentiality for growth (Rubin et al., 2015), although growth characterization on agar surface confirmed their importance for phototaxis movements (Figure 4.8A) (Bhaya et al., 1999). Growth performances on liquid medium indicate that these cell appendages are not related to sensing cell density and controlling cell division by cell-cell interaction (Figure 4.9). Nevertheless, these structures may be involved with the initiation of cell division, because cells from Δ*pilA1A2* colonies had a shorter lag phase with faster division rates than WT during the first day of growth (Figure 4.9C and D).

4.4 Conclusion

The identification of a cell-cell interaction mechanism controlling growth rates in *Synechocystis* reinforced the need to identify strategies to decrease or avoid the inhibitory effect of cell density on growth, allowing cells to keep faster division rates for longer periods until they will face medium or light limitations. The analyses performed in this chapter, together with those reported in the previous chapter, suggest that the cell-cell interaction mechanism cannot be downregulated just by environmental changes, although the length of lag phase seems sensitive to some of these changes. Further analyses of DNA levels and cell volume indicate that these two parameters are not coupled with cell division and, thus, adjustments of cell volume and DNA content are not the signals that trigger the starting of cell division. This observation also suggests that lag phase may not

be associated with energetic or metabolic limitations, because DNA and cell membrane synthesis request high amounts of ATP and carbon from photosynthesis. Hence, it may be possible that the signalling network triggered by the increase of cell density could still be present when cells are transferred to low cell density conditions and the starting of cell division may require a decrease of this signal, which possibly happens faster at higher temperatures. Molecular analyses indicate that pili structures are not involved with the onset of this signalling network generated by cell-cell interaction, but may present some regulatory role on lag phase. Therefore, further research effort is necessary to identify the nature of this signalling pathway and the proteins or protein complexes responsible for its onset and regulation, allowing the generation of cyanobacteria strains with higher biomass productivity.

4.5 Supplemental material

Supplemental table 4.1: Evolution of cell density, DNA content and cell volume during *Synechocystis* growth cycle

Relative cell density

Hours	18 L/6 D 26° C	18 L/6 D 32° C	6 L/2 D 26°C	6 L/2 D 32°C	LL 26° C	LL 32° C
0	1.00 ± 0.12	1.00 ± 0.14	1.00 ± 0.16	1.00 ± 0.17	1.00 ± 0.27	1.00 ± 0.14
6	1.03 ± 0.04	1.00 ± 0.20	0.91 ± 0.12	0.90 ± 0.14	0.97 ± 0.24	1.06 ± 0..14
18	1.05 ± 0.06	2.21 ± 0.19	0.92 ± 0.17	1.45 ± 0.19	1.07 ± 0.16	2.74 ± 0.23
24	1.03 ± .022	2.87 ± 0.33	1.12 ± 0.39	5.07 ± 0.88	1.92 ± 0.33	5.04 ± 0.34
48	7.82 ± 2.65	19.40 ± 1.29	13.28 ± 4.32	28.82 ± 2.15	19.51 ± 3.40	22.84 ± 2.10
72	32.56 ± 10.04	43.90 ± 4.20	41.02 ± 5.53	57.71 ± 4.08	49.86 ± 1.24	43.36 ± .150
96	66.46 ± 17.10	68.55 ± 9.92	65.50 ± 5.43	65.97 ± 12.45	63.02 ± 6.97	52.26 ± 1.97
120	80.62 ± 11.53	76.80 ± 11.43	85.22 ± 10.63	92.49 ± 16.30	87.12 ± 6.02	68.53 ± 2.41
144	102.77 ± 18.53	86.00 ± 19.56	96.88 ± 11.21	104.11 ± 1.65	100.95 ± 9.97	84.17 ± 3.86
168	102.77 ± 5.64	81.00 ± 15.39	109.17 ± 16.93	99.29 ± 18.97	104.26 ± 13.77	72.01 ± 8.40

Relative DNA content

Hours	18 L/6 D 26° C	18 L/6 D 32° C	6 L/2 D 26°C	6 L/2 D 32°C	LL 26° C	LL 32° C
0	1.00 ± 0.05	1.00 ± 0.03	1.00 ± 0.04	1.00 ± 0.08	1.00 ± 0.04	1.00 ± 0.01
6	1.54 ± 0.02	1.71 ± 0.05	1.10 ± 0.04	1.59 ± 0.34	0.99 ± 0.19	1.22 ± 0.39
18	4.70 ± 0.06	6.34 ± 0.54	3.04 ± 0.28	2.99 ± 0.37	4.44 ± 0.72	5.15 ± 0.65
24	4.30 ± 0.07	4.81 ± 0.23	4.36 ± 0.53	3.77 ± 0.17	6.55 ± 1.22	4.33 ± 0.32
48	3.03 ± 0.08	1.65 ± 0.06	2.65 ± 0.10	2.03 ± 0.05	2.50 ± 0.19	2.16 ± 0.06
72	1.79 ± 0.03	1.16 ± 0.04	1.31 ± 0.05	1.31 ± 0.03	1.37 ± 0.09	0.99 ± 0.06
96	1.36 ± 0.11	0.95 ± 0.02	1.05 ± 0.05	1.10 ± 0.01	1.29 ± 0.12	0.93 ± 0.07
120	1.27 ± 0.10	0.95 ± 0.04	1.05 ± 0.02	1.15 ± 0.06	1.19 ± 0.06	0.95 ± 0.05
144	1.15 ± 0.08	0.87 ± 0.01	1.03 ± 0.01	1.12 ± 0.04	1.16 ± 0.03	1.01 ± 0.05
168	1.22 ± 0.02	0.91 ± 0.06	0.99 ± 0.03	1.16 ± 0.02	1.21 ± 0.03	1.10 ± 0.04

Relative cell volume

Hours	18 L/6 D 26° C	18 L/6 D 32° C	6 L/2 D 26°C	6 L/2 D 32°C	LL 26° C	LL 32° C
0	1.00 ± 0.02	1.00 ± 0.01	1.00 ± 0.01	1.00 ± 0.02	1.00 ± 0.01	1.00 ± 0.01
6	2.01 ± 0.05	2.94 ± 0.03	2.47 ± 0.10	3.60 ± 0.11	2.26 ± 0.25	1.99 ± 0.10
18	6.08 ± 1.16	6.96 ± 0.62	8.14 ± 0.44	5.86 ± 0.52	6.53 ± 0.73	4.03 ± 0.16
24	6.38 ± 0.16	3.53 ± 0.10	8.53 ± 0.29	3.69 ± 0.37	7.62 ± 0.71	2.49 ± 0.12
48	3.58 ± 0.47	0.89 ± 0.02	3.31 ± 0.31	1.08 ± 0.02	1.94 ± 1.12	0.68 ± 0.04
72	1.35 ± 0.05	0.71 ± 0.05	1.19 ± 0.04	0.81 ± 0.02	0.97 ± 0.35	0.59 ± 0.05
96	1.12 ± 0.13	0.80 ± 0.10	0.82 ± 0.02	0.85 ±0.01	0.91 ± 0.26	0.65 ± 0.03
120	1.05 ± 0.15	0.89 ± 0.12	0.92 ± 0.03	0.99 ± 0.05	0.95 ± 0.24	0.75 ± 0.02
144	1.06 ± 0.13	1.02 ± 0.13	0.97 ± 0.04	0.97 ± 0.03	1.00 ± 0.23	0.84 ± 0.04
168	1.14 ± 0.10	1.15 ± 0.17	1.02 ± 0.01	1.07 ± 0.06	1.05 ± 0.18	0.89 ± 0.04

Values represent the means ± standard deviation (n = 3), and are relative to time zero. Significant differences, at 5% probability (unpaired Student's *t* test), between cells grown in similar light regimes but different temperatures are highlighted in blue (higher value) and yellow (lower value).

Supplemental table 4.2: Primers used in this chapter

Gene	Primer name	Sequence	Forward/ Reverse
sigF region	RS017	GGATCTGTGGTCTGGCAATGGC	Forward
	RS018	CAAATCAGGCAGGAGATTGCGG	Reverse
pilA1A2 region	RS019	TGGAGCTAATCAGCATGGTGGAC	Forward
	RS020	TCAGTCAAAGACTGCCCTGGAG	Reverse
kanamycin resistance	RS021	gatcggtaccgatatcGGGAAAGCCACGTTGTGTCTC	Forward
	RS022	cgatctgcagCTGAGGTCTGCCTCGTGAAG	Reverse
sigF	RS060	CACCAGCGAAAGCCTCAAAC	Forward
	RS061	ATGGTGCGCTTCCTTTCTCA	Reverse
pilA1	RS062	ACCGTGCCCAACAAGGTTAT	Forward
	RS063	CCATCAGGAGCTGGGACTTC	Reverse
pliA2	RS064	GCTGGAACTGCTTGTTGTGG	Forward
	RS065	TCAGCTTCCCTCGCTTTACC	Reverse

Small letter in the primers RS021 and RS022 represent the noncoding region of the kanamycin resistance gene

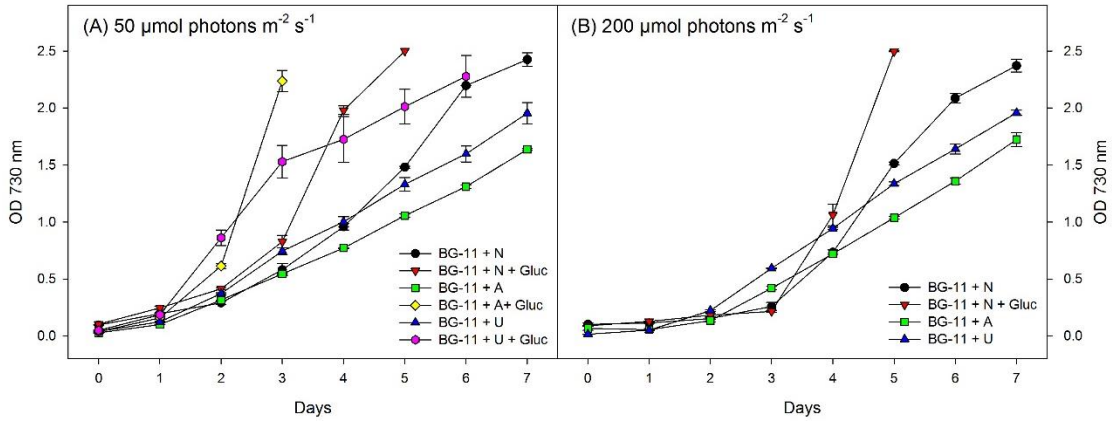

Supplemental Figure 4.1: Glucose tolerance test with *Synechocystis* sp. PCC 6803.
Synechocystis was cultured under (**A**) 50 and (**B**) 200 µmols photons m^{-2} s^{-1} in autotrophic and mixotrophic conditions using liquid BG-11 supplemented with nitrate, ammonium or urea. A, Ammonium; N, Nitrate; U, Urea; Gluc, glucose 0.2 mM.

Final Conclusion and Future Directions

The growth, metabolic and molecular analysis performed in this study showed that *Synechocystis* sp. PCC 6803 (hereafter termed *Synechocystis*) can achieve fast division rates using urea, a low-cost nitrogen source that does not require metabolic energy for uptake and hydrolysis, and releases CO_2 into to the cell during its assimilation. However, the negative effect of cell density on division rates was not due to metabolic limitations or deficiencies in culture conditions, suggesting that *Synechocystis* is likely able to monitor the increase of cell density by a cell-cell interaction mechanism, gradually decreasing its growth rates to avoid a future limitation of resources (light and nutrients). Changes in culture conditions failed to circumvent cell-cell interaction driven growth limitation, although these changes could influence the length of the lag phase. Curiously, the initiation of cell division was also not triggered when cells achieve a certain volume or DNA content. Hence, based on the metabolic and energetic demand for DNA and cell membrane synthesis (McHenry, 2011; Knoop et al., 2013; Lea-Smith et al., 2016) we can hypothesize that photosynthesis and metabolism were likely not limiting the onset of the logarithmic growth, and an additional regulation possibly controls the starting of cell division. Therefore, it may be possible that the signalling network initiated due to increases in cell density could lead to the accumulation of a molecule which is present in cells from linear to stationary phase. Thus, the restart of cell division in these cells would depend first on the decrease of density and subsequently, the depletion of this molecule levels, which probably would happen faster when cells are cultured in higher temperatures due to faster metabolic activities or instability of this signalling molecule.

For a better understanding of how growth is controlled by cell-cell interaction will be important to identify the proteins or proteins complexes present in the cell wall that are involved in sensing the increase in cell density. Zilliges et al. (2008) identified a protein on the cell surface of some strains of *Microcystis aeruginosa* PCC 7806 that is involved with cell-cell contacts and controls cell agglomeration. However, this protein is not present in *Synechocystis*. The existence of two pili structures in *Synechocystis* cell wall (Schuergers and Wilde, 2015) and their role on mobility and phototaxis, when cells are grown on agar surface (Bhaya et al., 2000), raised questions about the possibility of an additional sensorial function related to sensing cell density when cells are grown planktonically. The characterization of pili null mutants indicated that these structures are not involved in cell-cell interaction but may present a role in the onset of the logarithmic phase. Hence, further research effort is necessary to identify new candidates that may be related to cell-cell interaction. Due to the high number of proteins in *Synechocystis* cell

wall, most of them with unknown functions (Huang et al., 2004; Rajalahti et al., 2007; Wang et al., 2009), a possible alternative to select new candidates would be characterize the protein and carbohydrate composition of *Synechocystis* cell wall and exopolysaccharides layer, respectively, in the different stages of the growth cycle (i.e. lag, log, linear and stationary phases). Using this approach would allow to observe whether there are some differences in the cell wall composition over the growth cycle and select those proteins which present opposite behaviour with division rates (e.g. the increase of their levels is followed by a decrease on the growth rate).

The consequence of this cell-cell interaction mechanism, possibly mediated by proteins present on the cell wall, could be the increase in the cellular levels of some signal molecule. Recent findings show that *Synechocystis* present a signalling pathway regulated by light quality that controls the levels of cyclic dimeric guanosine monophosphate (c-di-GMP), a second messenger that is involved in the control of cell buoyancy and agglomeration (Agostoni et al., 2013). This molecule is also observed in heterotrophic bacteria and increases in its cellular levels lead cells to differentiate from motile to biofilm forms (Massie et al., 2012). In cyanobacteria, c-di-GMP synthesis is stimulated by blue light and higher levels of this messenger increase cell sedimentation and aggregation (Agostoni et al., 2016). However, an opposite behaviour would be expected in natural environments. Since blue light can penetrate deeper in the water column, the increase of blue light availability over the other wavelengths likely indicate that cells should increase their buoyancy and move upper in the water column to reach levels where the other wavelengths are more available. Additionally, variations on c-di-GMP levels did not affect the growth cycle, although higher levels of this molecule inhibit the growth of some bacteria (Ryjenkov et al., 2005). Hence, the absence of effect of c-di-GMP on growth could be due to the low light intensity in which these growth analyses were performed (35 µmols photons m^{-2} s^{-1}). Therefore, it would be interesting to determine the levels of c-di-GMP over the growth cycle under higher light conditions to observe how the variation in the levels of this second messenger correlates with growth rates or whether it is really not involved with the control of cell division.

Since this mechanism of cell-cell interaction is likely not controlled by a single gene, a candidate gene approach should not be solely used, and a better strategy to understand this regulation and identify the candidate genes related with it could be an evolution experiment. This strategy has been used to generate thermo-tolerant strains of *Synechocystis* and microalgae (Tillich et al., 2012; Tillich et al., 2014; Bonnefond et al.,

2017). Thus, the identification of the adequate selective pressures (e.g. high light intensity, to avoid self-shading/light limitation, and high and constant cell density, avoiding nutrient limitation) may allow that only cells with lower or absence of sensitivity to the cell-cell interaction be able to divide even in higher cell densities. These dividing cells can be isolated by fluorescence-activated cell sorting (FACS) (Basu et al., 2010; Doan and Obbard, 2012), based on their bigger volume, compared to cells that are not dividing. Another more precise approach would be to use GFP fluorescence, using promoters of genes involved in cell division and replication, and then use these transformed strains for random mutagenesis experiments. Due to the large number of non-causal mutations that happen simultaneously in different cells when using this approach, it will be necessary to sequence the whole populations by next-generation sequencing (NGS) to identify genes with higher frequencies of mutations. Those genes can represent the candidates related to the control of cell density by cell-cell interaction, which will be then validated by homologous recombination and phenotyping of the strains obtained.

List of Figures

List of Tables

References

Agostoni M, Koestler BJ, Waters CM, Williams BL, Montgomery BL (2013) Occurrence of cyclic di-GMP-modulating output domains in cyanobacteria: an illuminating perspective. mBio **4**

Agostoni M, Waters CM, Montgomery BL (2016) Regulation of biofilm formation and cellular buoyancy through modulating intracellular cyclic di-GMP levels in engineered cyanobacteria. Biotechnol. Bioeng. **113:** 311-319

Aichi M, Takatani N, Omata T (2001) Role of NtcB in activation of nitrate assimilation genes in the cyanobacterium *Synechocystis* sp. strain PCC 6803. J. Bacteriol. **183:** 5840-5847

Alfonso M, Perewoska I, Kirilovsky D (2000) Redox control of *psbA* gene expression in the cyanobacterium *Synechocystis* PCC 6803. Involvement of the cytochrome b6/f complex. Plant Physiol. **122:** 505-516

Alfonso M, Perewoska I, Kirilovsky D (2001) Redox control of *ntcA* gene expression in *Synechocystis* sp. PCC 6803. Nitrogen availability and electron transport regulate the levels of the NtcA protein. Plant Physiol. **125:** 969-981

Allen AE, Dupont CL, Oborník M, Horák A, Nunes-Nesi A, McCrow JP, Zheng H, Johnson DA, Hu H, Fernie AR (2011) Evolution and metabolic significance of the urea cycle in photosynthetic diatoms. Nature **473:** 203-207

Altermann W, Kazmierczak J (2003) Archean microfossils: a reappraisal of early life on Earth. Res. Microbiol. **154:** 611-617

Antia N, Harrison P, Oliveira L (1991) The role of dissolved organic nitrogen in phytoplankton nutrition, cell biology and ecology. Phycologia **30:** 1-89

Arteni AA, Ajlani G, Boekema EJ (2009) Structural organisation of phycobilisomes from *Synechocystis* sp. strain PCC6803 and their interaction with the membrane. BBA-Bioenerg. **1787:** 272-279

Asato Y (2003) Toward an understanding of cell growth and the cell division cycle of unicellular photoautotrophic cyanobacteria. Cell. Mol. Life Sci. **60:** 663-687

Asayama M, Imamura S (2008) Stringent promoter recognition and autoregulation by the group 3 σ-factor SigF in the cyanobacterium *Synechocystis* sp. strain PCC 6803. Nucleic Acids Res. **36:** 5297-5305

Atteia A, van Lis R, van Hellemond JJ, Tielens AGM, Martin W, Henze K (2004) Identification of prokaryotic homologues indicates an endosymbiotic origin for the alternative oxidases of mitochondria (AOX) and chloroplasts (PTOX). Gene **330:** 143-148

Azuma M, Osanai T, Hirai MY, Tanaka K (2011) A response regulator Rre37 and an RNA polymerase sigma factor SigE represent two parallel pathways to activate sugar catabolism in a cyanobacterium *Synechocystis* sp. PCC 6803. Plant Cell Physiol. **52:** 404-412

Badger MR, Price GD, Long BM, Woodger FJ (2006) The environmental plasticity and ecological genomics of the cyanobacterial CO_2 concentrating mechanism. J. Exp. Bot. **57:** 249-265

Baebprasert W, Jantaro S, Khetkorn W, Lindblad P, Incharoensakdi A (2011) Increased H_2 production in the cyanobacterium *Synechocystis* sp. strain PCC 6803 by redirecting the electron supply via genetic engineering of the nitrate assimilation pathway. Metab. Eng. **13:** 610-616

Bandyopadhyay A, Elvitigala T, Welsh E, Stöckel J, Liberton M, Min H, Sherman LA, Pakrasi HB (2011) Novel metabolic attributes of the genus *Cyanothece*,

comprising a group of unicellular nitrogen-fixing cyanobacteria. mBio **2:** e00214-00211

Basu S, Campbell HM, Dittel BN, Ray A (2010) Purification of specific cell population by fluorescence activated cell sorting (FACS). J. Vis. Exp.**:** 1546

Beck C, Hertel S, Rediger A, Lehmann R, Wiegard A, Kölsch A, Heilmann B, Georg J, Hess WR, Axmann IM (2014) Daily expression pattern of protein-encoding genes and small noncoding RNAs in *Synechocystis* sp. strain PCC 6803. Appl. Environ. Microbiol. **80:** 5195-5206

Beck C, Knoop H, Axmann IM, Steuer R (2012) The diversity of cyanobacterial metabolism: genome analysis of multiple phototrophic microorganisms. BMC Genomics **13:** 13-56

Becker EW (2007) Micro-algae as a source of protein. Biotechnol. Adv. **25:** 207-210

Bekker A, Holland HD, Wang PL, Rumble D, Stein HJ, Hannah JL, Coetzee LL, Beukes NJ (2004) Dating the rise of atmospheric oxygen. Nature **427:** 117-120

Belas R (2014) Biofilms, flagella, and mechanosensing of surfaces by bacteria. Trends Microbiol. **22:** 517-527

Belas R, Suvanasuthi R (2005) The ability of *Proteus mirabilis* to sense surfaces and regulate virulence gene expression involves FliL, a flagellar basal body protein. J. bacteriol. **187:** 6789-6803

Berg J, Tymoczko J, Stryer L (2002) The glyoxylate cycle enables plants and bacteria to grow on acetate. Biochemistry (Mosc). 5th ed. New York: WH Freeman Publisher. Available from http://www.ncbi.nlm.nih.gov/books/NBK22383

Bergman B, Gallon JR, Rai AN, Stal LJ (1997) N_2 fixation by non-heterocystous cyanobacteria. FEMS Microbiol. Rev. **19:** 139-185

Bergman B, Sandh G, Lin S, Larsson J, Carpenter EJ (2013) *Trichodesmium* – a widespread marine cyanobacterium with unusual nitrogen fixation properties. FEMS Microbiol. Rev. **37:** 286-302

Berla BM, Pakrasi HB (2012) Upregulation of plasmid genes during stationary phase in *Synechocystis* sp. strain PCC 6803, a cyanobacterium. Appl. Environ. Microb. **78:** 5448-5451

Berman-Frank I, Lundgren P, Chen Y-B, Küpper H, Kolber Z, Bergman B, Falkowski P (2001) Segregation of nitrogen fixation and oxygenic photosynthesis in the marine cyanobacterium *Trichodesmium*. Science **294:** 1534-1537

Berman-Frank I, Lundgren P, Falkowski P (2003) Nitrogen fixation and photosynthetic oxygen evolution in cyanobacteria. Res. Microbiol. **154:** 157-164

Bhaya D, Bianco NR, Bryant D, Grossman A (2000) Type IV pilus biogenesis and motility in the cyanobacterium *Synechocystis* sp. PCC6803. Mol. Microbiol. **37:** 941-951

Bhaya D, Watanabe N, Ogawa T, Grossman AR (1999) The role of an alternative sigma factor in motility and pilus formation in the cyanobacterium *Synechocystis* sp. strain PCC6803. PNAS **96:** 3188-3193

Bird C, Wyman M (2003) Nitrate/nitrite assimilation system of the marine picoplanktonic cyanobacterium *Synechococcus* sp. strain WH 8103: effect of nitrogen source and availability on gene expression. Appl. Environ. Microbiol. **69:** 7009-7018

Bonnefond H, Grimaud G, Rumin J, Bougaran G, Talec A, Gachelin M, Boutoute M, Pruvost E, Bernard O, Sciandra A (2017) Continuous selection pressure to improve temperature acclimation of *Tisochrysis lutea*. PLoS One **12:** e0183547

Bradley RW, Bombelli P, Lea-Smith DJ, Howe CJ (2013) Terminal oxidase mutants of the cyanobacterium *Synechocystis* sp. PCC 6803 show increased electrogenic activity in biological photo-voltaic systems. Phys. Chem. Chem. Phys. **15:** 13611-13618

Brennan L, Owende P (2010) Biofuels from microalgae - a review of technologies for production, processing, and extractions of biofuels and co-products. Renew Sust. Energ. Rev. **14:** 557-577

Brown AD (1976) Microbial water stress. Bacteriol. Rev. **40:** 803-846

Burnap RL (2015) Systems and photosystems: cellular limits of autotrophic productivity in cyanobacteria. Front. Bioeng. Biotechnol. **3:** 1-13

Burnat M, Herrero A, Flores E (2014) Compartmentalized cyanophycin metabolism in the diazotrophic filaments of a heterocyst-forming cyanobacterium. PNAS **111:** 3823-3828

Cassier-Chauvat C, Veaudor T, Chauvat F (2016) Comparative genomics of DNA recombination and repair in cyanobacteria: biotechnological implications. Front. Microbiol. **7:** 1809

Catling DC, Zahnle KJ, McKay CP (2001) Biogenic methane, hydrogen escape, and the irreversible oxidation of early earth. Science **293:** 839-843

Cavalcanti JHF, Esteves-Ferreira AA, Quinhones CGS, Pereira-Lima IA, Nunes-Nesi A, Fernie AR, Araújo WL (2014) Evolution and functional implications of the tricarboxylic acid cycle as revealed by phylogenetic analysis. Genome Biol. Evol. **6:** 2830-2848

Chang Y, Takatani N, Aichi M, Maeda S-i, Omata T (2013) Evaluation of the effects of PII deficiency and the toxicity of PipX on growth characteristics of the PII-less mutant of the cyanobacterium *Synechococcus elongatus*. Plant Cell Physiol. **54:** 1504-1514

Chávez S, Lucena JM, Reyes JC, Florencio FJ, Candau P (1999) The presence of glutamate dehydrogenase is a selective advantage for the cyanobacterium *Synechocystis* sp. strain PCC 6803 under nonexponential growth conditions. J. Bacteriol. **181:** 808-813

Chávez S, Reyes JC, Chauvat F, Florencio FJ, Candau P (1995) The NADP-glutamate dehydrogenase of the cyanobacterium *Synechocystis* 6803: cloning, transcriptional analysis and disruption of the *gdhA* gene. Plant Mol. Biol. **28:** 173-188

Chellamuthu VR, Alva V, Forchhammer K (2013) From cyanobacteria to plants: conservation of PII functions during plastid evolution. Planta **237:** 451-462

Crespo JL, García-Domínguez M, Florencio FJ (1998) Nitrogen control of the *glnN* gene that codes for GS type III, the only glutamine synthetase in the cyanobacterium *Pseudanabaena* sp. PCC 6903. Mol. Microbiol. **30:** 1101-1112

Cross JM, von Korff M, Altmann T, Bartzetko L, Sulpice R, Gibon Y, Palacios N, Stitt M (2006) Variation of enzyme activities and metabolite levels in 24 Arabidopsis accessions growing in carbon-limited conditions. Plant Physiol. **142:** 1574-1588

Davidson AL, Chen J (2004) ATP-binding cassette transporters in bacteria. Annu. Rev. Biochem. **73:** 241-268

Dexter J, Fu P (2009) Metabolic engineering of cyanobacteria for ethanol production. Energy Environ. Sci. **2:** 857-864

Díaz-Troya S, López-Maury L, Sánchez-Riego AM, Roldán M, Florencio FJ (2014) Redox regulation of glycogen biosynthesis in the cyanobacterium *Synechocystis* sp. PCC 6803: analysis of the AGP and glycogen synthases. Mol. Plant **7:** 87-100

Doan TTY, Obbard JP (2012) Enhanced intracellular lipid in *Nannochloropsis* sp. via random mutagenesis and flow cytometric cell sorting. Algal Res. **1:** 17-21

Dörrich AK, Mitschke J, Siadat O, Wilde A (2014) Deletion of the *Synechocystis* sp. PCC 6803 *kaiAB1C1* gene cluster causes impaired cell growth under light–dark conditions. Microbiology **160:** 2538-2550

Dubois M, Gilles KA, Hamilton JK, Rebers PA, Smith F (1956) Colorimetric method for determination of sugars and related substances. Anal. Chem. **28:** 350-356

Ducat DC, Way JC, Silver PA (2011) Engineering cyanobacteria to generate high-value products. Trends Biotechnol. **29:** 95-103

Dutta D, De D, Chaudhuri S, Bhattacharya S (2005) Hydrogen production by cyanobacteria. Microb. Cell Fact. **4:** 36

Eisenberg D, Gill HS, Pfluegl GMU, Rotstein SH (2000) Structure–function relationships of glutamine synthetases. BBA Protein Struct. Mol. Enzym. **1477:** 122-145

Eley JH (1988) Glyoxylate cycle enzyme activities in the cyanobacterium *Anacystis nidulans*. J. Phycol. **24:** 586-588

Ellison C, Brun YV (2015) Mechanosensing: a regulation sensation. Curr. Biol. **25:** R113-R115

Eriksen NT (2008) The technology of microalgal culturing. Biotechnol. Lett. **30:** 1525-1536

Espinosa J, Castells MA, Laichoubi KB, Contreras A (2009) Mutations at *pipX* suppress lethality of PII-deficient mutants of *Synechococcus elongatus* PCC 7942. J. Bacteriol. **191:** 4863-4869

Espinosa J, Castells MA, Laichoubi KB, Forchhammer K, Contreras A (2010) Effects of spontaneous mutations in PipX functions and regulatory complexes on the cyanobacterium *Synechococcus elongatus* strain PCC 7942. Microbiology **156:** 1517-1526

Espinosa J, Forchhammer K, Burillo S, Contreras A (2006) Interaction network in cyanobacterial nitrogen regulation: PipX, a protein that interacts in a 2-oxoglutarate dependent manner with PII and NtcA. Mol. Microbiol. **61:** 457-469

Espinosa J, Forchhammer K, Contreras A (2007) Role of the *Synechococcus* PCC 7942 nitrogen regulator protein PipX in NtcA-controlled processes. Microbiology **153:** 711-718

Espinosa J, Rodríguez-Mateos F, Salinas P, Lanza VF, Dixon R, de la Cruz F, Contreras A (2014) PipX, the coactivator of NtcA, is a global regulator in cyanobacteria. PNAS **111(23):** 2423-2430

Esteves-Ferreira AA, Cavalcanti JHF, Vaz MGMV, Alvarenga LV, Nunes-Nesi A, Araújo WL (2017a) Cyanobacterial nitrogenases: phylogenetic diversity, regulation and functional predictions. Genet. Mol. Biol. **40:** 261-275

Esteves-Ferreira AA, Inaba M, Obata T, Fort A, Fleming GT, Araújo WL, Fernie AR, Sulpice R (2017b) A novel mechanism, linked to cell density, largely controls cell division in *Synechocystis*. Plant Physiol. **174:** 2166-2182

Fay P (1992) Oxygen relations of nitrogen fixation in cyanobacteria. Microbiol. Rev. **56:** 340-373

Feria Bourrellier AB, Valot B, Guillot A, Ambard-Bretteville F, Vidal J, Hodges M (2010) Chloroplast acetyl-CoA carboxylase activity is 2-oxoglutarate–regulated by interaction of PII with the biotin carboxyl carrier subunit. PNAS **107:** 502-507

Finzi-Hart JA, Pett-Ridge J, Weber PK, Popa R, Fallon SJ, Gunderson T, Hutcheon ID, Nealson KH, Capone DG (2009) Fixation and fate of C and N in the

cyanobacterium *Trichodesmium* using nanometer-scale secondary ion mass spectrometry. PNAS **106:** 6345-6350

Florencio FJ, Marqués S, Candau P (1987) Identification and characterization of a glutamate dehydrogenase in the unicellular cyanobacterium *Synechocystis* PCC 6803. FEBS Lett. **223:** 37-41

Flores E, Frías JE, Rubio LM, Herrero A (2005) Photosynthetic nitrate assimilation in cyanobacteria. Photosynth. Res. **83:** 117-133

Flores E, Herrero A (2005) Nitrogen assimilation and nitrogen control in cyanobacteria. Biochem. Soc. T. **33:** 164-167

Fokina O, Chellamuthu V-R, Forchhammer K, Zeth K (2010a) Mechanism of 2-oxoglutarate signaling by the *Synechococcus elongatus* PII signal transduction protein. PNAS **107:** 19760-19765

Fokina O, Chellamuthu V-R, Zeth K, Forchhammer K (2010b) A novel signal transduction protein PII variant from *Synechococcus elongatus* PCC 7942 indicates a two-step process for NAGK–PII complex formation. J. Mol. Biol. **399:** 410-421

Fokina O, Herrmann C, Forchhammer K (2011) Signal-transduction protein P(II) from *Synechococcus elongatus* PCC 7942 senses low adenylate energy charge in vitro. Biochem. J. **440:** 147-156

Forcada-Nadal A, Forchhammer K, Rubio V (2014) SPR analysis of promoter binding of *Synechocystis* PCC6803 transcription factors NtcA and CRP suggests cross-talk and sheds light on regulation by effector molecules. FEBS lett. **588:** 2270-2276

Forcada-Nadal A, Palomino-Schätzlein M, Neira JL, Pineda-Lucena A, Rubio V (2017) The PipX protein, when not bound to its targets, has its signaling C-terminal helix in a flexed conformation. Biochem. **56:** 3211-3224

Forchhammer K (2004) Global carbon/nitrogen control by PII signal transduction in cyanobacteria: from signals to targets. FEMS Microbiol. Rev. **28:** 319-333

Forchhammer K, de Marsac NT (1995) Phosphorylation of the PII protein (*glnB* gene product) in the cyanobacterium *Synechococcus* sp. strain PCC 7942: analysis of in vitro kinase activity. J. Bacteriol. **177:** 5812-5817

Forchhammer K, Hedler A (1997) Phosphoprotein PII from cyanobacteria. Eur. J. Biochem. **244:** 869-875

Forchhammer K, Lüddecke J (2016) Sensory properties of the PII signalling protein family. FEBS Journal **283:** 425-437

Forchhammer K, Tandeau de Marsac N (1995) Functional analysis of the phosphoprotein PII (*glnB* gene product) in the cyanobacterium *Synechococcus* sp. strain PCC 7942. J. Bacteriol. **177:** 2033-2040

Foster JS, Singh AK, Rothschild LJ, Sherman LA (2007) Growth-phase dependent differential gene expression in *Synechocystis* sp. strain PCC 6803 and regulation by a group 2 sigma factor. Arch. Microbiol. **187:** 265-279

Frías JE, Mérida A, Herrero A, Martín-Nieto J, Flores E (1993) General distribution of the nitrogen control gene *ntcA* in cyanobacteria. J. Bacteriol. **175:** 5710-5713

Frommeyer M, Wiefel L, Steinbüchel A (2014) Features of the biotechnologically relevant polyamide family "cyanophycins" and their biosynthesis in prokaryotes and eukaryotes. Crit. Rev. Biotechnol. **36(1):** 153-164

García-Domínguez M, Florencio FJ (1997) Nitrogen availability and electron transport control the expression of *glnB* gene (encoding PII protein) in the cyanobacterium *Synechocystis* sp. PCC 6803. Plant Mol. Biol. **35:** 723-734

García-Domínguez M, Reyes JC, Florencio FJ (1997) Purification and characterization of a new type of glutamine synthetase from cyanobacteria. Eur. J. Biochem. **244:** 258-264

García-Domínguez M, Reyes JC, Florencio FJ (2000) NtcA represses transcription of *gifA* and *gifB*, genes that encode inhibitors of glutamine synthetase type I from *Synechocystis* sp. PCC 6803. Mol. Microbiol. **35:** 1192-1201

Ge X, Cain K, Hirschberg R (1990) Urea metabolism and urease regulation in the cyanobacterium *Anabaena variabilis*. Can. J. Microbiol. **36:** 218-222

Ginn HP, Pearson LA, Neilan BA (2010) NtcA from *Microcystis aeruginosa* PCC 7806 is autoregulatory and binds to the microcystin promoter. Appl. Environ. Microbiol. **76:** 4362-4368

Goda SK, Minton NP (1995) A simple procedure for gel electrophoresis and northern blotting of RNA. Nucleic Acids Res. **23:** 3357-3358

González López CV, García MdCC, Fernández FGA, Bustos CS, Chisti Y, Sevilla JMF (2010) Protein measurements of microalgal and cyanobacterial biomass. Bioresour. Technol. **101:** 7587-7591

Govindjee, Shevela D (2011) Adventures with cyanobacteria: a personal perspective. Front. Plant Sci. **2:** 28

Granata T (2017) Dependency of microalgal production on biomass and the relationship to yield and bioreactor scale-up for biofuels: a statistical analysis of 60+ years of algal bioreactor data. Bioenergy Res. **10:** 267-287

Grima EM, Fernández FA, Camacho FG, Chisti Y (1999) Photobioreactors: light regime, mass transfer, and scaleup. J. Biotechnol. **70:** 231-247

Gründel M, Knoop H, Steuer R (2017) Activity and functional properties of the isocitrate lyase in the cyanobacterium *Cyanothece* sp. PCC 7424. Microbiology **163:** 731-744

Guerreiro AC, Benevento M, Lehmann R, van Breukelen B, Post H, Giansanti P, Altelaar AM, Axmann IM, Heck AJ (2014) Daily rhythms in the cyanobacterium *Synechococcus elongatus* probed by high-resolution mass spectrometry–based proteomics reveals a small defined set of cyclic proteins. Mol. Cell Proteomics **13:** 2042-2055

Guerrero MG, Vega JM, Losada M (1981) The assimilatory nitrate-reducing system and its regulation. Annu. Rev. Plant Biol. **32:** 169-204

Hagemann M (2011) Molecular biology of cyanobacterial salt acclimation. FEMS Microbiol. Rev. **35:** 87-123

Hagemann M, Kern R, Maurino VG, Hanson DT, Weber APM, Sage RF, Bauwe H (2016) Evolution of photorespiration from cyanobacteria to land plants, considering protein phylogenies and acquisition of carbon concentrating mechanisms. J. Exp. Bot. **67(10):** 2963-2976

Harano Y, Suzuki I, Maeda S-i, Kaneko T, Tabata S, Omata T (1997) Identification and nitrogen regulation of the cyanase gene from the cyanobacteria *Synechocystis* sp. strain PCC 6803 and *Synechococcus* sp. strain PCC 7942. J. bacteriol. **179:** 5744-5750

Hauf W, Schmid K, Gerhardt ECM, Huergo LF, Forchhammer K (2016) Interaction of the nitrogen regulatory protein GlnB (PII) with biotin carboxyl carrier protein (BCCP) controls acetyl-CoA levels in the cyanobacterium *Synechocystis* sp. PCC 6803. Front. Microbiol. **7:** 1-14

He X, Ahn J (2011) Differential gene expression in planktonic and biofilm cells of multiple antibiotic-resistant *Salmonella typhimurium* and *Staphylococcus aureus*. FEMS Microbiol. Lett. **325:** 180-188

Heinrich A, Maheswaran M, Ruppert U, Forchhammer K (2004) The *Synechococcus elongatus* PII signal transduction protein controls arginine synthesis by complex formation with N-acetyl-l-glutamate kinase. Mol. Microbiol. **52:** 1303-1314

Hendriks JHM, Kolbe A, Gibon Y, Stitt M, Geigenberger P (2003) ADP-glucose pyrophosphorylase is activated by posttranslational redox-modification in response to light and to sugars in leaves of Arabidopsis and other plant species. Plant Physiol. **133:** 838-849

Hendry JI, Prasannan CB, Joshi A, Dasgupta S, Wangikar PP (2016) Metabolic model of *Synechococcus* sp. PCC 7002: prediction of flux distribution and network modification for enhanced biofuel production. Bioresour. Technol. **213:** 190-197

Herrero A, Muro-Pastor AM, Flores E (2001) Nitrogen control in cyanobacteria. J. Bacteriol. **183:** 411-425

Hihara Y, Kamei A, Kanehisa M, Kaplan A, Ikeuchi M (2001) DNA microarray analysis of cyanobacterial gene expression during acclimation to high light. Plant Cell **13:** 793-806

Hisbergues M, Jeanjean R, Joset F, Tandeau de Marsac N, Bédu S (1999) Protein PII regulates both inorganic carbon and nitrate uptake and is modified by a redox signal in *Synechocystis* PCC 6803. FEBS Lett. **463:** 216-220

Huang F, Hedman E, Funk C, Kieselbach T, Schröder WP, Norling B (2004) Isolation of outer membrane of *Synechocystis* sp. PCC 6803 and its proteomic characterization. Mol. Cell Proteomics **3:** 586-595

Huergo LF, Dixon R (2015) The emergence of 2-oxoglutarate as a master regulator metabolite. Microbiol. Mol. Biol. Rev. **79:** 419-435

Iijima H, Nakaya Y, Kuwahara A, Hirai MY, Osanai T (2015) Seawater cultivation of freshwater cyanobacterium *Synechocystis* sp. PCC 6803 drastically alters amino acid composition and glycogen metabolism. Front. Microbiol. **6:** 1-10

Imanaka H, Tanaka S, Feng B, Imamura K, Nakanishi K (2010) Cultivation characteristics and gene expression profiles of *Aspergillus oryzae* by membrane-surface liquid culture, shaking-flask culture, and agar-plate culture. J. Biosci. Bioeng. **109:** 267-273

Irmler A, Forchhammer K (2001) A PP2C-type phosphatase dephosphorylates the PII signaling protein in the cyanobacterium *Synechocystis* PCC 6803. PNAS **98:** 12978-12983

Jiang F, Wisén S, Widersten M, Bergman B, Mannervik B (2000) Examination of the transcription factor NtcA-binding motif by in vitro selection of DNA sequences from a random library. J. Mol. Biol. **301:** 783-793

Joseph A, Aikawa S, Sasaki K, Matsuda F, Hasunuma T, Kondo A (2014) Increased biomass production and glycogen accumulation in *apcE* gene deleted *Synechocystis* sp. PCC 6803. AMB Express **4:** 1-6

Kamennaya NA, Chernihovsky M, Post AF (2008) The cyanate utilization capacity of marine unicellular cyanobacteria. Limnol Oceanogr **53:** 2485-2494

Kaneko T, Sato S, Kotani H, Tanaka A, Asamizu E, Nakamura Y, Miyajima N, Hirosawa M, Sugiura M, Sasamoto S (1996) Sequence analysis of the genome of the unicellular cyanobacterium *Synechocystis* sp. strain PCC6803. II. Sequence determination of the entire genome and assignment of potential protein-coding regions. DNA Res. **3:** 109-136

Kanesaki Y, Shiwa Y, Tajima N, Suzuki M, Watanabe S, Sato N, Ikeuchi M, Yoshikawa H (2012) Identification of substrain-specific mutations by massively

parallel whole-genome resequencing of *Synechocystis* sp. PCC 6803. DNA Res. **19:** 67-79

Kasting JF, Siefert JL (2002) Life and the evolution of Earth's atmosphere. Science **296:** 1066-1068

Kim B-H, Ramanan R, Cho D-H, Choi G-G, La H-J, Ahn C-Y, Oh H-M, Kim H-S (2012) Simple, rapid and cost-effective method for high quality nucleic acids extraction from different strains of *Botryococcus braunii*. PLoS One **7:** e37770

Kim BH, Oh HM, Lee YK, Choi GG, Ahn CY, Yoon BD, Kim HS (2006) Simple method for RNA preparation from cyanobacteria. J. Phycol. **42:** 1137-1141

Kim HW, Vannela R, Zhou C, Rittmann BE (2011) Nutrient acquisition and limitation for the photoautotrophic growth of *Synechocystis* sp. PCC 6803 as a renewable biomass source. Biotechnol. Bioeng. **108:** 277-285

Kirilovsky D (2007) Photoprotection in cyanobacteria: the orange carotenoid protein (OCP)-related non-photochemical-quenching mechanism. Photosynth. Res. **93:** 7-16

Klähn S, Schaal C, Georg J, Baumgartner D, Knippen G, Hagemann M, Muro-Pastor AM, Hess WR (2015) The sRNA NsiR4 is involved in nitrogen assimilation control in cyanobacteria by targeting glutamine synthetase inactivating factor IF7. PNAS **112:** 6243-6252

Kleiner D (1981) The transport of NH_3 and HN_4^+ across biological membranes. BBA - Rev. Bioenerg. **639:** 41-52

Kloft N, Forchhammer K (2005) Signal transduction protein PII phosphatase PphA is required for light-dependent control of nitrate utilization in *Synechocystis* sp. strain PCC 6803. J. Bacteriol. **187:** 6683-6690

Kloft N, Rasch G, Forchhammer K (2005) Protein phosphatase PphA from *Synechocystis* sp. PCC 6803: the physiological framework of PII-P dephosphorylation. Microbiology **151:** 1275-1283

Knoll AH (2008) Cyanobacteria and earth history. *In* A Herrero, E Flores, eds, The Cyanobacteria: Molecular Biology, Genomics, and Evolution. Caister Academic Press, U.K., pp 1-20

Knoop H, Gründel M, Zilliges Y, Lehmann R, Hoffmann S, Lockau W, Steuer R (2013) Flux balance analysis of cyanobacterial metabolism: the metabolic network of *Synechocystis* sp. PCC 6803. PLoS Comput. Biol. **9:** e1003081

Kobayashi M, Rodríguez Ro, Lara C, Omata T (1997) Involvement of the C-terminal domain of an ATP-binding subunit in the regulation of the ABC-type nitrate/nitrite transporter of the cyanobacterium *Synechococcus* sp. strain PCC 7942. J. Biol. Chem. **272:** 27197-27201

Kobayashi M, Takatani N, Tanigawa M, Omata T (2005) Posttranslational regulation of nitrate assimilation in the cyanobacterium *Synechocystis* sp. strain PCC 6803. J. Bacteriol. **187:** 498-506

Komárek J, Kastovský J (2003) Coincidences of structural and molecular characters in evolutionary lines of cyanobacteria. Algol. Stud. **109:** 305-325

Kopečná J, Komenda J, Bučinská L, Sobotka R (2012) Long-term acclimation of the cyanobacterium *Synechocystis* sp. PCC 6803 to high light is accompanied by an enhanced production of chlorophyll that is preferentially channeled to trimeric photosystem I. Plant Physiol. **160:** 2239-2250

Kornberg H (2000) Krebs and his trinity of cycles. Nat. Rev. Mol. Cell Biol. **1:** 225-228

Koropatkin NM, Pakrasi HB, Smith TJ (2006) Atomic structure of a nitrate-binding protein crucial for photosynthetic productivity. PNAS **103:** 9820-9825

Krall L, Huege J, Catchpole G, Steinhauser D, Willmitzer L (2009) Assessment of sampling strategies for gas chromatography-mass spectrometry (GC-MS) based metabolomics of cyanobacteria. J. Chromatogr. B **877:** 2952-2960

Kuhl M, Chen M, Ralph PJ, Schreiber U, Larkum AWD (2005) Ecology: A niche for cyanobacteria containing chlorophyll d. Nature **433:** 820-820

Kuniyoshi TM, Gonzalez A, Lopez-Gomollon S, Valladares A, Bes MT, Fillat MF, Peleato ML (2011) 2-oxoglutarate enhances NtcA binding activity to promoter regions of the microcystin synthesis gene cluster. FEBS lett. **585:** 3921-3926

Labella JI, Obrebska A, Espinosa J, Salinas P, Forcada-Nadal A, Tremiño L, Rubio V, Contreras A (2016) Expanding the cyanobacterial nitrogen regulatory network: The GntR-like regulator PlmA interacts with the PII-PipX complex. Front. Microbiol. **7:** 1677

Laichoubi KB, Beez S, Espinosa J, Forchhammer K, Contreras A (2011) The nitrogen interaction network in *Synechococcus* WH5701, a cyanobacterium with two PipX and two PII-like proteins. Microbiology **157:** 1220-1228

Laichoubi KB, Espinosa J, Castells MA, Contreras A (2012) Mutational analysis of the cyanobacterial nitrogen regulator PipX. PLoS One **7:** e35845

Lamb JJ, Hill RE, Eaton-Rye JJ, Hohmann-Marriott MF (2014) Functional role of PilA in iron acquisition in the cyanobacterium *Synechocystis* sp. PCC 6803. PLoS One **9:** e105761

Law AE, Mullineaux CW, Hirst EM, Saldanha J, Wilson RI (2000) Bacterial orthologues indicate the malarial plastid gene *ycf24* is essential. Protist **151:** 317-327

Lazazzera BA (2000) Quorum sensing and starvation: signals for entry into stationary phase. Curr. Opin. Microbiol. **3:** 177-182

Lea-Smith DJ, Bombelli P, Dennis JS, Scott SA, Smith AG, Howe CJ (2014) Phycobilisome-deficient strains of *Synechocystis* sp. PCC 6803 have reduced size and require carbon-limiting conditions to exhibit enhanced productivity. Plant Physiol. **165:** 705-714

Lea-Smith DJ, Ortiz-Suarez ML, Lenn T, Nürnberg DJ, Baers LL, Davey MP, Parolini L, Huber RG, Cotton CAR, Mastroianni G, Bombelli P, Ungerer P, Stevens TJ, Smith AG, Bond PJ, Mullineaux CW, Howe CJ (2016) Hydrocarbons are essential for optimal cell size, division, and growth of cyanobacteria. Plant Physiol. **172:** 1928-1940

Lee H-M, Flores E, Herrero A, Houmard J, Tandeau de Marsac N (1998) A role for the signal transduction protein PII in the control of nitrate/nitrite uptake in a cyanobacterium. FEBS Lett. **427:** 291-295

Lee H-M, Vázquez-Bermúdez MF, de Marsac NT (1999) The global nitrogen regulator NtcA regulates transcription of the signal transducer PII (GlnB) and influences its phosphorylation level in response to nitrogen and carbon supplies in the cyanobacterium *Synechococcus sp*. strain PCC 7942. J. Bacteriol. **181:** 2697-2702

Leganés F, Blanco-Rivero A, Fernández-Piñas F, Redondo M, Fernández-Valiente E, Fan Q, Lechno-Yossef S, Wolk CP (2005) Wide variation in the cyanobacterial complement of presumptive penicillin-binding proteins. Arch. Microbiol. **184:** 234-248

Liu H, Zhang H, Niedzwiedzki DM, Prado M, He G, Gross ML, Blankenship RE (2013) Phycobilisomes supply excitations to both photosystems in a megacomplex in cyanobacteria. Science **342:** 1104-1107

Liu X, Sheng J, Curtiss III R (2011) Fatty acid production in genetically modified cyanobacteria. PNAS **108:** 6899-6904

Llácer JL, Contreras A, Forchhammer K, Marco-Marín C, Gil-Ortiz F, Maldonado R, Fita I, Rubio V (2007) The crystal structure of the complex of PII and acetylglutamate kinase reveals how PII controls the storage of nitrogen as arginine. PNAS **104:** 17644-17649

Llácer JL, Espinosa J, Castells MA, Contreras A, Forchhammer K, Rubio V (2010) Structural basis for the regulation of NtcA-dependent transcription by proteins PipX and PII. PNAS **107:** 15397-15402

Llácer JL, Fita I, Rubio V (2008) Arginine and nitrogen storage. Curr. Opin. Struct. Biol. **18:** 673-681

Lowry OH, Rosebrough NJ, Farr AL, Randall RJ (1951) Protein measurement with the folin phenol reagent. J. Biol. Chem. **193:** 265-275

Lu Y-M, Xiang W-Z, Wen Y-H (2011) *Spirulina* (*Arthrospira*) industry in Inner Mongolia of China: current status and prospects. J. Appl. Phycol. **23:** 265-269

Lüddecke J, Forchhammer K (2013) From PII signaling to metabolite sensing: a novel 2-oxoglutarate sensor that details PII-NAGK complex formation. PLoS One **8:** e83181

Lüddecke J, Forchhammer K (2015) Energy sensing versus 2-oxoglutarate dependent ATPase switch in the control of *Synechococcus* PII interaction with its targets NAGK and PipX. PLoS One **10:** e0137114

Lüddecke J, Francois L, Spät P, Watzer B, Chilczuk T, Poschet G, Hell R, Radlwimmer B, Forchhammer K (2017) PII protein-derived FRET sensors for quantification and live-cell imaging of 2-oxoglutarate. Sci. Rep. **7:** 1-13

Ludwig M, Bryant DA (2012) Acclimation of the global transcriptome of the cyanobacterium *Synechococcus* sp. strain PCC 7002 to nutrient limitations and different nitrogen sources. Front. Microbiol. **3:** 1-15

Luque I, Flores E, Herrero A (1994a) Molecular mechanism for the operation of nitrogen control in cyanobacteria. Embo Journal **13:** 2862-2869

Luque I, Flores E, Herrero A (1994b) Nitrate and nitrite transport in the cyanobacterium *Synechococcus* sp. PCC 7942 are mediated by the same permease. BBA - Bioenerg. **1184:** 296-298

Luque I, Zabulon G, Contreras A, Houmard J (2001) Convergence of two global transcriptional regulators on nitrogen induction of the stress-acclimation gene *nblA* in the cyanobacterium *Synechococcus* sp. PCC 7942. Mol. Microbiol. **41:** 937-947

Ma C-W, Lüddecke J, Forchhammer K, Zeng A-P (2014) Population shift of binding pocket size and dynamic correlation analysis shed new light on the anticooperative mechanism of P(II) protein. Proteins **82:** 1048-1059

Machado IMP, Atsumi S (2012) Cyanobacterial biofuel production. J. Biotechnol. **162:** 50-56

Mackay MA, Norton RS, Borowitzka LJ (1984) Organic osmoregulatory solutes in cyanobacteria. Microbiology **130:** 2177-2191

Maeda S-i, Murakami A, Ito H, Tanaka A, Omata T (2015) Functional characterization of the FNT family nitrite transporter of marine picocyanobacteria. Life **5:** 432-446

Maeda S-i, Omata T (2009) Nitrite transport activity of the ABC-type cyanate transporter of the cyanobacterium *Synechococcus elongatus*. J. Bacteriol. **191:** 3265-3272

Maheswaran M, Ziegler K, Lockau W, Hagemann M, Forchhammer K (2006) PII-regulated arginine synthesis controls accumulation of cyanophycin in *Synechocystis* sp. strain PCC 6803. J. Bacteriol. **188:** 2730-2734

Marbouty M, Mazouni K, Saguez C, Cassier-Chauvat C, Chauvat F (2009a) Characterization of the *Synechocystis* strain PCC 6803 penicillin-binding proteins and cytokinetic proteins FtsQ and FtsW and their network of interactions with ZipN. J. Bacteriol. **191:** 5123-5133

Marbouty M, Saguez C, Cassier-Chauvat C, Chauvat F (2009b) Characterization of the FtsZ-interacting septal proteins SepF and Ftn6 in the spherical-celled cyanobacterium *Synechocystis* strain PCC 6803. J. Bacteriol. **191:** 6178-6185

Marbouty M, Saguez C, Chauvat F (2009c) The cyanobacterial cell division factor Ftn6 contains an N-terminal DnaD-like domain. BMC Struct. Biol. **9:** 54-54

Marino GT, Asato Y (1986) Characterization of cell cycle events in the dark in *Anacystis nidulans*. Microbiology **132:** 2123-2127

Markou G, Georgakakis D (2011) Cultivation of filamentous cyanobacteria (blue-green algae) in agro-industrial wastes and wastewaters: a review. Appl. Energy **88:** 3389-3401

Martin W, Rujan T, Richly E, Hansen A, Cornelsen S, Lins T, Leister D, Stoebe B, Hasegawa M, Penny D (2002) Evolutionary analysis of *Arabidopsis*, cyanobacterial, and chloroplast genomes reveals plastid phylogeny and thousands of cyanobacterial genes in the nucleus. PNAS **99:** 12246-12251

Massie JP, Reynolds EL, Koestler BJ, Cong J-P, Agostoni M, Waters CM (2012) Quantification of high-specificity cyclic diguanylate signaling. PNAS **109:** 12746-12751

Mazouni K, Domain F, Cassier-Chauvat C, Chauvat F (2004) Molecular analysis of the key cytokinetic components of cyanobacteria: FtsZ, ZipN and MinCDE. Mol. Microbiol. **52:** 1145-1158

McCormick AJ, Bombelli P, Lea-Smith DJ, Bradley RW, Scott AM, Fisher AC, Smith AG, Howe CJ (2013) Hydrogen production through oxygenic photosynthesis using the cyanobacterium *Synechocystis* sp. PCC 6803 in a bio-photoelectrolysis cell (BPE) system. Energy Environ. Sci. **6:** 2682-2690

McHenry CS (2011) DNA Replicases from a Bacterial Perspective. Annu. Rev. Biochem. **80:** 403-436

Mehta PK, Hale TI, Christen P (1993) Aminotransferases: demonstration of homology and division into evolutionary subgroups. Eur. J. Biochem. **214:** 549-561

Messineo L (1966) Modification of the Sakaguchi reaction: spectrophotometric determination of arginine in proteins without previous hydrolysis. Arch. Biochem. Bioph. **117:** 534-540

Miao X, Wu Q, Wu G, Zhao N (2003) Sucrose accumulation in salt-stressed cells of *agp* gene deletion-mutant in cyanobacterium *Synechocystis* sp. PCC 6803. FEMS Microbiol. Lett. **218:** 71-77

Mikkat S, Effmert U, Hagemann M (1997) Uptake and use of the osmoprotective compounds trehalose, glucosylglycerol, and sucrose by the cyanobacterium *Synechocystis* sp. PCC 6803. Arch. Microbiol. **167:** 112-118

Mitamura O, Kawashima M, Maeda H (2000) Urea degradation by picophytoplankton in the euphotic zone of Lake Biwa. Limnology **1:** 19-26

Mitamura O, Saijo Y (1980) In situ measurement of the urea decomposition rate and its turnover rate in the Pacific Ocean. Mar. Biol. **58:** 147-152

Miyagishima Sy, Wolk CP, Osteryoung KW (2005) Identification of cyanobacterial cell division genes by comparative and mutational analyses. Mol. Microbiol. **56:** 126-143

Montesinos MaL, Muro-Pastor AMa, Herrero A, Flores E (1998) Ammonium/methylammonium permeases of a cyanobacterium: identification

and analysis of three nitrogen-regulated *amt* genes in *Synechocystis* sp. PCC 6803. J. Biol. Chem. **273:** 31463-31470

Mori T, Binder B, Johnson CH (1996) Circadian gating of cell division in cyanobacteria growing with average doubling times of less than 24 hours. PNAS **93:** 10183-10188

Mori T, Johnson CH (2001) Independence of circadian timing from cell division in cyanobacteria. J. Bacteriol. **183:** 2439-2444

Mulkidjanian A, Koonin E, Makarova K, Mekhedov S, Sorokin A, Wolf Y, Dufresne A, Partensky F, Burd H, Kaznadzey D, Haselkorn R, Galperin M (2006) The cyanobacterial genome core and the origin of photosynthesis. PNAS **103:** 13126 - 13131

Mullineaux C (2008) Phycobilisome-reaction centre interaction in cyanobacteria. Photosynth. Res. **95:** 175-182

Muramatsu M, Hihara Y (2011) Acclimation to high-light conditions in cyanobacteria: from gene expression to physiological responses. J. Plant Res. **125:** 11-39

Muramatsu M, Sonoike K, Hihara Y (2009) Mechanism of downregulation of photosystem I content under high-light conditions in the cyanobacterium *Synechocystis* sp. PCC 6803. Microbiology **155:** 989-996

Muro-Pastor AMa, Herrero A, Flores E (2001) Nitrogen-regulated group 2 sigma factor from *Synechocystis* sp. strain PCC 6803 involved in survival under nitrogen stress. J. Bacteriol. **183:** 1090-1095

Muro-Pastor MI, Florencio FJ (2003) Regulation of ammonium assimilation in cyanobacteria. Plant Physiol. Biochem. **41:** 595-603

Muro-Pastor MI, Reyes JC, Florencio FJ (1996) The $NADP^+$-isocitrate dehydrogenase gene (*icd*) is nitrogen regulated in cyanobacteria. J. Bacteriol. **178:** 4070-4076

Muro-Pastor MI, Reyes JC, Florencio FJ (2005) Ammonium assimilation in cyanobacteria. Photosynth. Res. **83:** 135-150

Nakasugi K, Neilan BA (2005) Identification of pilus-like structures and genes in *Microcystis aeruginosa* PCC7806. Appl. Environ. Microbiol. **71:** 7621-7625

Navarro F, Chávez S, Candau P, Florencio FJ (1995) Existence of two ferredoxin-glutamate synthases in the cyanobacterium *Synechocystis* sp. PCC 6803. Isolation and insertional inactivation of *gltB* and *gltS* genes. Plant Mol. Biol. **27:** 753-767

Neilson A, Doudoroff M (1973) Ammonia assimilation in blue-green algae. Arch. Microbiol. **89:** 15-22

Niu W, Kim Y, Tau G, Heyduk T, Ebright RH (1996) Transcription activation at class II CAP-dependent promoters: two interactions between CAP and RNA polymerase. Cell **87:** 1123-1134

Nogales J, Gudmundsson S, Knight EM, Palsson BO, Thiele I (2012) Detailing the optimality of photosynthesis in cyanobacteria through systems biology analysis. PNAS **109:** 2678-2683

Nunnery JK, Mevers E, Gerwick WH (2010) Biologically active secondary metabolites from marine cyanobacteria. Curr. Opin. Biotechnol. **21:** 787-793

Ochoa de Alda JAG, Esteban R, Diago ML, Houmard J (2014) The plastid ancestor originated among one of the major cyanobacterial lineages. Nat. Commun. **5:** 4937

Ohashi Y, Shi W, Takatani N, Aichi M, Maeda S-i, Watanabe S, Yoshikawa H, Omata T (2011) Regulation of nitrate assimilation in cyanobacteria. J. Exp. Bot. **62:** 1411-1424

Ohbayashi R, Watanabe S, Ehira S, Kanesaki Y, Chibazakura T, Yoshikawa H (2016) Diversification of DnaA dependency for DNA replication in cyanobacterial evolution. ISME J. **10:** 1113-1121

Ohbayashi R, Watanabe S, Kanesaki Y, Narikawa R, Chibazakura T, Ikeuchi M, Yoshikawa H (2013) DNA replication depends on photosynthetic electron transport in cyanobacteria. FEMS Microbiol. Lett. **344:** 138-144

Ohbayashi R, Yamamoto J-y, Watanabe S, Kanesaki Y, Chibazakura T, Miyagishima S-y, Yoshikawa H (2017) Variety of DNA replication activity among cyanobacteria correlates with distinct respiration activity in the dark. Plant Cell Physiol. **58:** 279-286

Okuhara H, Matsumura T, Fujita Y, Hase T (1999) Cloning and inactivation of genes encoding ferredoxin- and NADH-dependent glutamate synthases in the cyanobacterium *Plectonema boryanum*. Imbalances in nitrogen and carbon assimilations caused by deficiency of the ferredoxin-dependent enzyme. Plant Physiol. **120:** 33-42

Omata T, Andriesse X, Hirano A (1993) Identification and characterization of a gene cluster involved in nitrate transport in the cyanobacterium *Synechococcus* sp. PCC7942. Mol. Gen. Genet. **236:** 193-202

Omata T, Ohmori M, Arai N, Ogawa T (1989) Genetically engineered mutant of the cyanobacterium *Synechococcus* PCC 7942 defective in nitrate transport. PNAS **86:** 6612-6616

Ort DR, Zhu X, Melis A (2011) Optimizing antenna size to maximize photosynthetic efficiency. Plant Physiol. **155:** 79-85

Osanai T, Azuma M, Tanaka K (2007) Sugar catabolism regulated by light- and nitrogen-status in the cyanobacterium *Synechocystis* sp. PCC 6803. Photochem. Photobiol. Sci. **6:** 508-514

Osanai T, Imamura S, Asayama M, Shirai M, Suzuki I, Murata N, Tanaka K (2006) Nitrogen induction of sugar catabolic gene expression in *Synechocystis* sp. PCC 6803. DNA Res. **13:** 185-195

Osanai T, Oikawa A, Iijima H, Kuwahara A, Asayama M, Tanaka K, Ikeuchi M, Saito K, Hirai MY (2014) Metabolomic analysis reveals rewiring of *Synechocystis* sp. PCC 6803 primary metabolism by *ntcA* overexpression. Environ. Microbiol. **16:** 3304-3317

Oswald O, Martin T, Dominy PJ, Graham IA (2001) Plastid redox state and sugars: Interactive regulators of nuclear-encoded photosynthetic gene expression. PNAS **98:** 2047-2052

Pando BF, van Oudenaarden A (2010) Coupling cellular oscillators—circadian and cell division cycles in cyanobacteria. Curr. Opin. Genet. Dev. **20:** 613-618

Parmar A, Singh NK, Pandey A, Gnansounou E, Madamwar D (2011) Cyanobacteria and microalgae: a positive prospect for biofuels. Bioresource Technol. **102:** 10163-10172

Parnasa R, Nagar E, Sendersky E, Reich Z, Simkovsky R, Golden S, Schwarz R (2016) Small secreted proteins enable biofilm development in the cyanobacterium *Synechococcus elongatus*. Sci. Rep. **6:** 1-10

Paz-Yepes J, Flores E, Herrero A (2003) Transcriptional effects of the signal transduction protein P(II) (*glnB* gene product) on NtcA-dependent genes in *Synechococcus* sp. PCC 7942. FEBS Lett. **543:** 42-46

Paz-Yepes J, Herrero A, Flores E (2007) The NtcA-regulated *amtB* gene is necessary for full methylammonium uptake activity in the cyanobacterium *Synechococcus elongatus*. J. Bacteriol. **189:** 7791-7798

Pearce J, Carr NG (1967) The metabolism of acetate by the blue-green algae, *Anabaena variabilis* and *Anacystis nidulans*. J. Gen. Microbiol. **49:** 301-313

Pearce J, Leach C, Carr N (1969) The incomplete tricarboxylic acid cycle in the blue-green alga *Anabaena variabilis*. J. Gen. Microbiol. **55:** 371-378

Peschek GA, Obinger C, Paumann M (2004) The respiratory chain of blue-green algae (cyanobacteria). Physiol. Plant. **120:** 358-369

Pimentel JSM, Giani A (2014) Microcystin production and regulation under nutrient stress conditions in toxic microcystis strains. Appl. Environ. Microbiol. **80:** 5836-5843

Pinto F, Pacheco CC, Ferreira D, Moradas-Ferreira P, Tamagnini P (2012) Selection of suitable reference genes for RT-qPCR analyses in cyanobacteria. PLoS One **7:** e34983

Price DC, Chan CX, Yoon HS, Yang EC, Qiu H, Weber APM, Schwacke R, Gross J, Blouin NA, Lane C, Reyes-Prieto A, Durnford DG, Neilson JAD, Lang BF, Burger G, Steiner JM, Löffelhardt W, Meuser JE, Posewitz MC, Ball S, Arias MC, Henrissat B, Coutinho PM, Rensing SA, Symeonidi A, Doddapaneni H, Green BR, Rajah VD, Boore J, Bhattacharya D (2012) *Cyanophora paradoxa* genome elucidates origin of photosynthesis in algae and plants. Science **335:** 843-847

Price GD, Sültemeyer D, Klughammer B, Ludwig M, Badger MR (1998) The functioning of the CO_2 concentrating mechanism in several cyanobacterial strains: a review of general physiological characteristics, genes, proteins, and recent advances. Can. J. Bot. **76:** 973-1002

Quintero MaJ, Montesinos MaL, Herrero A, Flores E (2001) Identification of genes encoding amino acid permeases by inactivation of selected ORFs from the *Synechocystis* genomic sequence. Genome Res. **11:** 2034-2040

Quintero MJ, Muro-Pastor AM, Herrero A, Flores E (2000) Arginine catabolism in the cyanobacterium *Synechocystis* sp. strain PCC 6803 involves the urea cycle and arginase pathway. J. Bacteriol. **182:** 1008-1015

Rajalahti T, Huang F, Rosén Klement M, Pisareva T, Edman M, Sjöström M, Wieslander Å, Norling B (2007) Proteins in different *Synechocystis* compartments have distinguishing N-terminal features: a combined proteomics and multivariate sequence analysis. J. Proteome Res. **6:** 2420-2434

Rangel OA, Gómez-Baena G, López-Lozano A, Diez J, García-Fernández JM (2009) Physiological role and regulation of glutamate dehydrogenase in *Prochlorococcus* sp. strain MIT9313. Environ. Microbiol. Rep. **1:** 56-64

Rastogi RP, Sinha RP, Incharoensakdi A (2014) The cyanotoxin-microcystins: current overview. Rev. Environ. Sci. Biotechnol. **13:** 215

Raven JA, Kübler JE (2002) New light on the scaling of metabolic rate with the size of algae. J. Phycol. **38:** 11-16

Rees AP, Woodward EMS, Joint I (2006) Concentrations and uptake of nitrate and ammonium in the Atlantic Ocean between 60°N and 50°S. Deep Sea Res. Part 2 Top. Stud. Oceanogr. **53:** 1649-1665

Reyes J, Muro-Pastor M, Florencio F (1997) Transcription of glutamine synthetase genes (*glnA* and *glnN*) from the cyanobacterium *Synechocystis* sp. strain PCC 6803 is differently regulated in response to nitrogen availability. J. Bacteriol. **179:** 2678-2689

Reyes JC, Florencio FJ (1994) A new type of glutamine synthetase in cyanobacteria: the protein encoded by the *glnN* gene supports nitrogen assimilation in *Synechocystis* sp. strain PCC 6803. J. Bacteriol. **176:** 1260-1267

Rippka R, Deruelles J, Waterbury JB, Herdman M, Stanier RY (1979) Generic assignments, strain histories and properties of pure cultures of cyanobacteria. J. Gen. Microbiol. **111:** 1-61

Ritchie R (2006) Consistent sets of spectrophotometric chlorophyll equations for acetone, methanol and ethanol solvents. Photosynth. Res. **89:** 27-41

Rodriguez IB, Ho T-Y (2014) Diel nitrogen fixation pattern of *Trichodesmium*: the interactive control of light and Ni. Sci. Rep. **4:** 1-5

Romero-Lastra P, Sánchez MC, Ribeiro-Vidal H, Llama-Palacios A, Figuero E, Herrera D, Sanz M (2017) Comparative gene expression analysis of *Porphyromonas gingivalis* ATCC 33277 in planktonic and biofilms states. PLoS One **12:** e0174669

Rubin BE, Wetmore KM, Price MN, Diamond S, Shultzaberger RK, Lowe LC, Curtin G, Arkin AP, Deutschbauer A, Golden SS (2015) The essential gene set of a photosynthetic organism. PNAS **112:** E6634-E6643

Ruffing AM (2011) Engineered cyanobacteria: teaching an old bug new tricks. Bioeng. Bugs. **2:** 136-149

Ruppert U, Irmler A, Kloft N, Forchhammer K (2002) The novel protein phosphatase PphA from *Synechocystis* PCC 6803 controls dephosphorylation of the signalling protein PII. Mol. Microbiol. **44:** 855-864

Ryjenkov DA, Tarutina M, Moskvin OV, Gomelsky M (2005) Cyclic diguanylate is a ubiquitous signaling molecule in bacteria: insights into biochemistry of the GGDEF protein domain. J. bacteriol. **187:** 1792-1798

Saelices L, Galmozzi CV, Florencio FJ, Muro-Pastor MI (2011) Mutational analysis of the inactivating factors, IF7 and IF17 from *Synechocystis* sp. PCC 6803: critical role of arginine amino acid residues for glutamine synthetase inactivation. Mol. Microbiol. **82:** 964-975

Sakamoto T, Bryant DA (2001) Requirement of nickel as an essential micronutrient for the utilization of urea in the marine cyanobacterium *Synechococcus* sp. PCC 7002. Microbes Environ. **16:** 177-184

Sakamoto T, Inoue-Sakamoto K, Bryant DA (1999) A novel nitrate/nitrite permease in the marine cyanobacterium *Synechococcus* sp. strain PCC 7002. J. Bacteriol. **181:** 7363-7372

Sandh G, Ran L, Xu L, Sundqvist G, Bulone V, Bergman B (2011) Comparative proteomic profiles of the marine cyanobacterium *Trichodesmium erythraeum* IMS101 under different nitrogen regimes. Proteomics **11:** 406-419

Sant'Anna FH, Trentini DB, de Souto Weber S, Cecagno R, da Silva SC, Schrank IS (2009) The PII superfamily revised: a novel group and evolutionary insights. J. Mol. Evol. **68:** 322-336

Sasaki Y, Nagano Y (2004) Plant acetyl-CoA carboxylase: structure, biosynthesis, regulation, and gene manipulation for plant breeding. Biosci. Biotechnol. Biochem. **68:** 1175-1184

Sauer J, Görl M, Forchhammer K (1999) Nitrogen starvation in *Synechococcus* PCC 7942: involvement of glutamine synthetase and NtcA in phycobiliprotein degradation and survival. Arch. Microbiol. **172:** 247-255

Schatz D, Nagar E, Sendersky E, Parnasa R, Zilberman S, Carmeli S, Mastai Y, Shimoni E, Klein E, Yeger O (2013) Self-suppression of biofilm formation in the cyanobacterium *Synechococcus elongatus*. Environ. Microbiol. **15:** 1786-1794

Schenk PM, Thomas-Hall SR, Stephens E, Marx UC, Mussgnug JH, Posten C, Kruse O, Hankamer B (2008) Second generation biofuels: high-efficiency microalgae for biodiesel production. Bioenergy Res. **1:** 20-43

Schippers JHM, Nunes-Nesi A, Apetrei R, Hille J, Fernie AR, Dijkwel PP (2008) The Arabidopsis onset of leaf death5 mutation of quinolinate synthase affects nicotinamide adenine dinucleotide biosynthesis and causes early ageing. Plant Cell **20:** 2909-2925

Schirrmeister BE, de Vos JM, Antonelli A, Bagheri HC (2013) Evolution of multicellularity coincided with increased diversification of cyanobacteria and the Great Oxidation Event. PNAS **110(5):** 1791-1796

Schneider D, Fuhrmann E, Scholz I, Hess WR, Graumann PL (2007) Fluorescence staining of live cyanobacterial cells suggest non-stringent chromosome segregation and absence of a connection between cytoplasmic and thylakoid membranes. BMC Cell Biol. **8:** 39-39

Schuergers N, Wilde A (2015) Appendages of the cyanobacterial cell. Life **5:** 700-715

Schuurmans RM, Matthijs JCP, Hellingwerf KJ (2017) Transition from exponential to linear photoautotrophic growth changes the physiology of *Synechocystis* sp. PCC 6803. Photosynth. Res. **132(1):** 69-82

Schuurmans RM, van Alphen P, Schuurmans JM, Matthijs HCP, Hellingwerf KJ (2015) Comparison of the photosynthetic yield of cyanobacteria and green algae: different methods give different answers. PLoS One **10:** e0139061

Schwamborn M (1998) Chemical synthesis of polyaspartates: a biodegradable alternative to currently used polycarboxylate homo- and copolymers. Polym. Degrad. Stab. **59:** 39-45

Sekar S, Chandramohan M (2008) Phycobiliproteins as a commodity: trends in applied research, patents and commercialization. J. Appl. Phycol. **20:** 113-136

Sharif DI, Gallon J, Smith CJ, Dudley E (2008) Quorum sensing in Cyanobacteria: n-octanoyl-homoserine lactone release and response, by the epilithic colonial cyanobacterium *Gloeothece* PCC 6909. ISME J. **2:** 1171-1182

Shiloach J, Fass R (2005) Growing *E. coli* to high cell density - a historical perspective on method development. Biotechnol. Adv. **23:** 345-357

Singh S (1990) Regulation of urease activity in the cyanobacterium *Anabaena doliolum*. FEMS Microbiol. Lett. **67:** 79-84

Singh S (1992) Regulation of urease cellular levels in the cyanobacteria *Anacystis nidulans* and *Nostoc muscorum*. Biochem. Physiol. Pflanz. **188:** 33-38

Siryaporn A, Kuchma SL, O'Toole GA, Gitai Z (2014) Surface attachment induces *Pseudomonas aeruginosa* virulence. PNAS **111:** 16860-16865

Slade R, Bauen A (2013) Micro-algae cultivation for biofuels: cost, energy balance, environmental impacts and future prospects. Biomass Bioenerg. **53:** 29-38

Smith AJ, London J, Stanier RY (1967) Biochemical basis of obligate autotrophy in blue-green algae and *Thiobacilli*. J. Bacteriol. **94:** 972-983

Stal LJ (2008) Nitrogen fixation in cyanobacteria. *In* Encyclopedia of Life Sciences (ELS). John Wiley & Sons Ltd., pp 1 - 8

Steinhauser D, Fernie AR, Araújo WL (2012) Unusual cyanobacterial TCA cycles: not broken just different. Trends Plant Sci. **17:** 503-509

Stephan DP, Ruppel HG, Pistorius EK (2000) Interrelation between cyanophycin synthesis, L-arginine catabolism and photosynthesis in the cyanobacterium *Synechocystis* sp. strain PCC 6803. Z. Naturforsch. C Bio. Sci. **55:** 927-942

Steuer R, Knoop H, Machné R (2012) Modelling cyanobacteria: from metabolism to integrative models of phototrophic growth. J. Exp. Bot. **63:** 2259-2274

Steunou A-S, Jensen SI, Brecht E, Becraft ED, Bateson MM, Kilian O, Bhaya D, Ward DM, Peters JW, Grossman AR, Kuhl M (2008) Regulation of *nif* gene expression and the energetics of N_2 fixation over the diel cycle in a hot spring microbial mat. ISME J. **2:** 364-378

Stitt M, Schaewen A, Willmitzer L (1991) "Sink" regulation of photosynthetic metabolism in transgenic tobacco plants expressing yeast invertase in their cell wall involves a decrease of the Calvin-cycle enzymes and an increase of glycolytic enzymes. Planta **183:** 40-50

Straka L, Rittmann BE (2017) Effect of culture density on biomass production and light utilization efficiency of *Synechocystis* sp. PCC 6803. Biotechnol. Bioeng.

Su Z, Olman V, Mao F, Xu Y (2005) Comparative genomics analysis of NtcA regulons in cyanobacteria: regulation of nitrogen assimilation and its coupling to photosynthesis. Nucleic Acids Res. **33:** 5156-5171

Suzuki I, Horie N, Sugiyama T, Omata T (1995) Identification and characterization of two nitrogen-regulated genes of the cyanobacterium *Synechococcus* sp. strain PCC7942 required for maximum efficiency of nitrogen assimilation. J. Bacteriol. **177:** 290-296

Sweetlove LJ, Beard KF, Nunes-Nesi A, Fernie AR, Ratcliffe RG (2010) Not just a circle: flux modes in the plant TCA cycle. Trends Plant Sci. **15:** 462-470

Takatani N, Kobayashi M, Maeda S-i, Omata T (2006) Regulation of nitrate reductase by non-modifiable derivatives of PII in the cells of *Synechococcus elongatus* strain PCC 7942. Plant Cell Physiol. **47:** 1182-1186

Tamagnini P, Axelsson R, Lindberg P, Oxelfelt F, Wünschiers R, Lindblad P (2002) Hydrogenases and hydrogen metabolism of cyanobacteria. Microbiol. Mol. Biol. R. **66:** 1-20

Tandeau de Marsac N (1977) Occurrence and nature of chromatic adaptation in cyanobacteria. J. Bacteriol. **130:** 82-91

Tanigawa R, Shirokane M, Maeda S-i, Omata T, Tanaka K, Takahashi H (2002) Transcriptional activation of NtcA-dependent promoters of *Synechococcus* sp. PCC 7942 by 2-oxoglutarate in vitro. PNAS **99:** 4251-4255

Thurotte A, Lopez Igual R, Wilson A, Comolet L, Bourcier de Carbon C, Xiao F, Kirilovsky D (2015) Regulation of orange carotenoid protein activity in cyanobacterial photoprotection. Plant Physiol. **169:** 737-747

Tian J, Bryk R, Itoh M, Suematsu M, Nathan C (2005) Variant tricarboxylic acid cycle in *Mycobacterium tuberculosis*: identification of α-ketoglutarate decarboxylase. PNAS **102:** 10670-10675

Tillich UM, Lehmann S, Schulze K, Dühring U, Frohme M (2012) The optimal mutagen dosage to induce point-mutations in *Synechocystis* sp. PCC6803 and its application to promote temperature tolerance. PLoS One **7:** e49467

Tillich UM, Wolter N, Franke P, Dühring U, Frohme M (2014) Screening and genetic characterization of thermo-tolerant *Synechocystis* sp. PCC6803 strains created by adaptive evolution. BMC Biotechnol. **14:** 66

Ting CS, Rocap G, King J, Chisholm SW (2002) Cyanobacterial photosynthesis in the oceans: the origins and significance of divergent light-harvesting strategies. Trends Microbiol. **10:** 134-142

Tomitani A, Knoll AH, Cavanaugh CM, Ohno T (2006) The evolutionary diversification of cyanobacteria: molecular–phylogenetic and paleontological perspectives. PNAS **103:** 5442-5447

Touloupakis E, Cicchi B, Torzillo G (2015) A bioenergetic assessment of photosynthetic growth of *Synechocystis* sp. PCC 6803 in continuous cultures. Biotechnol. Biofuels **8:** 1-11

Ugwu C, Aoyagi H, Uchiyama H (2008) Photobioreactors for mass cultivation of algae. Bioresour. Technol. **99:** 4021-4028

Valladares A, Montesinos ML, Herrero A, Flores E (2002) An ABC-type, high-affinity urea permease identified in cyanobacteria. Mol. Microbiol. **43:** 703-715

van Alphen P, Hellingwerf KJ (2015) Sustained circadian rhythms in continuous light in *Synechocystis* sp. PCC6803 growing in a well-controlled photobioreactor. PLoS One **10:** e0127715

van de Meene AML, Hohmann-Marriott MF, Vermaas WFJ, Roberson RW (2006) The three-dimensional structure of the cyanobacterium *Synechocystis* sp. PCC 6803. Arch. Microbiol. **184:** 259-270

Vázquez-Bermúdez MaF, Herrero A, Flores E (2002) 2-Oxoglutarate increases the binding affinity of the NtcA (nitrogen control) transcription factor for the *Synechococcus glnA* promoter. FEBS Lett. **512:** 71-74

Vázquez-Bermúdez MF, Herrero A, Flores E (2000) Uptake of 2-oxoglutarate in *Synechococcus* strains transformed with the *Escherichia coli kgtP* gene. J. Bacteriol. **182:** 211-215

Vega-Palas M, Flores E, Herrero A (1992) NtcA, a global nitrogen regulator from the cyanobacterium *Synechococcus* that belongs to the Crp family of bacterial regulators. Mol. Microbiol. **6:** 1853-1859

Wang H-L, Postier BL, Burnap RL (2004) Alterations in global patterns of gene expression in *Synechocystis* sp. PCC 6803 in response to inorganic carbon limitation and the inactivation of *ndhR*, a LysR family regulator. J. Biol. Chem. **279:** 5739-5751

Wang Y, Xu W, Chitnis PR (2009) Identification and bioinformatic analysis of the membrane proteins of *Synechocystis* sp. PCC 6803. Proteome Sci. **7:** 1-12

Watanabe S, Ohbayashi R, Kanesaki Y, Saito N, Chibazakura T, Soga T, Yoshikawa H (2015) Intensive DNA replication and metabolism during the lag phase in cyanobacteria. PLoS One **10:** e0136800

Watzer B, Engelbrecht A, Hauf W, Stahl M, Maldener I, Forchhammer K (2015) Metabolic pathway engineering using the central signal processor P(II). Microb. Cell Fact. **14:** 1-12

Wijffels RH, Kruse O, Hellingwerf KJ (2013) Potential of industrial biotechnology with cyanobacteria and eukaryotic microalgae. Curr. Opin. Biotech. **24:** 405-413

Williams JGK (1988) Construction of specific mutations in photosystem II photosynthetic reaction center by genetic engineering methods in *Synechocystis* 6803. *In* Methods Enzymol, Vol 167. Academic Press, pp 766-778

Williams PJlB, Laurens LM (2010) Microalgae as biodiesel and biomass feedstocks: review and analysis of the biochemistry, energetics and economics. Energy Environ. Sci. **3:** 554-590

Xiong W, Brune D, Vermaas WF (2014) The γ-aminobutyric acid shunt contributes to closing the tricarboxylic acid cycle in *Synechocystis* sp. PCC 6803. Mol. Microbiol. **93:** 786-796

Xu K, Jiang H, Juneau P, Qiu B (2012) Comparative studies on the photosynthetic responses of three freshwater phytoplankton species to temperature and light regimes. J. Appl. Phycol. **24:** 1113-1122

Xu Y, Carr PD, Clancy P, Garcia-Dominguez M, Forchhammer K, Florencio F, Tandeau de Marsac N, Vasudevan SG, Ollis DL (2003) The structures of the

PII proteins from the cyanobacteria *Synechococcus* sp. PCC 7942 and *Synechocystis* sp. PCC 6803. Acta Crystallogr. D Biol. Crystallogr. **59:** 2183-2190

Yang C, Hua Q, Shimizu K (2002) Metabolic flux analysis in *Synechocystis* using isotope distribution from 13C-labeled glucose. Metab. Eng. **4:** 202-216

Yang F, Shen G, Schluchter WM, Zybailov B, Ganago A, Golbeck JH, Bryant DA (1999) Structural and functional analyses of cyanobacterial photosystem I. *In* GA Peschek, W Löffelhardt, G Schmetterer, eds, The phototrophic prokaryotes. Springer, Boston, MA, pp 21-33

Yang Q, Pando BF, Dong G, Golden SS, van Oudenaarden A (2010) Circadian gating of the cell cycle revealed in single cyanobacterial cells. Science **327:** 1522-1526

Yoshihara S, Geng X, Okamoto S, Yura K, Murata T, Go M, Ohmori M, Ikeuchi M (2001) Mutational analysis of genes involved in pilus structure, motility and transformation competency in the unicellular motile cyanobacterium *Synechocystis* sp. PCC6803. Plant Cell Physiol. **42:** 63-73

Young JD, Shastri AA, Stephanopoulos G, Morgan JA (2011) Mapping photoautotrophic metabolism with isotopically nonstationary 13C flux analysis. Metab. Eng. **13:** 656-665

Yu J, Liberton M, Cliften PF, Head RD, Jacobs JM, Smith RD, Koppenaal DW, Brand JJ, Pakrasi HB (2015) *Synechococcus elongatus* UTEX 2973, a fast growing cyanobacterial chassis for biosynthesis using light and CO_2. Sci. Rep. **5:** 1-10

Yu Y, You L, Liu D, Hollinshead W, Tang YJ, Zhang F (2013) Development of *Synechocystis* sp. PCC 6803 as a phototrophic cell factory. Mar. Drugs **11:** 2894-2916

Zalutskaya Z, Kharatyan N, Forchhammer K, Ermilova E (2015) Reduction of PII signaling protein enhances lipid body production in *Chlamydomonas reinhardtii*. Plant Sci. **240:** 1-9

Zavřel T, Sinetova MA, Búzová D, Literáková P, Červený J (2015) Characterization of a model cyanobacterium *Synechocystis* sp. PCC 6803 autotrophic growth in a flat-panel photobioreactor. Eng. Life Sci. **15:** 122-132

Zeth K, Fokina O, Forchhammer K (2014) Structural basis and target-specific modulation of ADP sensing by the *Synechococcus elongatus* P(II) signaling protein. J. Biol. Chem. **289:** 8960-8972

Zhang S, Bryant DA (2011) The tricarboxylic acid cycle in cyanobacteria. Science **334:** 1551-1553

Zhang S, Bryant DA (2015) Biochemical validation of the glyoxylate cycle in the cyanobacterium *Chlorogloeopsis fritschii* strain PCC 9212. J. Biol. Chem. **290:** 14019-14030

Zhang S, Qian X, Chang S, Dismukes GC, Bryant DA (2016) Natural and synthetic variants of the tricarboxylic acid cycle in cyanobacteria: Introduction of the GABA shunt into *Synechococcus* sp. PCC 7002. Front. Microbiol. **7:** 1-13

Zhao M-X, Jiang Y-L, He Y-X, Chen Y-F, Teng Y-B, Chen Y, Zhang C-C, Zhou C-Z (2010) Structural basis for the allosteric control of the global transcription factor NtcA by the nitrogen starvation signal 2-oxoglutarate. PNAS **107:** 12487-12492

Zilliges Y, Kehr J-C, Mikkat S, Bouchier C, de Marsac NT, Börner T, Dittmann E (2008) An extracellular glycoprotein is implicated in cell-cell contacts in the toxic cyanobacterium *Microcystis aeruginosa* PCC 7806. J. Bacteriol. **190:** 2871-2879